SANDIA REPORT

SAND97-0794 • UC-721
Unlimited Release
Printed August 1997

Waste Isolation Pilot Plant Disposal Room Model

B. M. Butcher

Prepared by
Sandia National Laboratories
Albuquerque, New Mexico 87185 and Livermore, California 94550

Sandia is a multiprogram laboratory operated by Sandia Corporation, a Lockheed Martin Company, for the United States Department of Energy under Contract DE-AC04-94AL85000.

Approved for public release; distribution is unlimited.



Sandia National Laboratories

SF2900Q(8-81)

Issued by Sandia National Laboratories, operated for the United States Department of Energy by Sandia Corporation.

NOTICE: This report was prepared as an account of work sponsored by an agency of the United States Government. Neither the United States Government nor any agency thereof, nor any of their employees, nor any of their contractors, subcontractors, or their employees, makes any warranty, express or implied, or assumes any legal liability or responsibility for the accuracy, completeness, or usefulness of any information, apparatus, product, or process disclosed, or represents that its use would not infringe privately owned rights. Reference herein to any specific commercial product, process, or service by trade name, trademark, manufacturer, or otherwise, does not necessarily constitute or imply its endorsement, recommendation, or favoring by the United States Government, any agency thereof or any of their contractors or subcontractors. The views and opinions expressed herein do not necessarily state or reflect those of the United States Government, any agency thereof or any of their contractors.

Printed in the United States of America. This report has been reproduced directly from the best available copy.

Available to DOE and DOE contractors from
Office of Scientific and Technical Information
PO Box 62
Oak Ridge, TN 37831

Prices available from (615) 576-8401, FTS 626-8401

Available to the public from
National Technical Information Service
US Department of Commerce
5285 Port Royal Rd
Springfield, VA 22161

NTIS price codes
Printed copy: A08
Microfiche copy: A01

SAND97-0794
Unlimited Release
Printed August 1997

Distribution
Category UC-721

Waste Isolation Pilot Plant Disposal Room Model

B.M. Butcher
WIPP Disposal Room Systems Department
Nuclear Waste Management Center
Sandia National Laboratories
P.O. Box 5800
Albuquerque, NM 87185-1341

ABSTRACT

This paper describes development of the conceptual and mathematical models for the part of the Waste Isolation Pilot Plant (WIPP) repository performance assessment that is concerned with what happens to the waste over long times after the repository is decommissioned. These models, collectively referred to as the "The Disposal Room Model," describe the repository closure process during which deformation of the surrounding salt consolidates the waste. First, the relationship of repository closure to demonstration of compliance with the Environmental Protection Agency (EPA) standard (40 CFR 191 Appendix C) and how sensitive performance results are to it are examined. Next, a detailed description is provided of the elements of the Disposal Room Model, such as the configuration of the waste disposal region, and properties selected for the salt, waste, and other potential disposal features such as backfill. Included in the discussion is an explanation of how the various models were developed over time. Other aspects of closure analysis, such as the waste flow model and method of analysis, are also described. Finally, the closure predictions used in the final performance assessment analysis for the WIPP Compliance Certification Application are summarized.

CONTENTS

ACRONYMS vi

EXECUTIVE SUMMARY vii

1.0 INTRODUCTION 1

1.1 The Relationship of WIPP Repository Closure to 40 CFR 191 Scenarios 2

2.0 CONCEPTUAL MODELS AND ASSUMPTIONS FOR LONG-TERM COMPLIANCE 3

2.1 The Closure Process 3
2.1.1 Undisturbed Performance 3
2.1.2 Human Intrusion 6
2.1.3 Summary 6

2.2 Sensitivity of Performance Assessment Results to Closure 7
2.3 Disposal Model Components 7

2.3.1 Repository Geometry and Other Calculational Constraints 7
2.3.2 Constitutive Relations 8
2.3.3 Waste and Backfill Fluid Flow Models 8
2.3.4 Method of Analysis 8

3.0 APPROXIMATIONS, ASSUMPTIONS AND MATHEMATICAL MODELS USED IN THE DISPOSAL ROOM MODEL 15

3.1 Repository Geometry and Other Calculational Constraints 15

3.1.1 Two-Dimensional Approximations of a Three-Dimensional Repository 15
3.1.2 Effect of Scale on Two-Dimensional Closure Calculations 16
3.1.3 Effect of Stratigraphy 18
3.1.4 The Disturbed Rock Zone 19
3.1.5 Gravity Effects 19
3.1.6 Half-Room vs. Quarter-Room Symmetry 21
3.1.7 Disposal Room Computational Configurations 22

3.2 Constitutive Relationships 23

3.2.1 Halite Creep Laws 23
3.2.2 Waste Compaction Models 25
3.2.3 Backfill Consolidation 30
3.2.4 Gas Generation 33
3.2.5 Fractures 35
3.2.6 Disturbed Rock Zone 36

3.3 Waste Flow Model 36

3.3.1 Flow Model 36
3.3.2 Permeability and Other Flow Properties 37
3.3.3 Initial Brine Content of the Waste 39
3.3.4 Wicking and Other Water Migration Mechanisms 40

3.4 Method of Analysis 40

3.4.1 Porosity Surface Data 41
3.4.2 Coupled Two-Phase-Flow Mechanical Closure Approach 42

3.5 Compliance Certification Application Calculation Results 43

3.5.1 Porosity Surface Results 43

4.0 REFERENCES 52

Figures

Figure A. Schematic relationship of the consolidation process to data inputs for performance assessment codes viii
Figure 1. Repository geometry models and assumptions 9
Figure 2. Constitutive relationships and assumptions. 10
Figure 3. Waste and backfill flow models and assumptions. 12
Figure 4. Methods of analysis. 13
Figure 5. Ideal packing of drums in rooms and 10-m-wide drifts (not to scale). 20
Figure 6. WIPP waste compaction model. 26
Figure 7. Final disposal room waste compaction curve for the CCA. 29
Figure 8. Gas generation histories assumed for calculations of the closure of a single disposal room with no backfill in an infinite array configuration, for the CCA 44
Figure 9. Porosity curves showing the variation in the closure history with gas content of a single disposal room (no backfill) in an infinite array configuration 45
Figure 10. Gas pressure curves showing the variation in the closure history with gas content of a single disposal room (no backfill) in an infinite array configuration 46
Figure 11. Gas generation histories assumed for calculations of the closure of the experimental region with no backfill 48
Figure 12. Void volume curves showing the variation in the closure history with gas content of the experimental region with no backfill in an infinite array configuration 49
Figure 13. Gas pressure curves showing the variation in pressure with time for different gas content of the experimental region with no backfill 50

Tables

Table 1. Simulated TRU Waste Compaction 28
Table 2. Summary of Base Values, Ranges, and Distributions for Crushed Salt/Bentonite Backfill Mechanical Properties 33

ACRONYMS

BRAGFLO	WIPP Brine and gas flow computer code
CCA	Compliance Certification Application
CCDFs	complimentary cumulative distribution functions
CFR	Code of Federal Regulations
CPU	central processing unit
DRZ	disturbed rock zone
EPA	Environmental Protection Agency
M-D	Multimechanism deformation
PA	Performance assessment
PHENIX	Hybrid computer code coupling SANTOS and TOUGH2
RH	remote handled
SANCHO	Dynamic relaxation, finite-element, deformation of solids computer program used by Sandia National Laboratories (predecessor of SANTOS)
SANTOS	Dynamic relaxation, finite-element, deformation of solids computer program used by Sandia National Laboratories
SPECTROM-32	Finite-element, deformation of solids computer program used by RE/SPEC, Inc.
TOUGH2	Multiphase fluid and heat flow computer code
TRU	transuranic
WIPP	Waste Isolation Pilot Plant

EXECUTIVE SUMMARY

The ability of salt to deform with time, eliminate voids, and create an impermeable barrier around waste is one of the principal reasons for locating the Waste Isolation Pilot Plant (WIPP) repository in a bedded salt formation. This "closure" process is a complex and interdependent series of events that begins after a region within the repository is excavated and filled with waste. It is important because it determines the density of the waste at any given time, thus controlling the flow of brine and gases through the waste and its capacity to release radionuclides. An objective of this paper is to document how the consolidation of the waste is predicted as a function of time using the Disposal Room Model, and provide some of the history of how the model evolved to its current state of development. The model described in the paper was used to calculate the closures for final performance assessment analyses related to the WIPP Compliance Certification Application.

The initial configuration of a waste-filled disposal room normally includes waste, any backfill that may be present, and an air gap between the roof and the top of the backfill as shown in Figure A. Backfill is absent in some representations of the disposal room. Assuming backfill is present, the figure shows schematically how consolidation over time changes the state of the waste (the conceptual model). Since the time required for such changes is long compared with any experiment that can be performed, projections are made by calculations. The results are in the form of data describing the state of consolidation of the waste (its void volume or porosity) as a function of time and gas content. This information is then transferred as data to the performance assessment code BRAGFLO, for application to compliance analyses.

The evolution of the consolidated state, as described by the mathematical form of the model, was calculated in the past using either of two finite-element structural response computer codes—SANTOS—developed by Sandia National Laboratories, or SPECTROM-32—developed by RE/SPEC. SANTOS or SPECTROM-32 represented the computational part of the model. Results from the SANTOS code (Version 2.00 in the Cray-J911/UNICOS 8.04 system configuration) were used for the Sandia WIPP Project preliminary performance assessment in December 1992, and SANTOS has been used exclusively for all more recent calculations. An advantage of having two independent codes available for these complex calculations was that one code was used to verify the results of the other, adding to the credibility of the results.

As in the solution of any problem involving complex physical processes, a detailed conceptual model and a large number of assumptions and mathematical models are required for disposal room calculations. The description of these elements, such as the configuration of the room and the mathematical models and properties selected for the salt, waste, and backfill, constitute the major portion of this paper in Chapter 3. Before beginning this documentation, however, the relationship of repository closure to demonstration of compliance with the Environmental Protection Agency standard (40 CFR 191 Appendix C) is described in Chapter 1. Discussion is limited to the long-term response of the repository (after decommissioning). Chapter 2 describes the conceptual model of closure and how sensitive performance assessment results are to closure. Chapter 2 also outlines the assumptions and mathematical components of the model, which are then addressed in Chapter 3. The calculated average room porosities ranged from 0.24 to 0.7 at 10,000 years given zero to high gas generation volumes.

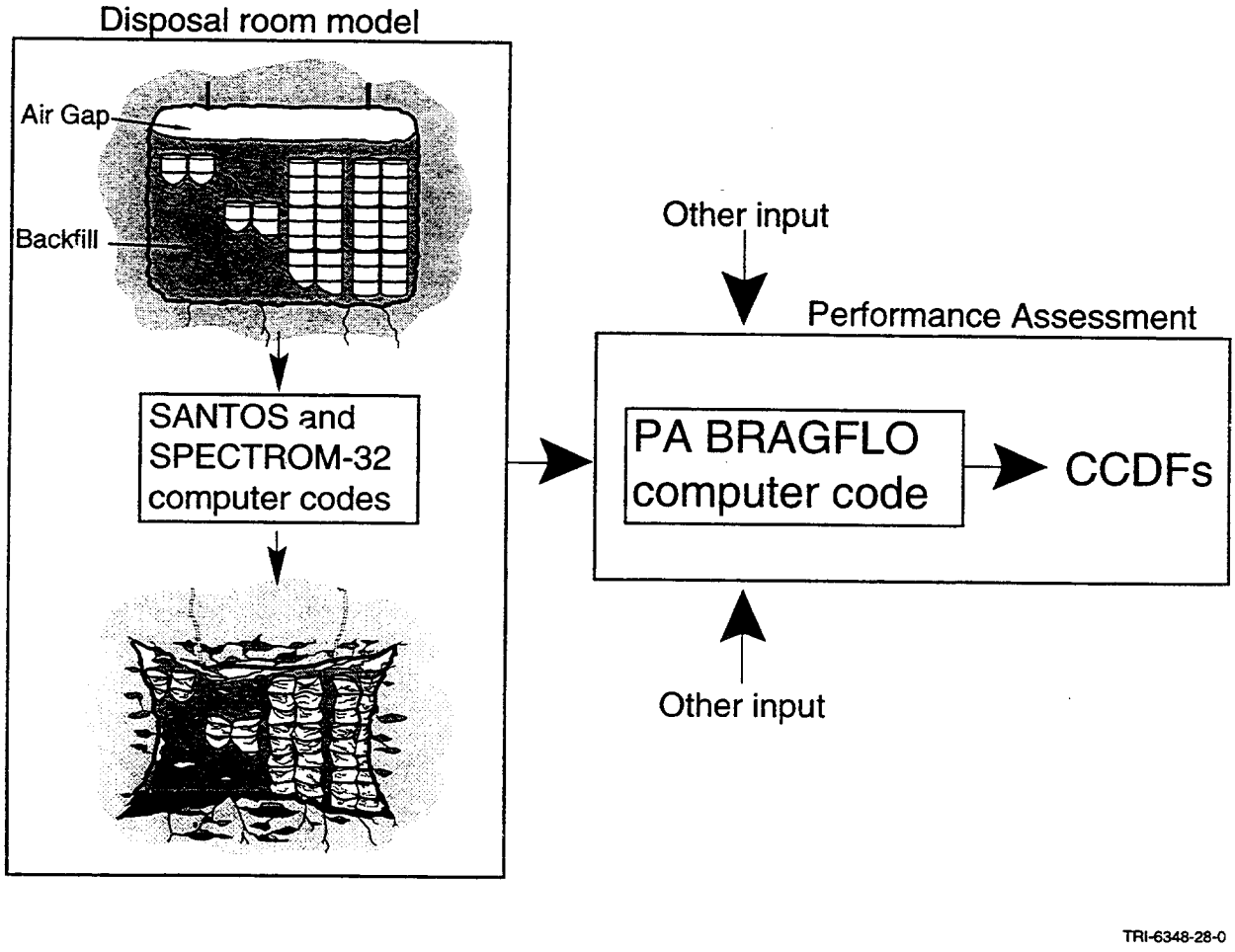


Figure A. Schematic of the relationship of the consolidation process to data inputs for performance assessment codes. (PA, performance assessment; CCDF, complementary cumulative distribution functions.)

1.0 INTRODUCTION

This paper describes the technical information required to address the part of the Waste Isolation Pilot Plant (WIPP) repository performance that is concerned with what happens to the waste and backfill after the repository is decommissioned, i.e., after the repository seals are in place and further access is not possible. This information was used to calculate closures for final performance assessment analyses related to the WIPP Compliance Certification Application (CCA).

The ability of salt to deform with time, eliminate voids, and create an impermeable barrier around the waste is one of the principal reasons for locating the WIPP repository in a bedded salt formation. This "closure" process is modeled as a complex and interdependent series of events that begins after a region within the repository is excavated and filled with waste. As an effect of excavation, the equilibrium state of the rock surrounding the repository is disturbed, and the rock begins to deform as it tries to return to an equilibrium state. At equilibrium, rock mass deformation ceases, and the waste and backfill have undergone as much compaction as is possible in response to the weight of the rock setting upon the repository (overburden).

The qualitative conceptual model of closure presented in this paper is similar to the model used in the December 1992 preliminary performance assessment (Sandia WIPP Project, 1992). This assessment provided limited information about the models and assumptions with regard to closure. This information can be found in Section 1.4.7 in the Sandia WIPP Project report (1992, pp. 1-42 to 1-46) addressing models, Section 2.5 in the Sandia WIPP Project report (1992, pp. 2-69 to 2-71) addressing code input parameters, and Section 4.2.2.2 in the WIPP PA Department document (WIPP PA Department, 1993, pp. 4-11 to 4-23) addressing how closure information is transformed into the data used in BRAGFLO. Closure information used for the December 1992 preliminary performance assessment was over 4 years old and did not reflect the many changes and improvements that have since been completed. In particular, all new results have been computed using the multimechanism deformation (M-D) constitutive relation for the creep of halite, instead of the steady-state reference creep law (Section 3.2.1 of this report).

The principal measure of compaction or closure of the repository is the pore volume, which continues to decrease until a state of quasi-equilibrium occurs. The description “quasi-equilibrium” is used because very small readjustments in the state of the repository are expected to continue for many thousands of years because of physical and chemical changes to the waste and equilibration of fluid flow processes. The fluids in the pore volume of this quasi-static state may or may not be at lithostatic pressure. The pore pressure depends on the properties of the fluid and whether the materials surrounding the pores have any time-independent strength. The assumption for the salt is that it will continue to deform until all stress gradients vanish. In contrast, some other materials, such as waste sludges, have permanent strength, which gives them the capacity to carry some of the overburden load. Under these circumstances, pore pressures may be reduced.

In all cases, the extent of compaction determines the properties of the waste that are important in performance assessment. These are as follows:

- The waste porosity controls the maximum volume that can exist in the waste for potential saturation with radionuclides or gas storage.
- The waste porosity influences waste permeability to both gas and brine, and therefore how fast fluids get in and out of the waste.
- The extent of compaction defines how resistant the waste is to removal when a drill

penetrates the repository during a human intrusion.

These concepts will now be discussed in terms of specific regulatory standards.

1.1 The Relationship of WIPP Repository Closure to 40 CFR 191 Scenarios

The closure scenarios addressed in the December 1992 preliminary performance assessment remain unchanged. Two sets of scenarios are important for 40 CFR 191 Appendix C (US EPA, 1985).[1] The first set is concerned with migration of contaminated brine away from the repository in its undisturbed state (WIPP PA Department, 1992, Section 4.1.1, pp. 4.2-4.5). In these scenarios, the state of compaction determines the maximum volume that can exist in the waste for potential saturation with brine, and how permeable the waste is to brine moving in and out of the repository. The actual amount of brine flow is determined by the coupling with brine flow through the Salado Formation and flow through shaft seals.

The second set of scenarios is concerned with human intrusion by drilling. In general, the amount of radioactive material released directly to the earth's surface depends on, among other factors, the strength of the waste at the time of the intrusion [40 CFR 191 Appendix C (US EPA, 1985)], and this in turn depends to some extent on the state of compaction. The starting point for estimating the release is to calculate the response of the undisturbed repository over 10,000 years. These results define the state of the repository at any given time; human intrusion interrupts this history, continues closure with new initial conditions, and produces a new repository closure history starting at the time of the intrusion. The drilling may penetrate a dense waste form or a porous form, depending on the previous history of repository conditions in regard to brine inflow and the history of the rate of gas production. A highly compacted waste form at the time of intrusion is desirable, because it will have much greater strength than a highly porous waste form, and therefore greater resistance to erosion and spall.

The compacted state of the waste, as reflected in its permeability, is also important at the time of human intrusion in controlling how fast contaminated brine or gas flows out of the waste and surroundings into the borehole. Examples of relationships between porosity, permeability, and other material properties are found in Freeze and Cherry (1979, p. 357). Another aspect of this issue is flow of brine through the waste from one borehole to another in the E1E2 scenario (WIPP PA Department, 1992, Section 4.1.1, pp. 4.2-4.5). In both cases, waste permeability helps to determine how readily this flow occurs. A subcategory of this issue is that release depends on how much contaminated brine exists in the waste before the intrusion, which depends on the waste porosity.

2.0 CONCEPTUAL MODELS AND ASSUMPTIONS FOR LONG-TERM COMPLIANCE

2.1 The Closure Process

2.1.1 Undisturbed Performance

[1] This was originally promulgated as 40 CFR 191 Appendix B (US EPA, 1985, p. 38088). It was subsequently remanded to the EPA (NRDC v. EPA, 824 F2d 1258 [1st Circ. 1987]), and was repromulgated as 40 CFR 191 Appendix C (US EPA, 1993, p. 66415). It is referenced as Appendix C throughout this position paper.

Repository closure is a complex and interdependent series of events that begin after a region within the repository is excavated and filled with waste. The evolution of closure is mathematically modeled as the Disposal Room Model (Butcher and Mendenhall, 1993), and it is important because it determines the density (porosity) of the waste at any given time, thus controlling flow of brine and gases through the waste and its capacity for storing fluids. Permeability and storage volume of the waste are dependent on the extent of closure, and in turn affect the extent of migration of radioactive and hazardous species. Since a room is one of the basic units of interest in defining the performance of the repository, its closure is often used in the examples that follow.

Room closure begins immediately after excavation because the cavity is at atmospheric pressure rather than in the undisturbed *in situ* state. Because loading of the salt is now nonuniform, the salt begins to deform with time and the volume of the cavity becomes smaller. Any free brine present in the surrounding rock can also begin to flow into the excavation at this time. Eventually, if the room were empty, closure would proceed to the point where the void volume created by the excavation would be eliminated, or filled with brine, and the surrounding halite would return to its undisturbed, uniform stress state. Backfill is placed in mines to hasten reaching an equilibrium condition and minimize subsidence, and may or may not be used in the WIPP.

Assume that a filled disposal room contains waste, salt backfill, and an air gap between the roof and the top of the backfill (Sandia WIPP Project, 1992, Figure 3.1-4, p. 3-13). The scenario for no backfill is similar. The idealized case will be described first where (1) the room remains unsaturated with brine during the time required to reach an equilibrium state and (2) the amount of gas produced is too small to affect the mechanical response of the waste and backfill. For this situation, the initial effect of closure will be to eliminate most of the air gap. Eventually, however, contact will be made between the surrounding halite, the waste, and any backfill. At this point, closure would largely cease if the strength of the waste and backfill is sufficient to support all of the rock above the room. If not, the room continues to close after the air gap is eliminated, gradually transferring load to the waste and backfill, and in the process consolidating them to denser states. Any fractures that have formed in the disturbed rock zone (DRZ), the region surrounding the repository room that may have been affected by the excavation process, also partially close as the waste and backfill exert back pressure at the room boundaries.

In the absence of substantial gas or brine, both the waste and the backfill will continue to consolidate and become denser, until load balance is achieved. The amount of consolidation and the time it takes is governed by the properties of the waste and backfill, the halite, and the dimensions and location of the room. Representation of salt backfill consolidation in past performance assessment calculations has been particularly complex because, like solid salt, it will continue to deform with time until most of the backfill void volume is eliminated. Compaction of the waste is simpler, because, as shown by compaction test results (Butcher et al., 1991b), it may be assumed to depend only on the load it supports. A time-independent material response is less complicated to analyze.

If no extraneous factors such as gas generation or brine inflow are present to alter the closure process, closure will continue to a maximum state of waste compaction at lithostatic pressure. For the baseline CCA assumption of no backfill, this state was assumed to be a porosity of 0.18 as defined in Section 3.2.2 of this report. The value of porosity quoted for this state in the performance assessment code BRAGFLO analyses (refer to Figure A for information on flow path) was different, because all porosity values in BRAGFLO are defined in terms of the initial volume of the repository (WIPP PA Department, 1993, Section 4.2.2.2, pp. 4-11 to 4-23), before any creep has had a chance to occur.

The BRAGFLO porosity definition preserves the void volume calculated from SANTOS:

Install Equation Editor and double-click here to view equation. (1)

where Install Equation Editor and double-click here to view equation. is the BRAGFLO porosity at time t, $\eta_v(t)$ is the instantaneous porosity at time t calculated from the Disposal Room Model, and $\eta_v(t = 0)$ is the initial porosity of the waste at $t = 0$. It follows that Install Equation Editor and double-click here to view equation.

The presence of either brine or gas in the waste voids (pores) interrupts the closure process. First, if brine is present and immobile in the waste or backfill, closure largely ceases when the void volume decreases to the point where the voids are completely filled (saturated) with brine. Consolidation continues only if the brine can flow elsewhere. Second, when gas is being generated, closure and consolidation continue until the gas (pore pressure) increases to the point where it begins to exert back pressure on the surrounding rock. Voids in the waste are assumed to be connected, causing the gas pressure to be uniform throughout the waste. Load transfer occurs according to the effective stress principle:

Install Equation Editor and double-click here to view equation. (2)

where σ_T is the stress associated with the overburden load of the overlying rock and brine, p is the pressure of the fluids in the pores, and σ_e is the effective stress that is applied to the waste skeleton (Freeze and Cherry, 1979, p. 53). In this process, the waste and backfill are considered to be skeleton structures immersed in a pore fluid, the gas. As the pore pressure increases, more of the weight of the overburden is transferred to the gas, until the gas pressure reaches lithostatic, at which time the gas and solid skeleton are both providing support. In the intermediate stages of this process, void volume reduction in the waste slows as gas pressure increases, until the porosity of the waste reaches a minimum value. Further consolidation ceases at this point, and will not begin again unless some of the gas is released. Brine inflow into the repository is also reduced as the gas pressure increases, and brine can even be expelled from the repository if the gas pressure becomes sufficiently high. During pressurization, gas release away from the waste can occur either by flow into the surrounding halite and marker beds, or by human intrusion, which will be discussed in the next section.

If the gas pressure increases above lithostatic pressure, it will eventually be high enough to lift the roof of the disposal room off the solid support. At this time the gas pressure will be supporting all of the overburden and large amounts of new gas storage volume will be created. New gas storage is produced by fracturing when the pore pressure exceeds the least *in situ* stress plus the tensile stress of the rock. Creation of this additional gas storage volume will limit the pressurization to slightly above lithostatic, and at present it is assumed to involve existing horizontal fractures, since this is the orientation for which the rock is weakest in tension. Creation of new gas storage volume may also occur at gas pressures below lithostatic pressure if local stresses are less than this value. Evidence that such a stress difference exists has yet to be acquired. Thus, the principal mechanism for limiting the gas pressure and creating large amounts of new storage volume is considered to be the opening of existing or new fractures in the interbeds. Human intrusion into the waste by drilling would have just the opposite effect. Gas pressure would be relieved as the gas flows up the borehole when the drill penetrates the waste, and more of the overburden load would be transferred back onto the waste

skeleton. If the load on the waste exceeds the load it has previously supported before the onset of gas pressurization, consolidation of the waste will begin again. Chemical and biological gas generation processes ongoing in the waste will influence how much additional waste consolidation occurs. In most cases this increment is expected to be small. Consolidation will also, for all practical purposes, end if the waste region becomes saturated with brine.

The processes associated with gas generation and migration described in the previous two paragraphs are clearly complex and highly coupled. In particular, exact descriptions of (1) the relationships between gas generation and brine availability, and (2) how the gas migrates away from the waste into the surrounding rock, become very difficult. To circumvent this overwhelming complexity, gas production in the Disposal Room Model has been parameterized. The parameterization process consists of assuming various gas production histories and calculating the corresponding closure histories. These results, referred to as "porosity surface" data, are then used in performance assessment calculations as described in Section 3.4 of this report.

Simplification of gas production by parameterization avoids the need for defining the exact details of gas production, such as (1) how the gas was generated, e.g., the amount of brine consumed during chemical reaction and where this brine came from; or (2) how much gas escaped from the waste is no longer required. Another assumption imposed by parameterization is that any brine present in the waste is incompressible and small enough in volume relative to the waste volume so as to be mechanically indistinguishable from the solid waste material that surrounds it. Solution of gas in brine is also assumed to be negligible. These are far-reaching assumptions and require demonstration, as discussed in Section 3.4 of this report, that the porosity surface approach still adequately represents the basic concepts introduced in this section.

2.1.2 Human Intrusion

For human intrusion by drilling, the assumption is made that the disposal room continues to close until gas pressurization becomes sufficient to prevent an additional decrease in porosity. This part of the repository history prior to the intrusion is identical with what would be predicted in the undisturbed repository calculation. As additional gas is generated, gas pressure continues to increase, transferring load-bearing capability from the waste skeleton to the pressure exerted by the gas according to the effective stress principle. The waste is assumed to behave as a time-independent, elastic-plastic material, similar to a metal, with unloading being largely elastic. The load transfer process may continue until the time of the intrusion. An extreme condition would be that if the pore pressure reaches lithostatic pressure, then the gas pressure alone is able to counter almost all of the weight of the overburden.

The effect of drilling is to drop almost instantaneously (compared to the time scale of creep closure) the gas pressure in the disposal room to a lower pressure. Since the gas pore pressure is now reduced, the waste skeleton must assume a greater portion of the load, and if this load exceeds the yield strength of the waste skeleton, as determined by the maximum stress it supported in the past, the compaction process may resume. Calculations have shown, however, that most of the compaction has already occurred before the time of most intrusions, with the exception of those intrusions in the 100- to 200-year period following waste emplacement, and therefore any additional compaction is likely to be small (see Butcher and Lincoln memo in Appendix A). This observation supported the assumption made in the December 1992 preliminary performance assessment that closure completely stops after the human intrusion (WIPP PA Department, 1993, Section 4.2.2.2, pp. 4-11 to 4-23). The same assumption was also made in the CCA. While a more exact analysis can be performed to determine the extent of additional compaction, the assumption of constant porosity was considered to be reasonable, and it greatly simplified the analysis of the repository over the remaining 10,000 years.

2.1.3 Summary

In summary, three processes are occurring during closure: (1) the volume of the excavation decreases as the salt deforms with time to consolidate and encapsulate the waste; (2) brine migrates toward the waste because fluid pressure adjacent to it is lower than the equilibrium fluid pressure that existed in the salt prior to excavation; and (3) decomposition, corrosion, and radiolysis processes within the waste generate gas, which exerts back pressure against closure. The presence of gas within the disposal room is important because gas pressurization may retard both the closure process and fluid flow. All three processes continue with time until the forces causing closure equilibrate with the backstress exerted by the waste, backfill, brine saturation, or gas pore pressurization. Even after equilibrium, the state of the waste can be disrupted at any time by inadvertent drilling into the repository. Because gas is released during an intrusion, the closure process may continue, or it may be impeded by brine inflow saturating the waste. Models for all the materials and processes affecting closure have been developed and incorporated into a computational method to quantitatively predict the closure histories under various conditions and their consequences.

2.2 Sensitivity of Performance Assessment Results to Closure

For 40 CFR 191 Appendix C, the principal issues influenced by closure are migration of contaminated brine and direct release of radioactive material during a human intrusion by drilling.

These processes are driven by the pore pressure and total gas content. Since the pore pressure in the waste is defined by its porosity and local gas content, the principal function of the Disposal Room Model is to determine the extent of compaction of the waste (its porosity) as a function of time. However, estimation of these states is not simple because they are determined early in the history of the repository by the tradeoff between waste densification and the increase in pore pressure caused by gas generation or brine inflow. Calculations show that compaction slows appreciably when the pore pressure (either gas or brine) increases to 10 to 20% of lithostatic pressure (lithostatic pressure is 14.8 MPa) (WIPP PA Department, 1993, Figure 4.2-6, p. 4-20).

The results of the December 1992 preliminary performance assessment imply that, in general, the final state of the disposal room is of secondary importance in regard to fluid transport through the repository (i.e., it does not have a strong effect on whether the repository is in compliance with the regulations). This conclusion is supported by other past calculations. However, the contribution of erosion and spalling mechanisms to direct release of waste during drilling can be substantial. The mechanical state of the waste or extent of closure at the time of the intrusion controls the release process in the sense that substantial gas generation early in the history of the repository, coupled with the changes introduced by decomposition of the waste, may lead to a low-strength waste form that is easily entrained in moving gas or brine.

2.3 Disposal Model Components

The Disposal Room Model for closure contains a number of conceptual submodels. The model requires assumptions about four basic types of information:

- Repository geometry and other calculational constraints
- Constitutive relations
- Waste and backfill fluid flow models
- Method of analysis

2.3.1 Repository Geometry and Other Calculational Constraints

The first part of the Disposal Room Model addresses the various aspects of the geometries assumed for disposal room closure predictions and the boundary loading conditions. Included in this module are decisions such as whether a single room or a panel of rooms should be considered, whether the calculation should be two-dimensional or three-dimensional, and the level of detail of the stratigraphy that should be assumed. All these issues must be addressed in order to define the geometry of the configuration selected for a specific numerical calculation. The flow diagram for this part of application of the Disposal Room Model is shown in Figure 1, which illustrates the decisions that have to be made. The models along the center vertical solid line in the diagram are the assumptions for CCA calculations. Each of the elements of Figure 1 and Figures 2, 3, and 4 is discussed in Chapter 3.

2.3.2 Constitutive Relations

Once the configuration is defined, the second part of the model is concerned with selecting models of the mechanical response for each region of the geometry, followed by definition of

appropriate material properties for each model. These models are frequently called constitutive relations, and include creep relationships for the halite, backfill if present, and a compaction model for the waste. Models for gas generation and fracture response are also required. This information must be provided for all regions of the configuration, and represents the bulk of the developmental effort for the Disposal Room Model. The flow diagram for this part of application of the Disposal Room Model is shown in Figure 2.

2.3.3 Waste and Backfill Fluid Flow Models

The third part of the model, though not at present used in the direct determination of closure, has application when closure is coupled with fluid flow in BRAGFLO calculations. These components include assumptions about the permeability of the waste and its initial brine content. The flow diagram for this information is shown in Figure 3.

2.3.4 Method of Analysis

The final part of the Disposal Room Model calculations is concerned with the method of analysis. This section addresses the question of how strong a coupling between brine and/or gas flow into and out of the disposal room must there be to obtain physically reasonable numerical solutions. A purely mechanical analysis with SANTOS (Version 2.00 on the Cray-J916/UNICOS 8.04 system configuration) in which an assumed or known gas generation history is prescribed (porosity surface approach described in Chapter 3, Section 3.4.1 [A-1]) is used for the CCA. The flow diagram for this part of application of the Disposal Room Model is shown in Figure 4.

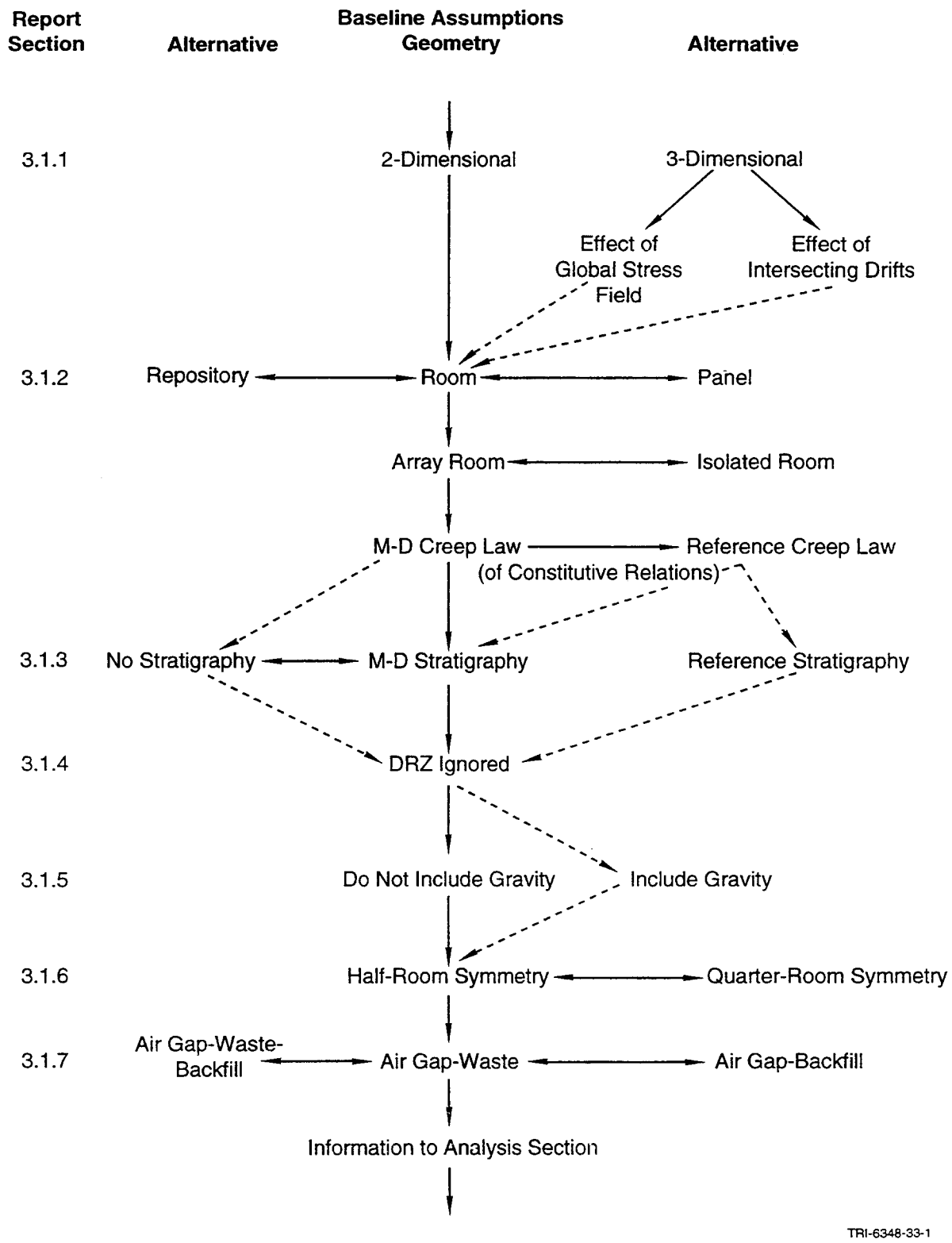


Figure 1. Repository geometry models and assumptions. The symbol ↔ indicates that the alternative can be substituted for the baseline assumption. Dashed lines indicate unlikely path options.

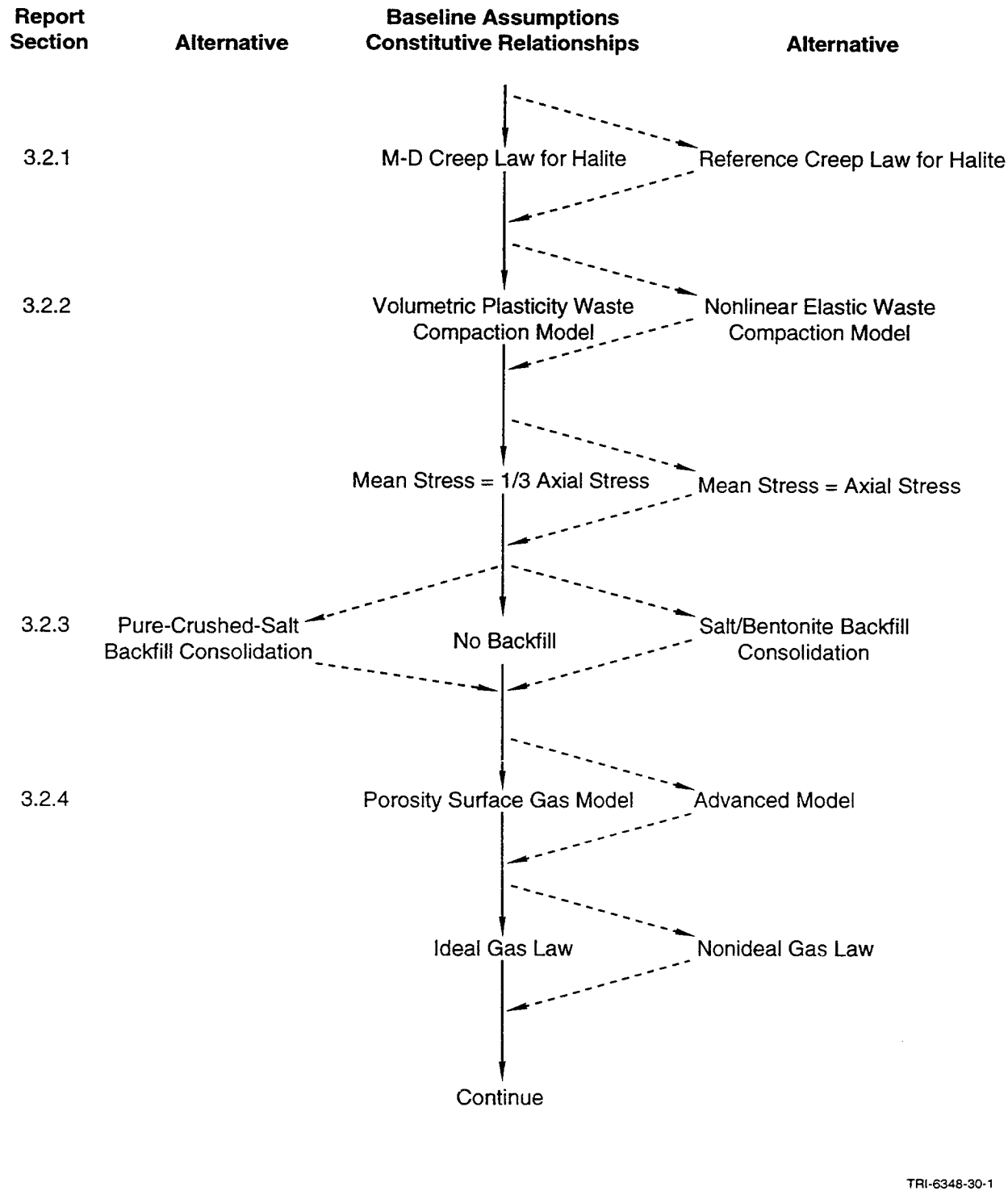


Figure 2. Constitutive relationships and assumptions. Dashed lines indicate unlikely path options.

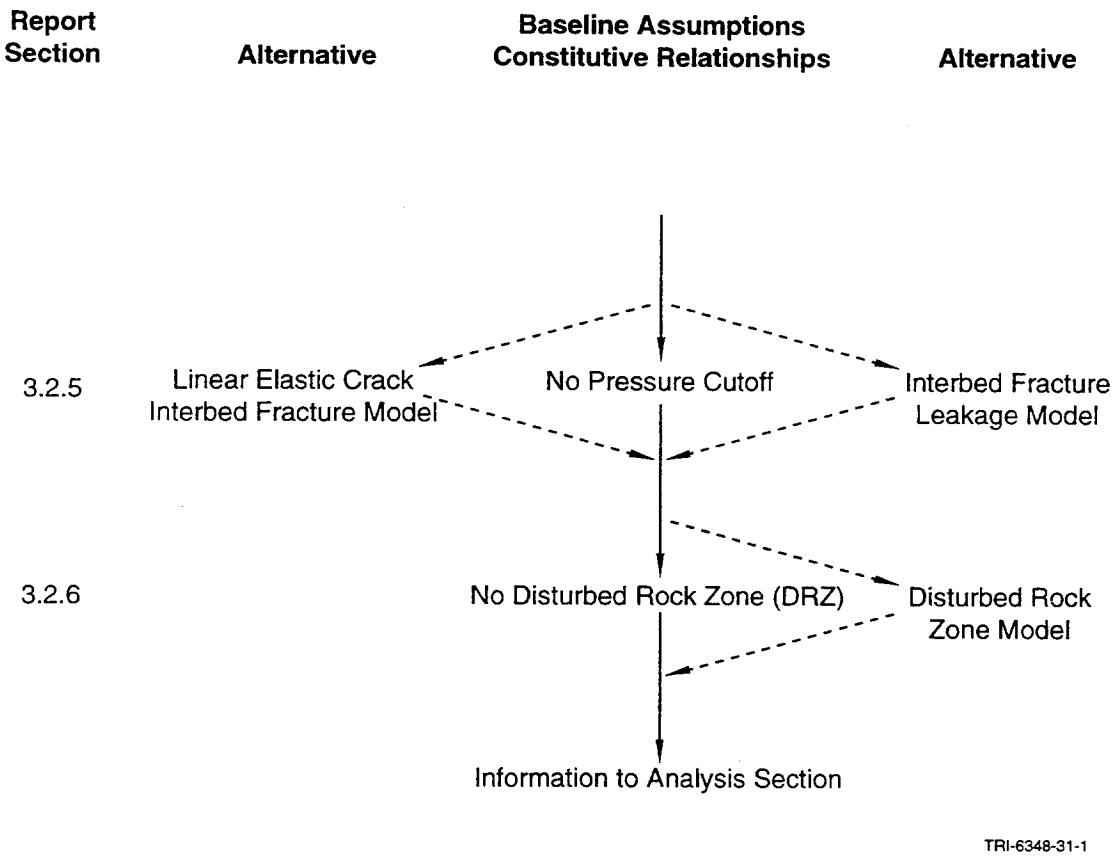


Figure 2. Constitutive relationships and assumptions (continued). Dashed lines indicate unlikely path options.

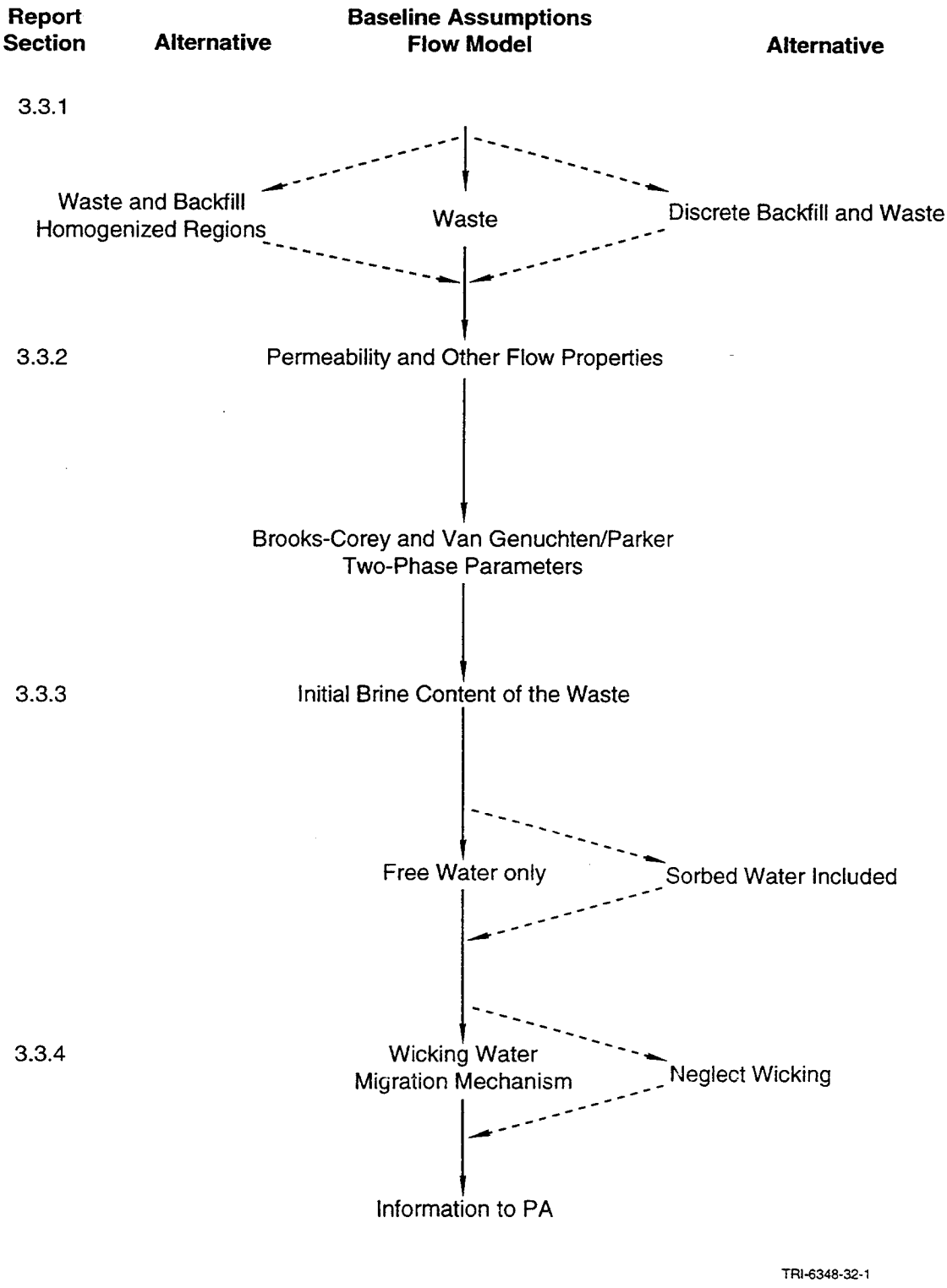


Figure 3. Waste and backfill flow models and assumptions. Dashed lines indicate unlikely path options.

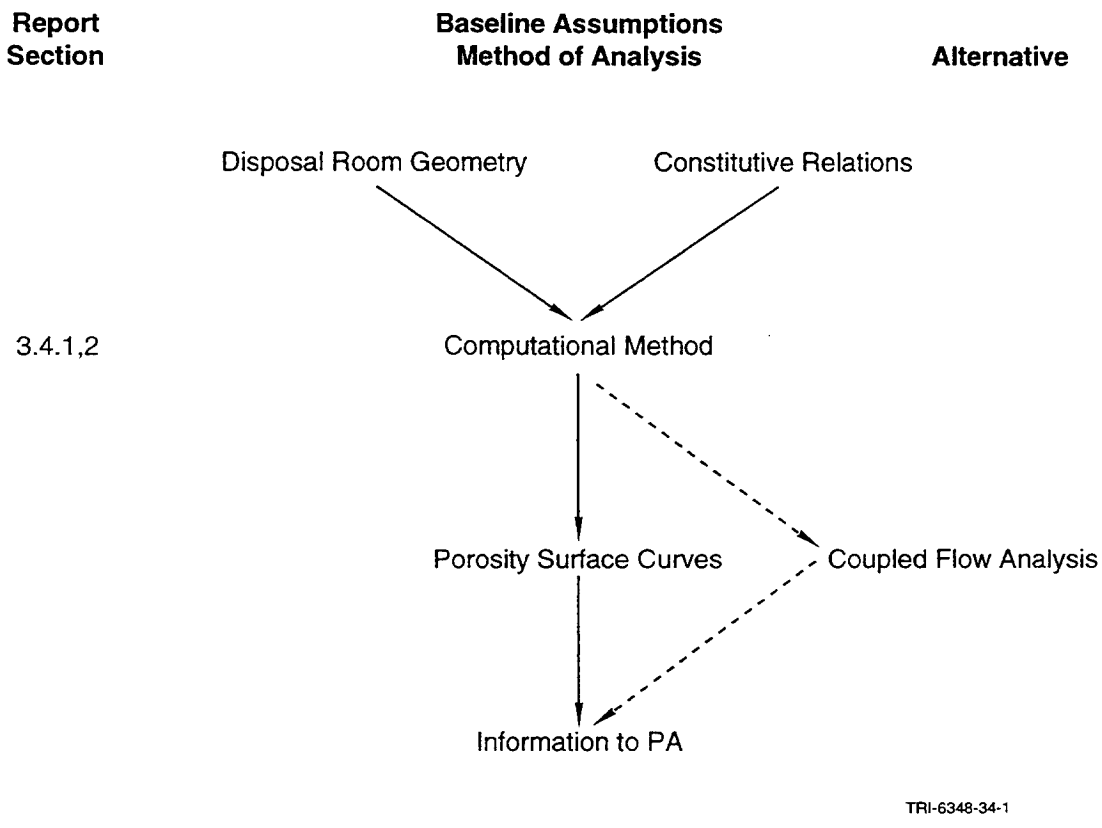


Figure 4. Methods of analysis. Dashed lines indicate unlikely path options.

THIS PAGE INTENTIONALLY LEFT BLANK

3.0 APPROXIMATIONS, ASSUMPTIONS AND MATHEMATICAL MODELS USED IN THE DISPOSAL ROOM MODEL

As described in Section 2.3, the Disposal Room Model for closure contains a number of subsidiary conceptual models. In this chapter, the assumptions and mathematical models for each of the components shown in Figures 1 to 4 are described.

3.1 Repository Geometry and Other Calculational Constraints

The following geometrical considerations and other computational assumptions must be addressed in regard to a repository closure calculation. This section provides information with regard to the conceptual model components shown in Figure 1.

- Must the repository be represented as three-dimensional, or can it be abstracted to a two-dimensional configuration?
- If two-dimensional, what is the effect of scale on two-dimensional closure calculations: can a single room be considered, or must all calculations be for a panel of rooms, or even the entire repository be represented?
- What stratigraphy should be used?
- Must the DRZ be considered?
- Must gravity be considered?
- If a single room is selected, should half-room or quarter-room symmetry be assumed?
- What is the nature of the waste and backfill and how are these to be emplaced within a storage area?

The implications of each of these questions and how they are at present resolved in repository calculations will be described in the following sections.

3.1.1 Two-Dimensional Approximations of a Three-Dimensional Repository

Ideally the Disposal Room Model should address the configuration of the entire repository, which is three-dimensional. However, the complexity of the repository geometry, the lack of efficient mathematical tools to address three-dimensional effects, and excessive solution times at present limit three-dimensional closure calculations to simpler abstractions of the waste storage areas. Closure for the CCA was modeled two-dimensionally, in the same manner as for the December 1992 preliminary performance assessment, and it is not likely that this situation will be improved by moving to the coarser grid spacing and simplified response models that are typical of the three-dimensional analyses that are technically feasible.

The potential error introduced by modeling closure as a two-dimensional process is expected to increase with time up to about 10 to 20 years, at which time closure estimates may be as much as 10% too much (Argüello, 1990). After this time the difference will begin to decrease as the three-dimensional closure "catches up" until there is little difference between two-dimensional and three-dimensional closure predictions. The basis for this estimate is taken from Argüello's three-dimensional calculations for closure at the intersection of an empty WIPP disposal room and one of its entryway drifts: after 12 years, the vertical closure of this region was estimated as 0.78 m in comparison to 0.88 m closure at the center of the room, where the state of stress is more two-dimensional. Horizontal

closure is observed to be similar. However, these results were for empty drifts and need to be extended to waste-filled rooms. For comparison, a room filled with waste and backfill, with no gas present, and a final porosity of about 0.2 is expected to have a total closure of about 2 m, rather than 4 m for an empty room, before reaching an equilibrium state. To expand this to a waste-filled room, room response during the first 0.78 m of closure is expected to differ little whether the room is empty or contains waste. Justification for this conclusion is that during the early stages of closure the waste has not been compacted to a sufficiently dense state to exert much backstress on the surrounding rock. After 0.78 m closure, which is about 40% of the total closure for a waste and backfilled room, the waste begins to stiffen up, and the difference between three-dimensional and two-dimensional closure of a waste-filled room begins to decrease. Thus, the assertion that the potential error in modeling closure two-dimensionally is of the order of 10% assumes that closure results for a filled room can be scaled from empty room results with regard to closure distance (but not to closure time).

While many factors influence closure on an individual basis, such as the presence of brine or gas, the assumption is made that no synergism is present that would prevent a situation involving combined effects from being abstracted to two dimensions. Therefore, a two-dimensional representation is considered adequate unless substantial gas is produced or brine inflow is excessive immediately after decommissioning.

3.1.2 Effect of Scale on Two-Dimensional Closure Calculations

Two-dimensional closure calculations can be for a single room, a single panel, or the entire repository. The state of development of numerical techniques for early closure predictions limited calculations to two types of configurations, an isolated single room or one of the rooms in an infinite array of rooms (Butcher and Mendenhall, 1993, Sections 4.3 and 4.4, pp. 4-3 to 4-8). Cross sections at the midpoint of rooms perpendicular to their lengths were examined. These two configurations bracket the two extremes of possible responses for two-dimensional response of rooms in a panel (Stone and Argüello, 1993). The array room configuration was generally preferred, because it was considered more representative of the majority of rooms in a panel. It is the basis for the data used in the CCA. The lateral boundaries for an isolated room calculation must be placed a long way away from the room, increasing the number of elements that must be considered.

Almost all calculations at present are performed on an array room configuration. The reason for this approximation is that computer resources are insufficient at this time to permit routine panel-type predictions, and even if the resources were available, it is not clear that the increased detail of the predictions would provide that much additional information.

To illustrate the sensitivity of closure to configuration, an example has shown that after 150 years of closure, results for an empty array room differ from the average results for a single panel by a factor of 0.87 (Stone and Argüello, 1993, Figure 6, p. A-130). That is, closure of an array room is faster than the average closure of a panel by 13%. This discrepancy is considered to persist for a relatively short time. The panel calculation was based on a symmetry plane along the length of the panel. The panel consisted of seven rooms, labeled one through seven starting from the farthest end. Two access ways located down the center of the repository were also included, using the centerline of the mine as a second plane of symmetry. In this configuration, room one at the end of the panel model was closest in nature to an isolated room, and room four in the middle of the panel model had approximately the same symmetry as a single array room.

Closure of different empty rooms was referenced in the panel calculation to closure of room four, typical of a single array room, with all other rooms closing slower (Stone and Argüello, 1993, Figures 7 and 8, p. A-131). At 150 years, the average closure of all of the rooms in the panel was 0.91 of the closure of room four, and room four was on the order of 0.96 of the closure of a single array room (Stone and Argüello, 1993, Figure 13, p. A-134). The significance of the 150 years is that this is the time it takes for the ceiling in room four to touch the floor, and the ceiling in all other rooms touch the floor shortly afterward. The reader is reminded, however, that these are empty rooms. For comparison, as mentioned in Section 3.1.1, (G-1), a room filled with waste and backfill, with no gas present, and a final porosity of about 0.2 would have approximately 2 m vertical closure. Two meters correspond to the distance that room four in the panel would close in about 40 years.

In any case, we would expect that the factor 0.87 (0.96×0.91) represents approximately the greatest difference to be expected between panel results and single array room results, with this difference eventually vanishing with time, because all regions in the repository will eventually close to nearly the same final states. This hypothesis is based on the assumption that filled room closure results scale as empty room closure results with regard to closure distance (but not to closure time). Thus, the uncertainty introduced by failing to apply this correction to array room closure to make it representative of panels is at present not considered critical. The exception to this conclusion would be if substantial gas is produced, or brine inflow is important soon after decommissioning (0 to 100 years). Under such circumstances, the compaction of the waste would be reduced, changing the available gas storage volume. Little evidence currently exists to support this hypothesis, and enough information probably exists to correct for it, if necessary. Additional calculations to evaluate closure on a panel scale have not been performed.

For repository-scale calculations, two-dimensional representations of the entire repository, which require smearing of repository features into a cylindrical (axisymmetrical) configuration, with its axis vertical to the plane of the repository, are sometimes used. While this configuration may be necessary for estimates of the distances of crack propagation in interbeds and related more global problems, the assumptions used in constructing equivalent axisymmetric waste regions and other aspects of the repository obscure the mechanics of closure sufficiently to make this type of analysis of questionable value in examination of the details.

3.1.3 Effect of Stratigraphy

3.1.3.1 DESCRIPTION

The WIPP is described as located in the massive Salado Formation of marine bedded salts. Vertically, at room scale, the formation is not homogeneous halite, but rather halites interspersed with thin interbeds, clay seams, and other geological structures (December 1992 preliminary performance assessment, Sandia WIPP Project, 1992, Figure 2.2-3, p. 2-7). Stratigraphic layers are modeled as separate layers of materials, and clay seams and partings have been modeled as friction slide lines, which are surfaces in the configuration along which slip can occur according to a Coulomb friction law (Stone et al., 1981). The dip of the repository is not considered important in regard to closure. This section addresses the question of whether any of this structure influences repository closure.

3.1.3.2 DISCUSSION

Methods for modeling various components of the stratigraphy have been available for some time. In many cases, however, the results of the calculations were not reconciled with *in situ* closure measurements, even when large arbitrary changes in material property values were considered (Morgan, 1993a, pp. A-92 to A-94). The analyses were found to be in much better agreement with *in situ* test closure results when (1) the formation was entirely halite (all-salt stratigraphy) (Morgan, 1993b, pp. A-67 to A-69) and (2) strains computed from the reference creep law were adjusted by a factor of E/12.5, where E is Young's modulus (Morgan, 1993b, pp. A-92 to A-94). These assumptions were made for many past analyses.

To improve upon early representations of the stratigraphy, a new stratigraphy description was defined coincident with development of the M-D Creep Model (Munson et al., 1989a,b). This stratigraphy description will be referred to as the M-D stratigraphy. Whereas the reference creep law assumes steady-state conditions, transient creep response is an important part of the M-D model (see Section 3.2.1 [C-1]). This and other improvements are observed to cause accelerated closure during the initial part of the repository response. For some analyses, however, the disposal room calculations are primarily focused on the long-term state of the repository, in which case the small increments of strain introduced by the transient portion of the model represent an increasingly smaller part of the total strain as the total creep strain increases. Calculated histories using the combined M-D descriptions (creep law + stratigraphy) were shown to be in agreement with extensive *in situ* closure data, and therefore it is considered the baseline model for the response of the formation surrounding the repository.

Under very conservative assumptions, gas pressurization of the repository can approach lithostatic pressure, raising the possibility that existing fractures, or fracture initiation and propagation within the interbeds, partings, and clay seams, will open to provide storage volume for the excess gas. The assumption is made that the presence of these fractures, even when open, does not greatly alter the mechanics of repository closure, and they are not modeled explicitly as part of the stratigraphy. The basis for this assumption is that fracture opening occurs only when the pore pressure exceeds lithostatic pressure, and that room closure is almost complete in several hundred years before fractures begin to develop. If the pressure drops, they will close first before closure resumes. More information on this subject is available in Section 3.2.5. It is emphasized that the fracture insensitivity conclusion applies only to mechanical closure. Fracturing in the interbeds is expected to strongly influence the distance of

gas migration away from the interbeds.

In summary, most calculations in the past, including those for the December 1992 preliminary performance assessment, were performed assuming all-salt stratigraphy and the reference creep law with the E/12.5 approximation. However, a simplification of M-D stratigraphy as discussed in Stone (1997) will be used in conjunction with the M-D creep law for the CCA calculations.

3.1.4 The Disturbed Rock Zone

Changes in the mechanical and flow characteristics of rock surrounding an excavation are observed. For WIPP these changes occur in the halite and interbed regions immediately adjacent to the rooms and access ways, in the zone called the disturbed rock zone (DRZ). The DRZ is expected to have slightly different mechanical properties than either the halite or backfill, although these are at present undefined.

While porosity and fractures within the DRZ will influence fluid flow and may provide gas storage volume, the present assessment is that the DRZ does not play an important role in controlling the compacted states of the waste and backfill. The issue is how soon how much of its enhanced porosity is squeezed out by closure, and whether fractures can be held open, or reopen by gas pressurization. These details of the DRZ storage volume are best addressed in the fluid flow part of performance analyses.

The reason the changing state of the DRZ is not expected to influence compaction is that most of its porosity is likely to be eliminated by closure by the time any substantial gas pressurization of the repository occurs, i.e., the DRZ porosity is assumed to decrease rapidly, because of backstress exerted by the waste. For example, crushed-salt backfill, which has much greater porosity than the DRZ, is predicted to undergo extensive consolidation from an initial porosity of 30 to 40%, to 5% porosity in 15 to 30 years (Butcher and Mendenhall, 1993, Figure 5-2, p. 5-6). Further justification for not including it in the Disposal Room Model is that the DRZ porosity is largely fracture porosity, which is likely to be eliminated more easily than void porosity in the backfill and the void volume of the DRZ is small in comparison to the void volume of the waste. Any brine in the DRZ fractures is expected to drain or be forced into the waste by closure. Thus, while very little is known about the DRZ, its effect on the mechanical response of the repository is expected to be of secondary importance.

3.1.5 Gravity Effects

Gravity effects in closure calculations are expressed primarily in the variation of the vertical component of the *in situ* stress state with depth from the earth's surface. Because of creep in the halite, horizontal stress components are assumed to be identical and equal to the vertical stress.

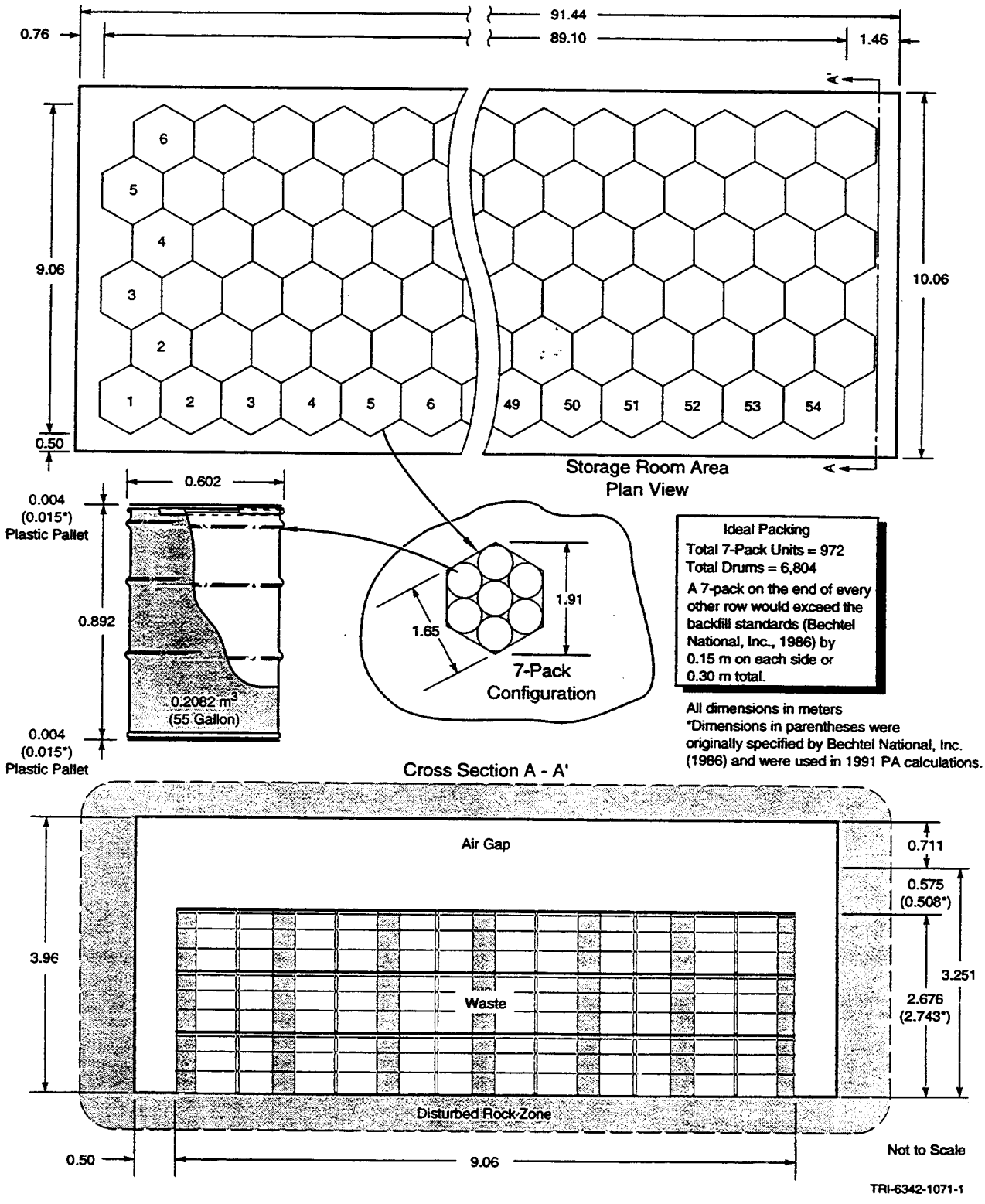


Figure 5. Ideal packing of drums in rooms and 10-m-wide drifts (not to scale). (From Sandia WIPP Project, 1992, Figure 2.1-4, p. 3.5.)

Specification of the initial stress field for the entire geometrical configuration assumed for disposal room analyses is required. Sometimes the vertical variation of the *in situ* stress from top to bottom of the finite element mesh has been specified. Other times, the *in situ* stress has been assigned a constant value throughout the mesh configuration representative of the lithostatic stress at the repository horizon. Assumption of a uniform stress state is a degenerate case of the geostatic case in which vertical stress variation caused by gravitational body forces is neglected, and thus constitutes simplification of the analyses. The assumption has been justified by demonstrating that closure predictions based on an initial uniform state of *in situ* stress are in essential agreement with calculations that include body forces. Thus, this approximation is widely used for closure analyses that are uncoupled from fluid flow, and was used for the December 1992 preliminary performance assessment. In contrast, gravitational effects must be included in calculations involving two-phase fluid flow, because of the density differences between gases and liquids.

3.1.6 Half-Room vs. Quarter-Room Symmetry

A quarter-room rather than a half-room representation of a disposal room can be used to save computer time if gravitational and stratigraphy effects can be demonstrated to be unimportant in regard to the mechanical response to the halite. Half-room symmetry refers to the fact that since the vertical centerline of the disposal room cross-section is coincident with a vertical plane of symmetry, only one-half of the room need be included in calculations, thus reducing the number of elements that have to be considered. Quarter-room symmetry refers to the assumption that the top half of the room is modeled as a mirror image of the bottom half of the room in computing closure. In quarter-room symmetry, a second horizontal plane of symmetry is introduced at midheight, so that elements for only a quarter of the room cross- section need be considered.

The use of the quarter-room representation began when central processing unit (CPU) times for solution of closure problems were excessive, and closure data from it was used for the December 1992 preliminary performance assessment modeling of a full panel. By increasing the symmetry of the problem, fewer elements were required and solution time shortened. Inherent in the use of this model are the assumptions that gravitational forces do not greatly affect the material response near the room, that the surroundings can be represented as all salt, and assumptions regarding the air gap located between the backfill and the roof of the room. Quarter-room symmetry assumes that the air gap and any backfill are divided equally both above and below the waste. The magnitude of the error introduced by this approximation is always suspect, however, even though past calculations suggest that it is small.

Because the half-room model is a better representation of the disposal room, particularly with regard to the gap between the roof of the room and the waste, its use has been adopted even though calculations may require a little more computer CPU time. Additional information about closure surface configurations can be found in Butcher and Mendenhall (1993).

3.1.7 Disposal Room Computational Configurations

The configuration of a disposal room for the CCA is waste with an air gap between the roof and the top of the waste. The values of the parameters for the CCA calculations are given in Butcher (1997).

The normal disposal room configuration consists of waste in drums stacked in units of seven, three drums high, in waste storage (disposal) rooms 4 m (13 ft) high, 10 m (33 ft) wide, and 91.4 m (300 ft) long, as shown in Figure 5 (Sandia WIPP Project, 1992, Figure 3.1-4, p. 3-5). Current plans for waste emplacement in the repository include thin plastic slipsheets separating the layers of drums stacked in a disposal room (Sandia WIPP Project, 1992, Figure 3.1-4, p. 3-11). These slipsheets, and the drum casings, are similar to materials already present in the waste and are treated as part of the waste mass, rather than being explicitly represented in the model. For computational purposes, the absolute maximum (perfect) packing of 6804 drums within the room is selected (Sandia WIPP Project, 1992, Figure 3.1-4, p. 3-11), even though it is unlikely in practice that so many drums can actually be emplaced within the room. This assumption constitutes a worst case in terms of waste concentration. Misalignment of seven-pack units relative to each other and other emplacement problems are likely to make the packing less dense. Computational methods are also insufficient to resolve effects introduced by emplacement of different types of waste in different regions of the room. Hence the waste is assumed to be a homogeneous mixture throughout the repository.

The waste properties depend on the waste inventory. The transuranic waste form is a combination of metals, sorbents, cellulose, rubber and plastics, and sludges. The waste is modeled as an average mixture of these components, which changes in properties as the respective amounts of each component change in the inventory projections. The waste inventory assumptions for the CCA closure calculations were taken from the February 1995 revision of the baseline inventory report (Baseline Inventory Report, 1995). The property values and their origins used for constructing and averaging the compaction curve for the waste are given in Tables 5 and 6 of Butcher (1997). The initial average waste density is 559.5 kg/m^3, and the average solid density of the waste is 1757 kg/m^3, which corresponds to an initial average waste porosity of 0.681. The volume of solids in a single disposal room is 551.2 m^3, and the initial average porosity of the undeformed disposal room (waste + void volume = 3644 m^3) is 0.849.

The storage volume configuration assumed for the waste differs from past calculations because there is no backfill: the space between the drums is empty. Since modeling the extreme detail of the 7-pack packing and the space between drums for the entire room was beyond the capability of the numerical technique, an assumption about the waste configuration was required in order to have an accurate continuum representing the waste response. The void space between the drums was eliminated by assuming that each waste drum deformed laterally from a cylindrical cross-section to a close-packed configuration with its neighbors during the early phases of closure.

The justification for this assumption was that little force is required to laterally deform a drum. As the distance between the walls decreased, the drums were assumed to be pushed together at very low stress levels, eliminating space between them. These stress levels were considered to have negligible effect on later consolidation of the waste. The consequence of this assumption is that elimination of any resistance of the waste to lateral closure until all the space is eliminated would imply a greater than expected rate of closure at early times. Thus, this assumption leads to a conservative performance assessment because it implies a faster buildup of gas pressure, which is the driver for releases.

Based on the no lateral resistance assumption, the waste was specified to occupy a modified continuum width of 7.35 m and length of 87.85 m, as defined by Equation 2 in Stone (1997). The height of the waste during this lateral consolidation was assumed to remain unchanged.

3.2 Constitutive Relationships

Mathematical mechanical response models and properties for each material present in the repository and its surroundings must be defined once the geometrical configuration for the closure calculation is established. The following material models, or constitutive relations, are available.

- Halite creep laws
- Waste compaction models
- Backfill consolidation
- Gas generation
- Fractures

The discussion of salt and salt/bentonite backfill is included in this section because of the consideration of these materials in past closure analyses, even though no backfill is at present planned for the CCA baseline design. The assumptions of these models and how they are used in closure analyses will be described in the following sections.

3.2.1 Halite Creep Laws

Halite (salt) has the unique characteristic of being able to deform with time under low shear stresses. This mechanical property causes mined cavities or voids in bedded or domal salt formation to decrease in volume (close) with time. Once waste is emplaced in the repository, the salt is observed in calculations to rapidly consolidate around it, reduce any void volume that could eventually fill with brine, and eventually surround the waste with a tight, impermeable barrier. For evaluation of repository performance, a mathematical model of salt creep is used to predict the length of time required to achieve various degrees of closure.

3.2.1.1 REFERENCE CREEP LAW

Historically, two mathematical laws have been used to describe creep of halite. The reference creep law proposed by Krieg (1984) was based on a comprehensive examination of all data relevant to WIPP salt prior to 1984, and was used extensively for disposal room calculations until 1993. An elastic/secondary steady-state creep relationship was defined. The second law, the M-D description (Munson et al., 1989a,b), has been used since then, because it more accurately represents the early part of closure. The rationale for limiting the description to secondary, steady-state creep, rather than including a primary or transient creep function, was that long enough periods of time were under consideration to render transient effects of lesser importance. This conclusion was based on the expectation that any transition to steady state would occur quickly and transient strain would be limited in magnitude. The assumption was made that the preponderance of the deformation would be from steady-state creep. Therefore, total strains several hundreds of years after decommissioning and later, predicted from steady-state creep rates, would be only slightly in error.

A reference stratigraphy for the region surrounding the disposal rooms was also recommended for use with the reference creep law, as were reference mechanical properties for dominant nonhalite features such as anhydrite and polyhalite marker beds and clay seams (Krieg, 1984). This information was used for calculations addressing comparisons with early closure data from the first underground experimental tests initiated at the WIPP. However, comparison of closure estimates with early closure data almost immediately indicated that mined openings in the WIPP were closing approximately three times faster than was predicted with the reference creep law (Morgan, 1993b, pp. A-92 to A-94, and conclusions). As a consequence, simple fixes to the reference creep law were instituted. Major changes involved dividing the Young's modulus value of the reference creep law by a factor of 12.5, and greatly simplifying the stratigraphy of the Disposal Room Model, eventually changing it to a uniform formation of 100% halite (Morgan, 1993b, pp. A-92 to A-94, and conclusions). The stratigraphy simplification was possible because closure results assuming inelastic response for the anhydrite and polyhalite parts of the stratigraphy did not differ greatly from the all-halite results. While a mechanistic justification for reduction of the moduli was not apparent at that time, some justification for simplifying the stratigraphy existed because of major uncertainty in modeling stratigraphic features. A major problem was representation of displacements or slip along clay seams. With the modulus and stratigraphy changes, closure estimates using the modified reference creep law and stratigraphy were found to be in better agreement with closure data (Morgan, 1993b, Figure 6, pp. A80, A81).

3.2.1.2 MULTIMECHANISM DEFORMATION (M-D) MODEL

After examination of a number of possible explanations for the inadequacy of the original reference creep law, a second model for the creep of salt was provided by Munson (Munson et al., 1989a,b). This model differs from the original reference creep law and stratigraphy recommendations in several ways. First, Munson proposed a different flow rate for the way in which one- and two-dimensional stress states are generalized to three-dimensional stress states. Second, based on further study, Munson constructed a different stratigraphy for the rock surrounding the repository, and proposed a different value for the coefficient of friction controlling slippage along clay seams. A third contribution was to include a description of primary (transient) creep in the constitutive model to represent initial deformations during and immediately after underground mining activities. The reader is referred to additional discussion of Munson’s model in Munson (1992, pp. A-115, A-116). Currently accepted material

parameter values are given in Table 3 of Butcher (1997). Closure estimates with it have been shown to be in agreement with a much larger and more recent gathering of closure data.

3.2.2 Waste Compaction Models

Halite in the roof contacts the waste and backfill as a room closes, and applies a load to the waste and backfill (if present). Initially, the waste and the backfill cannot support such a load, and the two begin to consolidate. Waste compaction models describe how much load must be exerted by the surrounding rock to consolidate the waste to a given porosity or density.

Two representations of the waste have been investigated in the past. The first, the volumetric plasticity model, was used in many of the early SANCHO calculations (Weatherby et al., 1991), and remains the recommended compaction description. A second representation, the Nonlinear Elastic Waste Model, was used in early calculations by RE/SPEC, but had certain physical consistency limitations, which made its use questionable.

The volumetric plasticity (crushable foam) model (Weatherby et al., 1991) is a yield surface in principal stress space, which is a surface of revolution with its axis centered about the hydrostat and the open end pointing into the compression direction. The open end is capped with a plane that is at right angles to the hydrostat. The deviatoric part is elastic-perfectly plastic so the surface of revolution is stationary in stress space. The volumetric part has variable strain hardening so the end plane moves outward during volumetric yielding. Volumetric hardening is defined by a set of pressure-volumetric strain relations derived from the experimental compaction data. Because the model does not specifically include time, a correction was applied to the data for time-dependent deformation (creep), especially for the plastics in the waste (Butcher et al., 1991b). The model also imposed the flow rule that the deviatoric strains produce no volume change (associated flow).

I think it is actually non-associated flow when the stress state is on the surface of revolution. The yield surface can depend on pressure, but the flow potential does not.

The experimental data used for the volumetric plasticity model and their interpretation are in the form of axial stress vs. density curves and are summarized in Butcher et al. (1991b) and Luker et al. (1991). The steps involved in deriving repository-averaged compaction data from the experimental results are shown in Figure 6, the WIPP Waste Compaction Model, and the results reproduced in Table 1 are for an assumed waste inventory of 122 kg/m^3 metals waste, 40 kg/m^3 sorbents such as vermiculite, 170 kg/m^3 cellulose, 84 kg/m^3 rubber and plastics, and 143.5 kg/m^3 sludges (Baseline Inventory Report, 1995). These results were used in the final disposal room waste compaction calculations for the CCA (Figure 7).

The derived average compaction curve data for the waste are limited to only one direction of loading (axial stress versus porosity). Thus, certain assumptions about the magnitude of lateral stresses acting on the waste during compaction were required in order to construct a three-dimensional volumetric plasticity description from this information. The extremes of possible response are that if no lateral stress acts on the waste, then the mean stress is one third of the axial stress,$\sigma_m = \sigma_a/3$; or if the lateral stress is equal to the axial stress, then the mean stress is equal to the axial stress, $\sigma_m = \sigma_a$ (Butcher et al., 1991b, p. 72). Calculations made

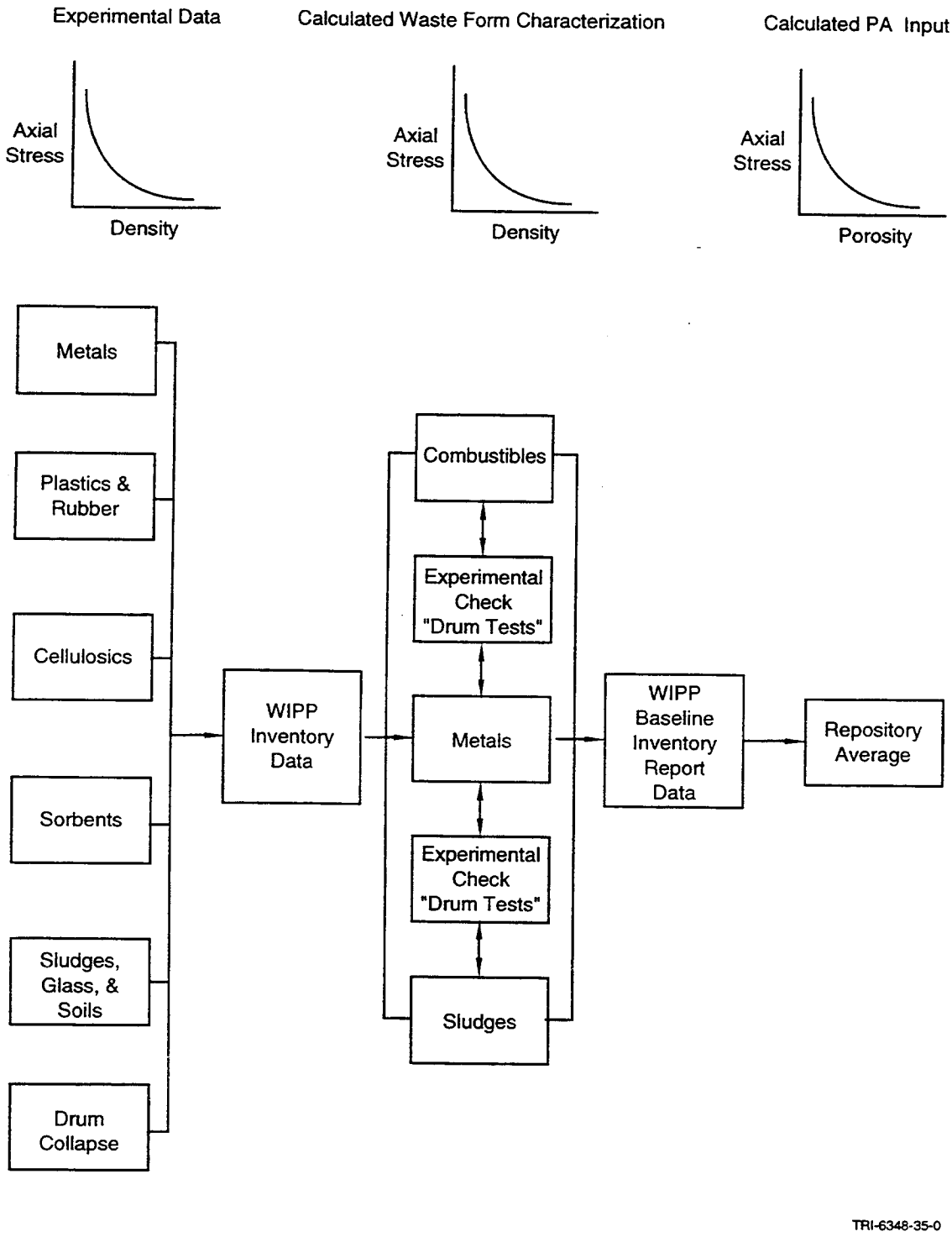


Figure 6. WIPP waste compaction model.

No, Figure 4 in Callahan (1993) reports 0.18 room porosity and 0.36 waste porosity at t=200 years when sigma_m = sigma_a.

with the $\sigma_m = \sigma_a$ assumption predict consolidation to unrealistically high porosity (on the order of 0.6) when no gas is present compared with calculations made with the $\sigma_m = \sigma_a/3$ assumption (Callahan, 1993, Figure 4, p. A-30).

Experimental tests do not easily resolve the question of which assumption should be used. The full-scale drum compaction tests, performed to determine the compaction characteristics of the waste, provided records of the axial load required to compact the waste as a function of drum height (Butcher et al., 1991b, p. 49). Thus, the average stress acting on the waste in only one direction was measured. This is only part of the information required to develop a compaction model; that is, the stresses acting on the waste in all three orthogonal directions must be specified in a mathematical model of compaction for computer code calculations (Butcher et al., 1991b, p. 72).

The reason stresses in all three directions were not measured in the tests was that the waste was contained in drums and was heterogeneous, with the consequence that there was no good way of measuring these stresses. Furthermore, the uncertainty introduced by not measuring these stresses was not considered large enough to justify the immense effort that would be required to develop such measurement techniques. Indirect guidance with regard to which of the relationships between axial stress and lateral stress is more representative of mechanical response during waste compaction is provided by the compaction test results, which showed that there were no large increases in drum diameter during compaction of either metallic or combustible waste (Butcher et al., 1991b, p. 52). Instead, the waste appeared to compact one-dimensionally, without obvious bulging of the drums or lateral expansion to rupture. These observations suggest that the steel containers were strong enough to prevent any lateral waste expansion, at least during the early parts of the tests. In contrast, drums of sludge did bulge (Butcher et al., 1991b, p. 52), but the volumetric portion of sludges in the waste was considered small enough to ignore in making the zero lateral stress assumption. The dominant conceptual model assumption was, therefore, that most of the waste is compacted in essentially a one-dimensional mode, without much lateral expansion, which is best represented by the $\sigma_m = \sigma_a/3$ assumption.

Current estimates of compaction are for as-received waste, with no correction for decomposition or corrosion with time. Some reviewers suggest that the final state of compaction of the waste should be considerably greater, i.e., its final porosity would be considerably less for the fully degraded state, and therefore the assumption of the unreacted properties is misleading. Implicit in their assumption is that the waste first compacts and then degrades.

They propose that during degradation, the biodegradable waste will simply vanish, with additional closure eliminating the space that is occupied. This would not alter the average porosity greatly, because it is dominated by the metal waste. For corrosion, however, the volume of the unreacted iron would eventually become insufficient to accommodate the volume of the solid corrosion products, with the consequence that the extra volume would be created at the expense of a reduction in the available void volume. This process would represent a decrease in average porosity of the waste. An alternative conceptual model is that the waste degrades before it attains the fully compacted state. This model is considered more representative of waste response.

Table 1. Simulated TRU Waste Compaction Data

Axial Stress (MPa)	Porosity	Axial Stress (MPa)	Porosity
0.000	0.681	11.663	0.240
1.600	0.680	11.868	0.235
1.818	0.659	12.077	0.231
2.013	0.641	12.301	0.227
2.233	0.622	12.508	0.223
2.460	0.604	12.727	0.219
2.671	0.588	12.941	0.215
2.886	0.572	13.163	0.211
3.109	0.556	13.369	0.207
3.310	0.543	13.584	0.203
3.518	0.530	13.804	0.200
3.739	0.516	14.800	0.183
3.950	0.504		
4.158	0.492		
4.383	0.480		
4.591	0.469		
4.802	0.459		
5.028	0.447		
5.239	0.438		
5.459	0.428		
5.662	0.419		
5.883	0.410		
6.092	0.401		
6.309	0.392		
6.530	0.384		
6.734	0.376		
6.945	0.368		
7.160	0.361		
7.378	0.353		
7.596	0.346		
7.817	0.339		
8.022	0.332		
8.235	0.326		
8.453	0.319		
8.659	0.313		
8.872	0.307		
9.094	0.301		
9.302	0.295		
9.524	0.290		
9.730	0.284		
9.951	0.279		
10.155	0.274		
10.367	0.269		
10.590	0.263		
10.805	0.258		
11.011	0.254		
11.231	0.249		
11.449	0.144		

Source: Butcher et al., 1991b.

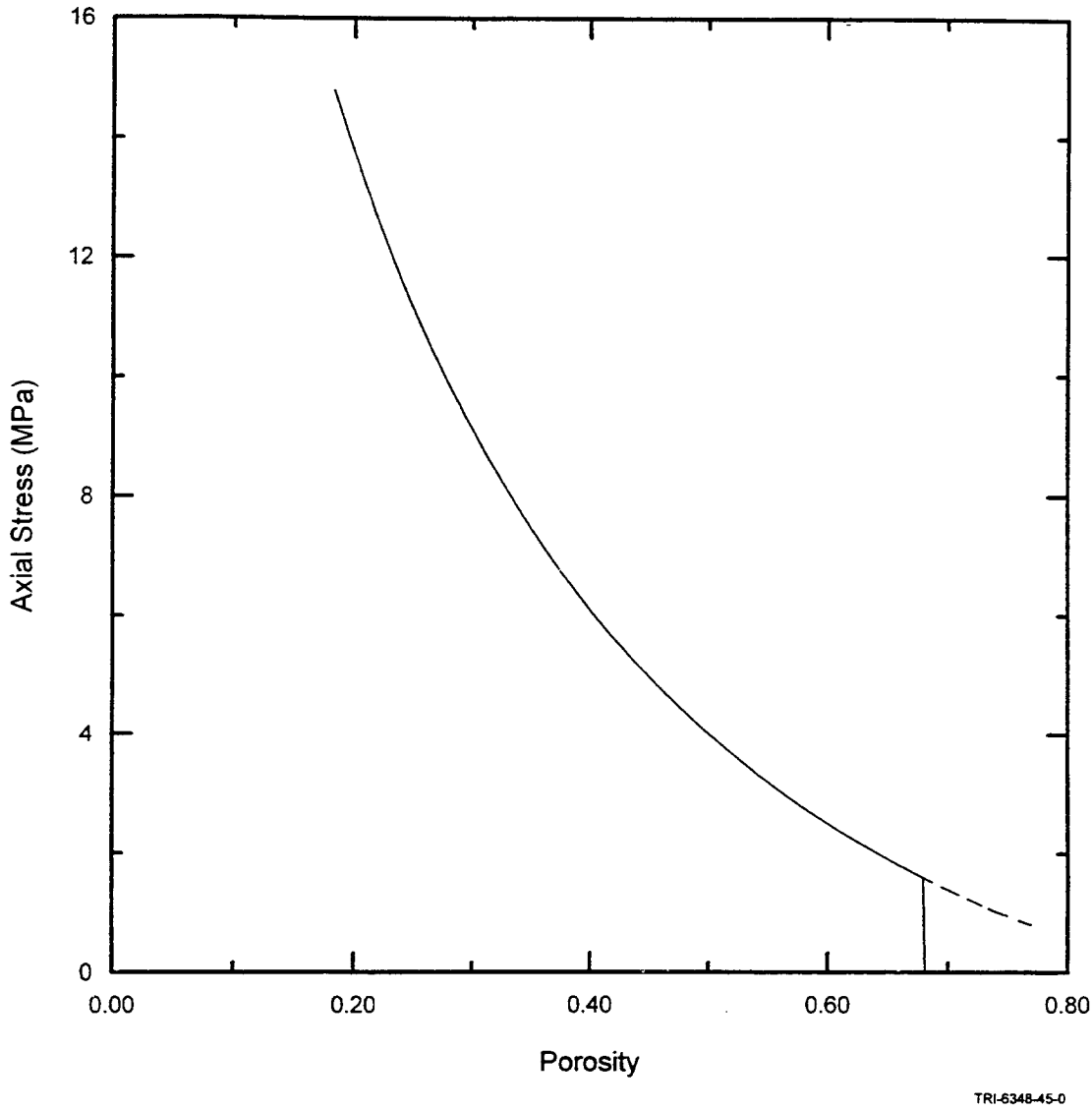


Figure 7. Final disposal room waste compaction curve for the CCA.

Quantitative estimates of degraded waste response have been limited to the currently accepted conceptual model (degradation during compaction), because it is not clear that the corrosion products would fully intrude into the void space if corrosion occurred in a confined volume. These estimates suggest that the porosity of the corroded and biodegraded waste would be comparable to that of the unreacted waste, even though the cellulosics have been totally consumed. These estimates are based on the assumption that the residual solid corrosion products will behave as a well-graded granular material. Data on the compaction characteristics of such materials were obtained from tests on well-graded granular magnetite, representing Fe_3O_4, and well-graded limonite material (Luker et al., 1991). Limonite, a hydrous ferric oxide of variable composition, is a major ore of iron. It was chosen because it was readily available as sample material and represents compounds more closely resembling hydroxides. The reason the calculated porosities were comparable to the estimates for unreacted waste was attributed to the fact that the theoretical solid densities of the corrosion products are much less than the solid density of iron, and the mixtures investigated in the experimental program did not compact easily. For example, magnetite, with a grain density of 5180 kg/m^3, compacted to a density of about 3100 kg/m^3; and limonite, with a grain density of 2700 kg/m^3 (average value), compacted to about 1400 kg/m^3 at lithostatic stress (Luker et al., 1991, p. 700). The conclusion from this comparison was that the difference between reacted and unreacted compaction states at lithostatic pressure was too small to attempt to compensate for them in closure calculations. Also noted in this comparison was the fact that only about 37% by weight of the waste is subject to chemical or biological change, an observation that reduces the effects of waste degradation on the average waste response.

A decision about which model or combination of assumptions is more representative of the eventual state of the waste is therefore also considered of secondary importance because none of the models are considered to have much effect on the waste permeability (see Section 3.3.2.1), and the waste gas storage volume remains a small portion of the potential maximum gas storage volume. However, for cuttings release, the first conceptual model of compaction followed by degradation would probably produce a denser, higher-strength final waste form, less prone to spallation and erosion phenomena.

The Nonlinear Elastic Waste Model for waste compaction arose from early work by RE/SPEC. The assumption was made for this model that waste responded in a nonlinear elastic manner by assuming that the three individual waste types involving metals, combustibles, and sludges are analogous to three nonlinear springs in series. An inconsistency occurs, however, when the model is applied to the condition of plane strain. In order to maintain the condition of zero total out-of-plane strain for the large strains that might be encountered during compaction, the computed out-of-plane stress can become unrealistically large, and of different sign (compressive) than the stress predicted using the volume plasticity model (Labreche et al., 1995). The model will not work, therefore, without an arbitrary and physically unreasonable fix, whereas the volume plasticity model works very well.

3.2.3 Backfill Consolidation

Although extensive theoretical and experimental studies of the time-dependent consolidation of salt backfill have been performed in the past to determine its advantages, no plans at present exist for backfilling the waste regions of the WIPP. Nevertheless, a salt backfill consolidation model is available in the Disposal Room Model if it is necessary to model backfill as

a design alternative in the future. The reader is cautioned, however, that because a backfill model was not required for the CCA, the best available values for its parameters have not been subjected to a full quality assurance review, a step that would be necessary before the model could be included in a formal performance assessment.

Assuming a repository is backfilled with crushed salt, halite in the roof contacts the backfill during closure, and the backfill consolidates. However, unlike the waste, which has a unique porosity value associated with each applied stress, crushed-salt-based backfill will continue to creep consolidate with time, even if under constant stress. Backfill consolidation models describe creep consolidation as a function of applied stress and time.

Backfill descriptions for both pure-crushed-salt backfill and salt/bentonite backfill are based on the Sjaardema and Krieg (1987) creep consolidation model. The crushed-salt part of the model was used for the December 1992 preliminary performance assessment. The Sjaardema and Krieg model describes the volumetric response of the backfill in terms of the rate of change of backfill density as a function of the hydrostatic or mean pressure and current density as a function of time. Definition of the effect of shear stresses on backfill deformation is also required to generalize the model for numerical analyses because constitutive equations for numerical calculations include deviatoric stress and strain components related to shear. Shear components under most circumstances are assumed not to produce any change in volume. In the Sjaardema and Krieg model, the volumetric part of consolidation captures almost all of the consolidation response, because the backfill undergoes large changes in density.

Two different ways of representing the effect of the deviatoric stresses are available (Callahan and DeVries, 1991, p. 13; Sjaardema and Krieg, 1987, p. 30). Since no experimental data exist to discriminate among models, the choice of model for a specific calculation depends on the numerical code used for the calculation. The lack of specificity is not considered critical, however, because the deviatoric strains are typically very small relative to the volumetric strains. To justify this assumption, backfill consolidation predictions using both deviatoric stress descriptions have been compared and found to be similar. The method used by Sjaardema and Krieg has been adopted as the recommended model.

Consolidation of pure crushed-salt backfill is observed to occur rapidly, with porosities decreasing to less than 10% within 40 years (Butcher et al., 1991a, Figure 4-4, p. 28). Salt/bentonite backfill is predicted to consolidate to states with low permeability within a comparable period (Butcher et al., 1991a, Figure 4-5, p. 29). This observation implies that long-term room closure is dominated by the waste consolidation process; i.e., since the time scale for backfill consolidation is much shorter than the time scale for waste consolidation, the exact time at which the backfill reaches an acceptable level of consolidation is less important and exact resolution of which deviatoric stress model best represents the backfill is unnecessary.

The creep consolidation model, in its simplest form, is given by Sjaardema and Krieg (1987; Equation 2.1.2, p. 11 and Equation 3.3.2, p. 25):

Install Equation Editor and double-click here to view equation.

(3)

where ρ is the backfill density at time t, dr/dt is the rate of change of the backfill density with

respect to time, ρ_0 is the initial backfill density, K is the bulk modulus, P is the pressure (positive in compression), dP/dt is the rate of change in pressure (mean stress) over time, and B_0, B_1, and A_b are constants with the currently accepted values given in Table 2 (Labreche et al., 1995, Table 3-11). Parameter values are for information only because the report has not been formally reviewed according to WIPP quality assurance procedures. Therefore values from the report cannot be used for performance assessment without further quality assurance qualification.

The values of these parameters were derived from Holcomb and Shields (1987). The value for B_0 in Table 2 reflects a recent change that requires reevaluation of its range.

An assumption in deriving values for the creep parameters is that sufficient moisture exists in the salt (greater than 0.5%) (Butcher et al., 1991a, p. 42) to cause it to consolidate as a "wet salt," as opposed to a salt containing no moisture. Moisture content is a design parameter that can be controlled during emplacement to ensure that this criterion is met. The general ability of the mathematical representation used by Sjaardema to physically represent salt consolidation is also supported by creep tests of salt/bentonite backfill, which shows a similar response.

An additional feature of the model is a variation of the elastic moduli with density. The bulk modulus and shear modulus is given by Sjaardema and Krieg (1987, Equations A1 and A2, p. 59):

Install Equation Editor and double-click here to view equation. (4)

and

Install Equation Editor and double-click here to view equation. (5)

where K_0, K_1, G_0, and G_1 are constants. Currently accepted values for the bulk modulus equation are also given in Table 2, and were derived from Holcomb and Hannum (1982) and Holcomb and Shields (1987). Embedded in the derivation of these ranges and distribution is the assumption that the solid density of rock salt ranges from 2098 to 2160 kg/m^2, with a median value of 2140 kg/m^2. The shear modulus relationship is required for the deviatoric (shear) stress part of the model, and is assumed to have the same stress dependence as K. The value of G_0 was 12.4 GPa (Krieg, 1984). The elastic constants are not considered to sensitively influence backfill consolidation.

Table 2. Summary of Base Values, Ranges, and Distributions for Crushed Salt/Bentonite Backfill Mechanical Properties

Parameter (Units)	Base Value	Range	Distribution
K_0 (MPa)	0.0176	0.0103 - 0.0854	Uniform
K_1 (m^3/kg)	0.00653	0.00701 - 0.00540	Uniform
A_b (m^3/kg)	–0.0173	$\mu = -0.01739$ $\sigma = 2.21$	Normal
B_0 (kg/$m^3 \cdot s^{-1}$)	$1.3 \cdot 10^5$	$\mu[\ln(B_0)] = 15.55 - 2.659 \cdot B_1$ $Var[\ln(B_0)] = 8.61 + 3.650 \cdot B_1$	Log normal
B_1 (MPa^{-1})	0.82	0.61 - 2.35	Uniform
ρ_0 (kg/m^3)	1400	1200 - 1600	Uniform

Source: Labreche et al. (1995).

3.2.4 Gas Generation

Gas within the repository will increase in pressure during closure and exert backpressure on the surrounding rock. Sources are gas already present in the waste and repository, gas generated during biodegradation of various components of organic waste, corrosion of metals, and radiolysis. The function of this part of the Disposal Room Model is to determine the gas pressure given the amount of gas within the limits of the disposal rooms and accessways, and the extent of void volume available for storage (Brown and Weatherby, 1993, p. A-7).

The present practice for calculating gas pressures in SANTOS closure calculations is to either assume gas generation rates or use a lookup table of gas production (Brown and Weatherby, 1993, p. A-7). The exact details of gas production, such as (1) how the gas was generated, e.g., the amount of brine consumed during chemical reaction and where this brine came from; or (2) how much gas escaped from the waste, were not considered because the gas source was treated parametrically. Given a number of moles of gas within the repository as a function of time, the void volume available for gas storage at a given time is determined and used to compute the gas pressure using the ideal gas law (Brown and Weatherby, 1993, p. A-7). A porosity surface approach is required because a fully coupled analysis of closure based on detailed descriptions of salt creep, waste consolidation, brine flow in or out of the waste, gas production, and gas migration away from the waste into the interbeds is not technically feasible. As a consequence, a two-step process has been developed. This porosity surface approach begins by computing the extent of closure for various assumed gas contents with the SANTOS code. The method of coupling closure with the coupled fluid flow interactions related to gas production is to determine porosities for actual waste contents by interpolation of this data in the WIPP performance assessment code BRAGFLO (WIPP PA Department, 1993, pp. 4-18 to 4-23).

Inherent in this process is the assumption that the porosity - gas pressure values for a given amount of gas are independent of the previous gas generation history. Thus, the closure data provided by SANTOS can be thought of as representing a surface, with any gas generation history computed by BRAGFLO constrained to fall on this surface.

Since exact histories of gas generation are not known for the closure calculations, an arbitrary set of gas generation conditions must be selected. These conditions must span all gas generation potentials likely to be encountered. The reason for this requirement is to avoid any uncertainty that might occur if gas production predictions from BRAGFLO fell outside the closure data. That is, extrapolation of conditions outside the range of data is considered unacceptable. The bounds for assumed gas production for SANTOS were (1) no gas is generated or (2) all the potential gas-generating material is consumed. The gas generation rates for SANTOS were the fastest rates possible, those for waste completely immersed in brine. The consequences of any slower rates can be obtained by interpolation between curves. To preserve a link with reality, the gas generation input parameter values for SANTOS calculations were approximately the same as values used in past performance assessments. Because the gas generation histories used in SANTOS calculations are simply a device used to introduce a given amount of gas in the waste at various times, we did not need to update our assumptions to be consistent with all the changes in the nature of reaction products, generation rates, and variations in waste inventory that are required for the CCA.

For PA analyses, the amount of gas in the repository is calculated with the code BRAGFLO, converted to a gas pressure, and coupled with the closure data by interpolation on the basis of pressure (WIPP PA Department, 1993, Section 4.2.2.2 , pp. 4-11 to 4-23). To put closure calculation results in a form that can be used in PA analyses, closure states in terms of porosity as a function of moles of gas and time are converted to pressure and volume states corresponding to various gas contents. Redefinition of the porosity values is included in this transformation, because the porosity determined in the closure calculation is defined in terms of the current volume of the waste, and the porosity used in BRAGFLO is defined in terms of the initial volume of the waste (WIPP PA Department, 1993, Section 4.2.2.2, pp. 4-11 to 4-23). Calculation of a new state of the repository in BRAGFLO begins by some additional analysis of the BRAGFLO results at the end of the previous time step. Since pore pressure and gas generation rates are allowed to vary spatially in BRAGFLO, pore pressure and gas content over the waste area are first averaged, and the gas content transformed to a form that can be compared with the porosity surface data. The effect of brine occupying some or part of the pores, although not explicitly included in SANTOS, is correctly represented in BRAGFLO because of the use of average pore pressure as a variable. Given the average pressure and gas content, a new porosity for the waste area is then defined by interpolation of the porosity surface data. The new porosity is assumed to be constant and spatially invariant over the new time step. The flow solution is then iterated to obtain new gas contents, brine saturations, and pressures at the end of the new time step. The pore pressure in the waste area is determined using a nonideal gas law. When iteration is complete, new pressure and gas amounts are again averaged volumetrically to determine a new porosity for the next part of the calculations.

Questions are also frequently raised about how brine availability is coupled with the quantity of gas produced in mechanical closure calculations. Since corrosion of iron uses up brine as one of the reactants, this coupling causes the corrosion process to be self-limiting, because eventually sufficient gas pressurization may prevent additional brine from entering the repository. The same discussion about the need for exact coupling between the gas generation model

ultimately used by performance assessment and the closure data can also be evoked with regard to the coupling with brine content. Brine availability is already embedded into the closure results in the sense that a set of closure (void volume or porosity) curves are constructed from pressure histories that span all of the gas pressure histories that might be encountered within the repository. These curves span conditions from zero gas generation, which represents the case where no brine would be present in the waste, to conditions for which all of the waste is submerged in brine. Additional discussion about coupling fluid flow and closure will be presented in Section 3.4.2 of this report.

3.2.5 Fractures

As described in Section 3.1.3, gas pressurization of the repository can approach lithostatic pressure, raising the possibility that existing fractures, or fracture initiation and propagation within the interbeds, partings, and clay seams will open to provide storage volume for the excess gas. Opening of fractures by gas pressurization is considered to occur primarily within the interbeds, because they contain evidence of preexisting fracturing (Borns, 1985) and therefore have very low tensile strength. Fracturing is also assumed to be oriented horizontally, in a manner consistent with the observed fracture networks (Borns, 1985).

The assumption is currently made in closure analyses that suitable estimates of closure are possible without specific consideration of fracture models. Fracture openings are expected to act as gas pressure-limiting devices: once the gas pressure within the repository becomes approximately equal to lithostatic pressure, pressurization ceases and any additional gas causes flow out through the interbeds. Fracture opening in this context refers to unlimited opening of the fractures by mechanical means, as for example is produced by hydraulic pressurization of formations to stimulate gas and oil recovery. The gas pressure required to open fractures in this manner, the critical fracture pressure, is in most cases very close to lithostatic pressure.

Since fracture in the interbeds is assumed to have little effect on closure, except for its pressure-limiting effects, inclusion of a detailed fracture model in the Disposal Room Model is not necessary at this time. Instead, an accurate representation of closure is possible by (1) determining the amount of closure at the point where the critical fracture pressure is first reached, and (2) assigning that value of porosity to the waste thereafter, unless the pressure starts to decrease.

While this simplified procedure is considered a sufficient first approximation of closure, it does not circumvent the need for a detailed fracture model to determine crack dimensions and their effect on fluid flow in regard to other aspects of performance. Should representation of fracturing become necessary in the future for calculation of disposal room response, options are available for describing gas-induced fracturing. A first step would be to represent interbed gas in the gas generation model, since the rate of closure of the repository depends on the pressure of the gas contained within the waste boundaries. This is the amount of gas generated less the amount that flows away from the waste region. It is sufficient, therefore, to represent interbed gas storage in fractures as a leakage term in the gas generation model.

3.2.6 Disturbed Rock Zone

As discussed in Section 3.1.4, porosity and fracture within the DRZ will influence fluid

flow and may provide gas storage volume. DRZ porosity occurs at the expense of porosity in the room. The issue is how much of it is squeezed out by closure, and whether it can be reopened by gas pressurization. While porosity and fracture within the DRZ will influence fluid flow and other factors such as whether communication paths to anhydrite interbeds exist, these parameters are not expected to have much effect on the mechanical part of closure. No simplified model of the DRZ is at present in closure codes and implementation of such a model would be a major effort. Therefore, a present assessment is that the DRZ is not important because most of the enhanced porosity is eliminated by closure by the time any substantial gas pressurization of the repository occurs; i.e., the DRZ is assumed to close rapidly because of backstress exerted by the waste, and it is not an important part of the gas storage volume within and immediately adjacent to the waste.

3.3 Waste Flow Model

The third part of the model having to do with fluid flow parameters is not currently used in the direct determination of closure. Instead, these parameters are used in performance assessment to predict fluid flow through the repository with the BRAGFLO code, and are included in this chapter for the sake of completeness. The model components that will be addressed are:

- Flow model
- Permeability and other flow properties
- Initial brine content of the waste
- Wicking and other water migration mechanisms

Some parts of these models are computationally intensive for the repetitious calculations required for performance assessment complimentary cumulative distribution functions (CCDFs); however, in most cases they are amendable to separate studies to evaluate the effects that they might have on repository performance.

3.3.1 Flow Model

The flow model within a disposal room and within the repository as a whole predicts how fast fluids will flow in and out of the waste. The current model is based on the assumption of two-phase Darcy flow. A detailed discussion of the mathematical form of the two-phase Darcy flow model is not given in this section because it is discussed in many other references (see, for example, Freeze et al., 1995a)

Fluid flow modeling within a disposal room has two important considerations: (1) fluid distribution in the waste and backfill and flow within the room and repository, and (2) fluid flow to and from the Salado Formation. The first aspect influences the rate of fluid movement within a room, or flow from one location to another. This may affect the rate of gas generation, for example, due to the fluid transit time from one part of the room to another. Although the total amount of brine available for gas generation would not change, the rate at which it would be used up might change. The second aspect influences the fluid exchange with the surrounding Salado Formation. For example, when the repository pressure is sufficient to drive out gas from the repository, it may also drive out brine as well, altering the total amount of brine available for gas generation. The details of fluid flow within the room may control the amount of brine driven out of the room by the gas. This aspect may also come into play in evaluating flow up a human

intrusion borehole, which may be affected by room fluid flow parameters and their distribution.

The current modeling of flow within the repository is based on homogenizing room contents into the large computational volumes necessary for PA calculations. However, as mentioned above, heterogeneity of the room contents may influence gas and brine behavior in the room as well as fluid flow to and from the Salado Formation. At present only homogeneous representations of the rooms have been considered. Thus, the effect of heterogeneous contents on repository performance is unknown at present, and while it is too detailed to address in current performance assessment modeling, it can be addressed in separate studies.

3.3.2 Permeability and Other Flow Properties

The permeability of waste and backfill at a given time can influence repository performance by controlling how rapidly gas or brine can flow through the waste. These parameters will be discussed first in this section, because their magnitudes have influenced decisions about how detailed a description of flow through the waste is required for performance evaluation. The permeability of a material is assumed to be related to its porosity.

3.3.2.1 WASTE PROPERTIES

Tests on simulated unprocessed waste have shown compacted material permeabilities on the order of 10^{-12} to 10^{-16} m^2 to brine at lithostatic pressure (full compaction of the waste) (Luker et al., 1991; WIPP PA Division, 1991, p. PA 101 [Table 4]). While the lower bound value for a permeability of 10^{-16} m^2 is still much higher than that for the surrounding salt, it may be lower than fractured interbeds, open boreholes, or borehole plugs.

The value for the average permeability of the waste remains the same as for previous iterations of performance assessment. For computational ease in the 12/91 preliminary comparison with 40 CFR 191 Appendix C (WIPP PA Division, 1991, Section 3.4.7, pp. 3-130 to 3-134), the assumption was made in evaluating the permeability of an average drum that the permeabilities of each component were uniformly distributed from the minimum to maximum values for each waste form. Consequently, the distribution of local permeability (i.e., the effective permeability of a collapsed drum) was the weighted sum of uniform distributions, the weights being percent by volume of each component. The volume percents of the components were 40% combustibles, 40% metals/glass, and 20% sludge. This analysis concluded that the expected (mean) permeability of waste on the scale of a drum would be 1.7×10^{-13} m^2. For the December 1992 preliminary performance assessment, a median value of 1×10^{-13} m^2 was used and was assumed to be independent of porosity (Sandia WIPP Project, 1992, Table 3.4-1, pp. 3-56, 3-57), because inclusion of a dependence between porosity and permeability in the calculations was not considered worth the minor effect it would have on the results. It should also be noted that the permeability value used represents the lowest value considered likely (no gas generation), and is associated with the maximum possible compaction of the waste. If gas generation limits waste compaction, making the waste even more porous, then it could be even more permeable. The significance of the increase in permeability related to gas production will be discussed later in this section. A permeability value of 1.7×10^{-13} m^2 was used for the CCA.

No WIPP-specific two-phase property measurements for waste are available, nor is any

measurement program planned at this time. The past values of two-phase flow parameters used in performance assessment analyses were based on a fragmented mixture of clay, sandstone, and volcanic sand investigated by Brooks and Corey. These values are given in the Sandia WIPP Project document (1992, Table 3.4-1, pp. 3-56, 3-57), and are subject to minor changes for the CCA calculations.

The justification for not being very precise in the values and model used for fluid flow in the waste is based on the observation that performance assessment studies have shown that the permeability of a computational volume has to be at least within three orders of magnitude of the permeability of the adjacent computational volumes in series to make any contribution to the time needed for brine to flow through the configuration. Flow through the high-permeability element is for all practical purposes instantaneous. Similarly, for volumes in parallel, if the difference in permeability is greater than a factor of 1000, all flow is concentrated in the high- permeability element and for all practical purposes it occurs instantaneously relative to parallel flow through the high-permeability elements.

To place the observation about the critical flow path in context, the WIPP waste is confined between layers of very low permeability (intact halite permeability $<10^{-21}$ m^2). Therefore, the waste is much more permeable than the halite and may be expected to be the dominant path for the flow of fluids. The flow path through the repository is expected to be short compared with the external flow paths for brine migration (through seals and up shafts or boreholes, etc.). Thus, the assumption of a permeability on the order of 10^{-13} m^2 or greater is considered to be analogous to assuming that there is little restriction of flow of either gas or brine within the waste. This assumption constitutes a bound with regard to gas or brine migration. Another way of summarizing this conclusion is that the permeability description is such that in estimating brine migration away from the repository, practically no credit is given to the time it takes for brine to flow through the waste. The consequences of this position with regard to fluid flow through degraded waste into a borehole during a human intrusion may have to be examined in more detail in the future.

3.3.2.2 BACKFILL FLOW PROPERTIES

While substantial permeability data for crushed-salt backfill and salt/bentonite backfill exist (Butcher et al., 1991a), data on two-phase flow properties for these backfills do not exist. Crushed-salt backfill was the baseline backfill assumed for the December 1992 preliminary performance assessment analyses. Consolidation calculations for backfill show that consolidation of pure-crushed-salt backfill occurs rapidly, with porosities decreasing to less than 10% within 40 years, including closure of the air gap (Butcher et al., 1991a). Permeability to brine rapidly decreases to 10^{-19} m^2. Salt/bentonite backfill is predicted to consolidate to states with low permeability within a comparable period (Butcher et al., 1991a). Based on the fact that (1) the backfill consolidates rapidly to low permeability states more typical of the surrounding halite, and (2) that it represents a smaller portion of the disposal room contents than the waste, the assumption is that a detailed description of backfill permeability is probably unimportant.

3.3.3 Initial Brine Content of the Waste

The initial water content of the waste is another parameter that is not currently used in the direct determination of closure. Instead, this parameter is important for estimation of gas generation rates with the BRAGFLO code because it defines how much brine is immediately available for the corrosion reaction.

The initial free liquid content is assumed to be a combination of liquid in the waste and brine in the backfill, if backfill is present. All of the liquid is assumed to be either brine or water with no volume correction. A median value of 7% was used for the initial free water saturation of the waste and backfill in the December 1992 preliminary performance assessment (Sandia WIPP Project, 1992, Table 3.4, pp. 3-56, 3-57). In the absence of backfill, this value has since been revised to a mean of 0.06%, with a minimum of 0 and a maximum of 1.5%, based on EG&G/Idaho National Engineering Laboratory data and transportation restrictions on the amount of free liquid that the waste can contain. For CCA analyses, a constant conservative value of 1.5% was used, which is equal to the maximum value expected.

The present free water saturation for the waste refers to unbound water within the waste. In contrast, materials such as dry portland cement, vermiculite, and other sorbents have intentionally been added to the waste to sorb excess water. This bound water is sometimes proposed as a source of water for corrosion, in which case the amount of water initially available within the waste would become much greater than assumed at present. Water transfer between the sorbents and their surroundings is a process that has not been addressed. It represents a complex tradeoff between the sorbents' chemical affinity for water and the robustness of the chemical reactions, i.e., the ability of the corrosion processes to extract water from the sorbents. The assumption is that it would be a coupled diffusion/vapor transport process, likely to be very slow, and therefore unimportant because of the availability of brine from the surrounding rock. Because it is reasonable to consider it unimportant, this source of water has not been considered in any of the past performance assessments.

3.3.4 Wicking and Other Water Migration Mechanisms

Wicking is the ability of a material to carry a fluid by capillary action above the level it would normally seek in response to gravity. Unsaturated zones in granular materials are controlled by the same capillary forces. Since the present gas generation model defines drastically different rates depending upon whether the waste is in direct contact with liquid brine or surrounded by water vapor, the physical extent of these regions could be important. A parameter defining the extent of wicking in the waste was included in the CCA analyses.

Enhanced water-vapor transport in the gas phase because of the thermal gradients caused by the heat from remote-handled (RH) waste has also been proposed. The concern is that condensation of water in colder parts of the waste/backfill regions may cause a greater portion of the waste to be in contact with liquid water than anticipated. While the magnitude of this effect has not been quantitatively determined, it is considered of secondary importance. However, the thermal gradient issue is also considered of lesser importance, but it can be addressed, if necessary, with the more detailed flow models that are available.

3.4 Method of Analysis

Once the computational configuration and material properties for a closure problem are defined, the computational approach must be selected. Two options are possible:

- A purely mechanical finite strain analysis with SANTOS (Stone, 1997) in which an assumed or known gas generation history is prescribed (porosity surface approach) (Butcher and Mendenhall, 1993, pp. 7-1 to 7-9)
- A coupled flow - mechanical analysis with either TOUGH2 (Pruess, 1991; Freeze et al., 1995a,b) or PHENIX (see Larson memo in Appendix B) in which the dependence of gas generation on brine availability is part of the analysis

Selection of the method of analysis depends on how strong the coupling between fluid flow and mechanical closure must be to adequately represent the response under consideration. The extent of gas generation, and how it controls brine flow into or out of the repository, is clearly the major consideration in this decision.

The porosity surface method was computed for the December 1992 preliminary performance assessment using the structural response code SANCHO (Stone et al., 1985). After those calculations, SANCHO was declared obsolete because of its slow running time, and replaced by the code SANTOS. The SANTOS code is vectorized for improved run time, and has the same physical and mathematical models as contained in SANCHO with exactly the same constitutive relations. It also contains several new options which had been difficult, if not impossible, to implement in SANCHO, such as a method of representing contact of the backfill/waste region with the roof of the excavation.

3.4.1 Porosity Surface Data

The porosity surface concept evolved to compensate for the absence of detailed definition of gas generation within the repository. The concept involves selection of a set of gas generation histories that span all of the gas generation histories likely to be encountered within the repository. Closure corresponding to a specific history is then derived from interpolation between the baseline curves for various amounts of gas. Gas generation histories must be assumed because of the dependence of gas production on brine availability and because structural codes such as SANTOS have no way of estimating this quantity of gas.

The present Disposal Room Model focuses on the "porosity surface" approach, because results from this type of calculation are in a form that performance assessment can use. The coupled flow analysis is used to check the degree to which this approach correctly represents closure during complex gas generation histories. Inherent in this strategy is the present performance assessment position that implementation of a two-phase flow, structural mechanics code capability is not practical because of the large number of calculations that are required for assessments and the excessive computer time that it would take to obtain results from these calculations. Furthermore, based on supporting evidence presented later in this and subsequent sections, we believe at this time that brine content and gas generation can be decoupled from closure via the "porosity surface" approach.

Several direct verifications of the porosity surface method of transferring data to BRAGFLO have been completed. The sequence of steps in this verification process is (1) recovery of several gas generation histories and the changes in repository porosity with time that they produce from vectors spanning the range of repository conditions encountered in the BRAGFLO December 1992 preliminary performance assessment calculations; (2) these gas generation histories are then used to define gas production for SANTOS closure predictions; (3) the loop is completed by comparing the SANTOS porosity-time results with the initial porosity results from BRAGFLO. Differences in the two sets of data would be observed if the porosity surface data were not correctly implemented and converged in BRAGFLO. Exact agreement is not anticipated because of different extrapolation methods and numerical procedures in BRAGFLO. Comparison of the results showed that good agreement was in fact obtained, with the exception of a case in which the repository was largely saturated with brine. To examine the consequences of high brine saturation, the deviating calculation was repeated, specifying the volume of brine in the waste as a function of time in addition to the gas production in the SANTOS analysis. Good agreement was obtained in the revised analysis when the brine inventory was included. Our interpretation of these results is that the present method of representing closure using BRAGFLO is satisfactory, even for the most severe repository conditions.

3.4.2 Coupled Two-Phase-Flow Mechanical Closure Approach

Two approaches have been developed should there be a need for better representation of the coupled effects of fluid flow and mechanical closure (Freeze et al., 1995a,b). The first approach utilized the multiphase flow code, TOUGH2 (Pruess, 1987, 1991), as the basis for implementing the process coupling. Salt was modeled as a fluid phase having high viscosity, increasing the number of simulated phases considered in the calculation to three (gas, brine, and salt). Room closure was represented by the salt phase flowing into the disposal room. The flow properties of the fluid salt phase were calibrated so that the flow of salt into the disposal room would simulate room closure as predicted in strictly mechanical room closure simulations. Fully coupled simulations using the calibrated salt viscosity were then performed completely within TOUGH2. The second approach utilized the PHENIX code to explicitly couple SANTOS room closure estimates with TOUGH2 fluid flow and room pressure estimates at each time step. Neither of these approaches has been developed to the point where the complex calculations required for the performance assessment studies are feasible.

For the TOUGH2 "fluid-phase-salt" approach, a three-phase, three-component (water, air, "dead" oil) equation-of-state module was created. Darcy flow of the third "dead" oil phase resulted in "fluid" salt that was representative of salt creep. Room closure was represented by the fluid salt phase flowing into the disposal room. Resistance to closure (e.g., salt inflow) was provided by room pressurization caused by gas generation and by waste and backfill consolidation. The effects of waste and backfill consolidation were simulated using an artificial boundary within the disposal room to further oppose salt inflow. A calibration process was employed to derive salt phase flow parameters (e.g., viscosity) and properties of the artificial boundary that reproduced the room closures and pressures predicted using the computer code SANCHO (Stone et al., 1985) in past performance assessments. This approach, identified as the boundary backstress method, is described in Freeze et al. (1993, 1995a). The porosity surface approach was also implemented directly into TOUGH2 in this study and the result found to be consistent with the BRAGFLO process.

Predictions of gas pressurization and flow with the fluid flow code TOUGH2 can also be coupled with SANTOS closure estimates through PHENIX for more exact estimates of the dependence of gas generation histories on brine availability (see Larson memo in Appendix B). The PHENIX code simply allows the two other codes to communicate with each other. These calculations are more complex than "porosity surface" calculations and require more computer time. Therefore they are required mainly for verification of the adequacy of simplifying assumptions in a performance assessment. Extensive calculations with this approach have not been made because the conditions under which the porosity surface approach is inadequate have not been encountered and, in some cases, calculations with it are technically infeasible. Nevertheless, it is a potential method of verification of repository closure performance assessment predictions and therefore may be of increasing interest in the future.

3.5 Compliance Certification Application Calculation Results

3.5.1 Porosity Surface Results

The models and assumptions for the CCA are the same as those shown in Figures 1 through 4 of this report. The major exception from past analyses is that the repository is assumed not to be backfilled. Two sets of porosity surface data were obtained, one set for the north end (experimental) region of the repository (Argüello, 1994, in Appendix C), which is assumed to be empty, and one for the disposal area, where the only contents of the room are waste drums stacked three drums high (Stone, in preparation). The results are shown in Figures 8 through 13. The M-D halite creep model and an approximate stratigraphy were used for these calculations.

3.5.1.1 WASTE STORAGE REGIONS

Gas generation histories assumed for calculations of the closure of a single disposal room with no backfill in an infinite array configuration are shown in Figure 8. Each curve is labeled with a value for "f." The histories are selected to span the range of gas generation expected for the repository (see Section 3.2.4) and do not represent actual gas generation histories determined by BRAGFLO. A maximum gas potential of 3200 moles/drum is used, which would occur if all the cellulosics and plastics in the inventory were decomposed.

Porosity curves showing the variation in the closure history with gas content of a single disposal room (no backfill) in an infinite array configuration are shown in Figure 9. Each curve is labeled with the value of "f" corresponding to its gas generation history in Figure 8. These curves are for a sealed room; for performance assessment, actual gas contents within the waste at a given time are to be determined with BRAGFLO, and interpolations between the curves in this and corresponding figures will be used to determine waste porosities as described in Section 3.2.4.

The data points shown in Figure 9 indicate when the gas pressure reaches lithostatic pressure (14.8 MPa) in each calculation. If the assumption is made that the gas pressure in the waste can never exceed lithostatic pressure because of gas leakage into the interbeds, then closure would cease at this point on each curve. The porosity of the waste would remain constant, as shown for one of the curves by the dashed line. All other curves that would be limited by this constraint would also exhibit the same type of behavior: constant porosity in time beyond the critical time at which the gas pressure reaches lithostatic pressure. In fact, the region accessed by BRAGFLO is expected to be almost always limited to the lower region of this figure below the pressure cutoff, without involving any expansion of the room (the portions of the curves beyond the critical times). While closure calculations could be terminated at the data points, once the pressure limit is reached, we choose to continue the calculations to 10,000 years. The reason for this continuation is that termination presupposes that the BRAGFLO analyses will, in fact, be pressure limited and unduly constrain the closure process.

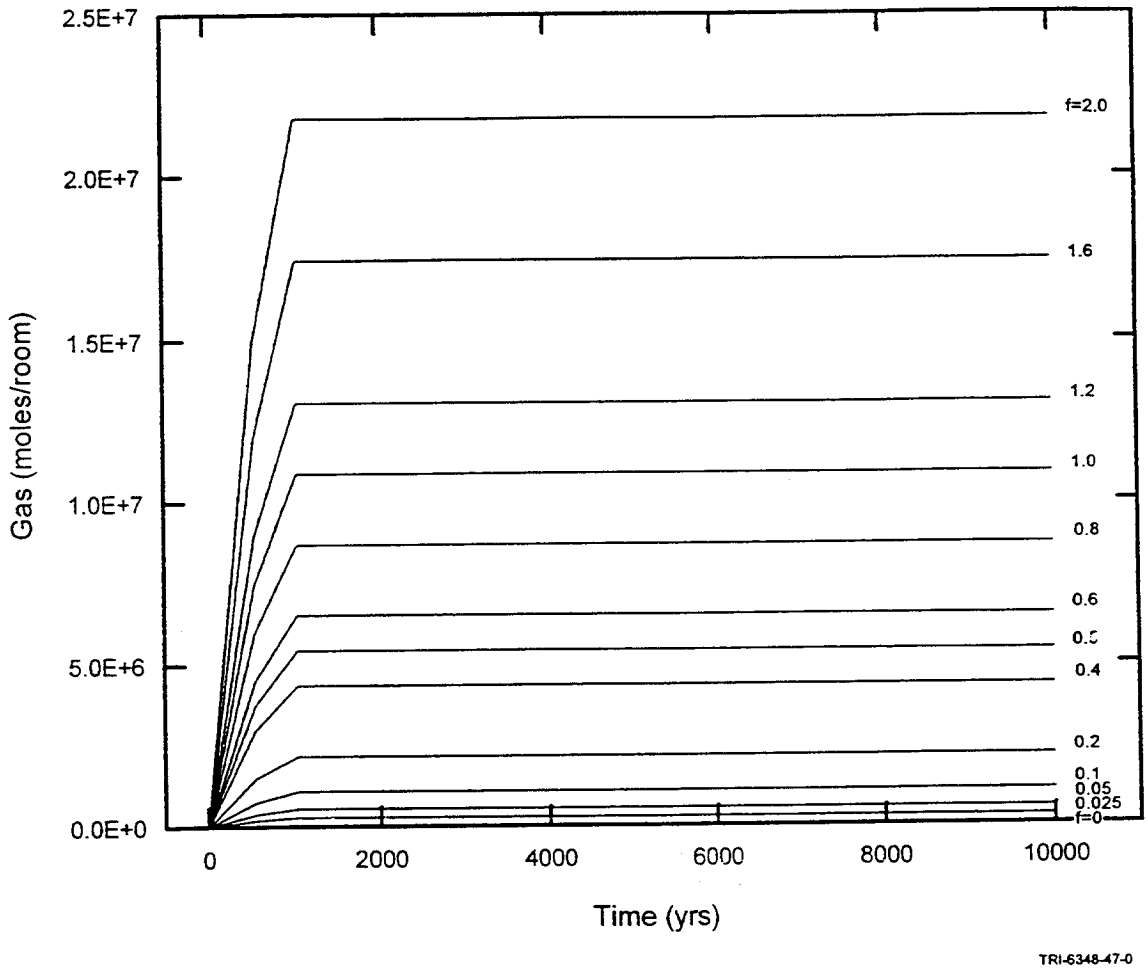


Figure 8. Gas generation histories assumed for calculations of the closure of a single disposal room with no backfill in an infinite array configuration, for the CCA. Each curve is labeled with a value for "f" to identify it (from Stone, 1997).

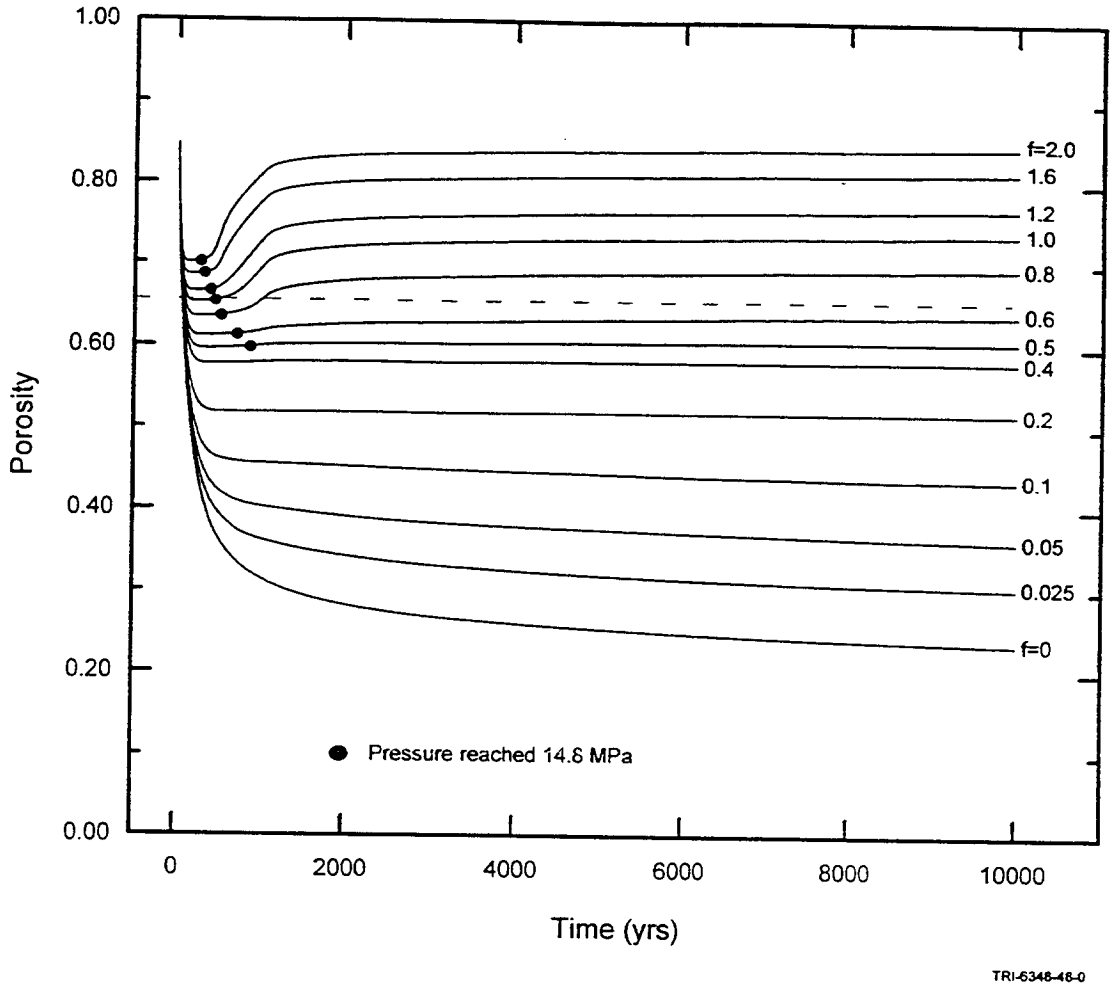


Figure 9. Porosity curves showing the variation in the closure history with gas content of a single disposal room (no backfill) in an infinite array configuration (from Stone, 1997). Each curve is labeled with a letter corresponding to the value for "f" representing its corresponding assumed gas generation history in Figure 7. The data points in the figure indicate when the gas pressure reaches lithostatic pressure (14.8 MPa) in each calculation. If the assumption is made that the gas pressure in the waste can never exceed lithostatic pressure, because of gas leakage into the interbeds, then closure would cease at this point. Under this condition, the porosity of the waste would then remain constant, as shown for one of the curves by the dashed line. All other curves that would be limited by this constraint would also exhibit the same type of behavior.

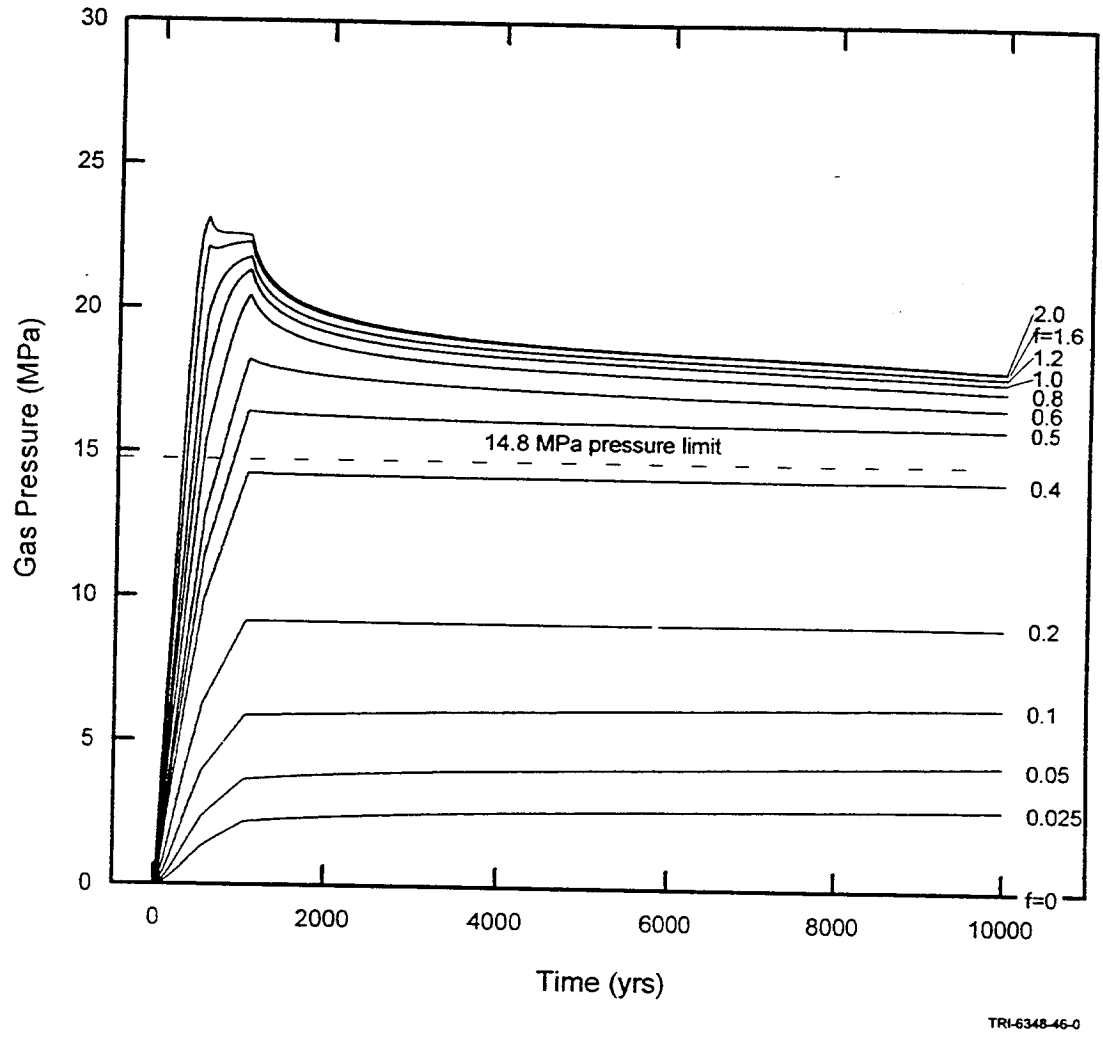


Figure 10. Gas pressure curves showing the variation in the closure history with gas content of a single disposal room (no backfill) in an infinite array configuration (from Stone, 1997). Each curve is labeled with a letter corresponding to its the value of "f" representing assumed gas generation history in Figure 7. BRAGFLO results are expected to show that gas leakage away from the waste prevents buildup of gas pressure much above lithostatic pressure (14.8 MPa), limiting it as shown by the dashed line in the figure (see Section 3.2.5 of this paper).

Gas pressure curves showing the variation in the closure history with the gas content of a single disposal room (no backfill) in an infinite array configuration are shown in Figure 10. Each curve is labeled with the value of "f" corresponding to its assumed gas generation history in Figure 8. As discussed in the previous paragraph, BRAGFLO results are expected to show that gas leakage away from the waste prevents buildup of gas pressure much above lithostatic pressure (14.8 MPa), limiting it as shown by the dashed line in the figure (see Section 3.2.5). The complete curves for the sealed room, for pressures above lithostatic, are provided as input for BRAGFLO, however, because of the unlikely event that the leakages included in the performance assessment calculations are not enough to limit the pressure. This approach ensures that no constraints in the form of artificial limits on closure response are placed on the data when they are passed to BRAGFLO: only the parts of the curves relevant to performance are accessed by BRAGFLO; the rest of the curves are simply ignored.

3.5.1.2 EXPERIMENTAL REGIONS

Gas generation histories assumed for calculations of the closure of the experimental region with no backfill are shown in Figure 11. Each curve is labeled with a letter to identify it. The histories are selected to span the range of gas generation expected (see Section 3.2.4), with the assumption that gas accumulates from other regions of the repository, and do not represent actual gas generation histories as determined by BRAGFLO. A maximum gas potential of 3200 moles/drum for the waste is used.

Void volume curves showing the variation in closure history with gas content of the experimental region with no backfill in an infinite array configuration are shown in Figure 12. Each curve is labeled with a letter corresponding to its assumed gas generation history in Figure 11. These curves are for a sealed region; for performance assessment, actual gas contents within the region at a given time are determined using BRAGFLO, and interpolations between the curves in this and corresponding figures are used to determine void volumes as described in Section 3.2.4. Void volumes are used because nothing is in the rooms and therefore the porosity always has a value of 1.

As for the disposal room porosity curves in Figure 8, the data points shown in Figure 11 indicate when the gas pressure reaches lithostatic pressure (14.8 MPa) in each calculation. If the assumption is made that the gas pressure in the waste can never exceed lithostatic pressure, because of gas leakage into the interbeds, then closure would cease at these points. The void volume of the waste would remain constant, as shown for one of the curves by the dashed line. All other curves that would be limited by this constraint would also exhibit the same type of curve: constant porosity in time beyond the respective data points.

Gas pressure curves showing the variation in closure history with gas content of the experimental region with no backfill are shown in Figure 13. Each curve is labeled with a letter corresponding to its assumed gas generation history in Figure 11. BRAGFLO results are expected to show that gas leakage away from the waste prevents buildup of gas pressure much above lithostatic pressure (14.8 MPa), limiting it as shown by the dashed line in the figure (see

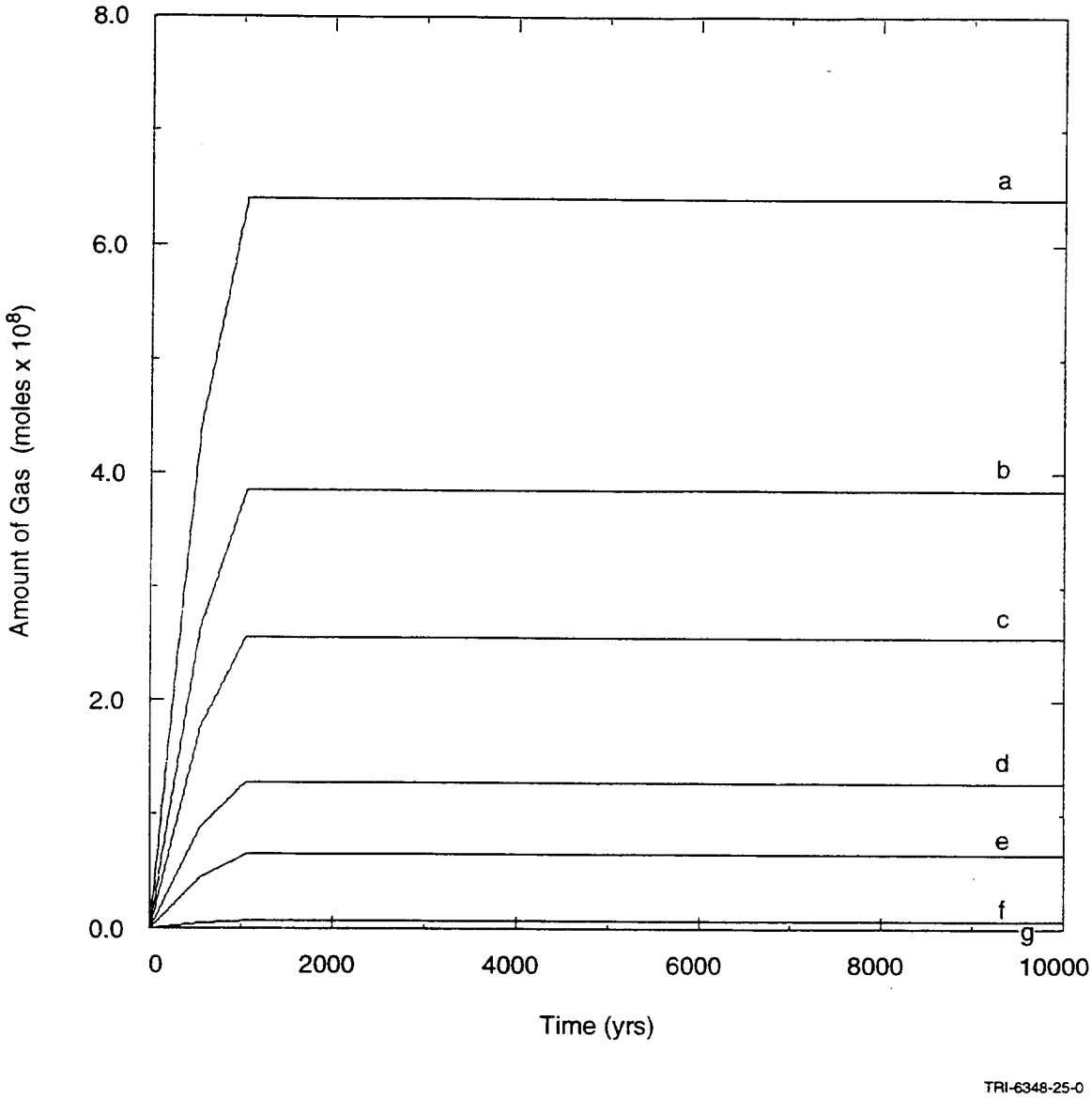


Figure 11. Gas generation histories assumed for calculations of the closure of the experimental region with no backfill (from Argüello, 1994, in Appendix C). Each curve is labeled with an identifying letter.

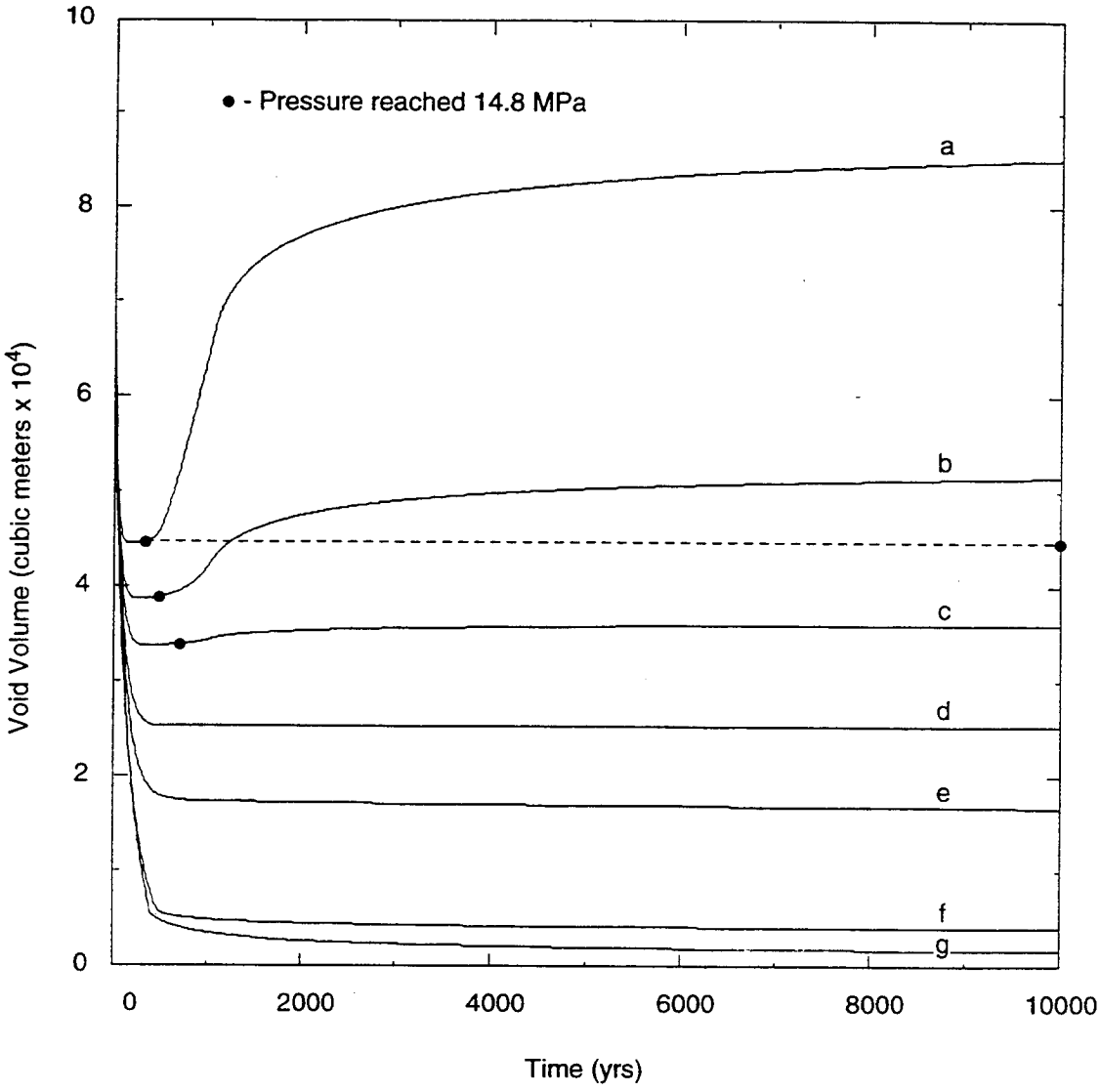


Figure 12. Void volume curves showing the variation in the closure history with gas content of the experimental region with no backfill in an infinite array configuration (from Argüello, 1994, in Appendix C). Void volumes rather than porosities are used because nothing is in the rooms, and therefore the porosity always has a value of 1. As for the disposal room porosity curves in Figure 8, the data points shown in the figure indicate when the gas pressure reaches lithostatic pressure (14.8 MPa) in each calculation. If the assumption is made that the gas pressure can never exceed lithostatic pressure, because of gas leakage into the interbeds, then closure would cease at this point. The porosity would remain constant, as shown for one of the curves by the dashed line. All other curves that would be limited by this constraint would also exhibit the same type of behavior.

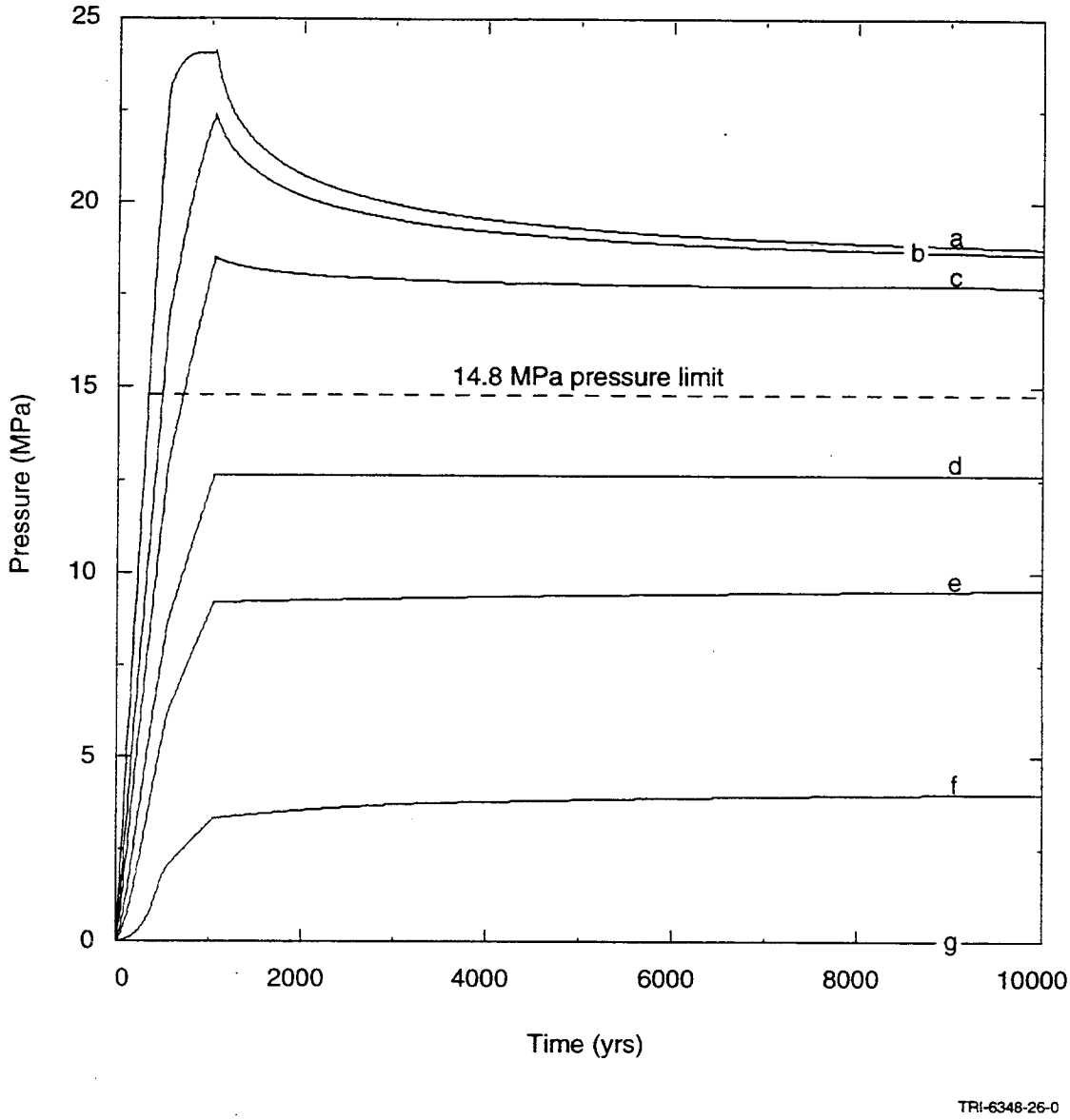


Figure 13. Gas pressure curves showing the variation in pressure with time for different gas content of the experimental region with no backfill (from Argüello, 1994, in Appendix C). Each curve is labeled with a letter corresponding to its corresponding assumed gas generation history in Figure 10. BRAGFLO results are expected to show that gas leakage away from the waste prevents buildup of gas pressure much above lithostatic pressure (14.8 MPa), limiting it as shown by the dashed line in the figure (see Section 3.2.5 of this paper).

Section 3.2.5). The complete curves for the sealed region are provided as input for BRAGFLO, in the remote event that leakages included in the performance assessment calculations are not enough to limit the pressure and it rises above lithostatic pressure, if only for a very short time.

The information presented in Figures 11 through 13 has not been used for the CCA because its use in BRAGFLO is considered to be an unnecessary expenditure of computer time. Instead, these curves were used to define a constant porosity of 0.18 for the region, which corresponds to a "hydrostatic" pressure of 7.8 MPa at 10,000 years. This simplification is justified because calculations have shown that the part of performance assessments provided by the BRAGFLO calculations are not sensitive to which description of closure is used. This information completes the description of the history of development of the final porosity surface conceptual model and data used in the CCA.

4.0 REFERENCES

Argüello, J.G. 1990. "Analysis of WIPP Disposal Room and Entryway Drift Intersection," *Rock Mechanics Contributions and Challenges: Proceedings of the 31st U.S. Symposium, Colorado School of Mines, Golden, CO, June 18-20, 1990.* Eds. W.A. Hustrulid and G.A. Johnson. SAND89-2282C. Brookfield, VT: A.A. Balkema. 329-336.

Argüello, J.G. 1994. "Backfill Sensitivity Study—Creep Closure Behavior of an `Equivalent' Empty Room at the North End of the WIPP Subjected to Gas Generation." Memo to B.M. Butcher, August 19. See Appendix C.

Baseline Inventory Report. 1995. *Waste Isolation Pilot Plant Transuranic Waste Baseline Inventory Report.* Report CAO-94-1005, Revision 1. [Carlsbad, NM]: WIPP Technical Assistance Contractor for U.S. Department of Energy. *(Available from the National Technical Information Service (NTIS), Springfield, VA as DE95009613/XAB.)*

Bechtel National, Inc. 1986. *Design Validation Final Report.* DOE-WIPP-86-010. San Francisco, CA: Bechtel National, Inc. *(Available from the NTIS, Springfield, VA as DE87003412/XAB.)*

Borns, D.J. 1985. *Marker Bed 139: A Study of Drillcore From A Systematic Array.* SAND85-0023. Albuquerque, NM: Sandia National Laboratories.

Brown, W.T., and J.R. Weatherby. 1993. "Appendix A: Influence of Gas Generation Potential and Gas Generation Rate on the Performance of CH-TRU Disposal Rooms," *A Summary of the Models Used for the Mechanical Response of Disposal Rooms in the Waste Isolation Pilot Plant with Regard to Compliance with 40 CFR 191, Subpart B.* B.M. Butcher and F.T. Mendenhall. SAND92-0427. Albuquerque, NM: Sandia National Laboratories. A-5 through A-25.

Butcher, B.M. 1997. *A Summary of the Sources of Input Parameter Values for the Waste Isolation Pilot Plant Final Porosity Surface Calculations.* SAND97-0796. Albuquerque, NM: Sandia National Laboratories.

Butcher, B.M., and R.C. Lincoln. 1993. "Completion of Milestone DR11M, 5/31/93, Which States That a Method will be Provided to PA for Defining the Effects of Human Intrusion from the Porosity Surface Data (No Brine Flow); WBS 1.1.1.2.3." Memo to D.R. Lincoln, May 28. See Appendix A.

Butcher, B.M., and F.T. Mendenhall. 1993. *A Summary of the Models Used for the Mechanical Response of Disposal Rooms in the Waste Isolation Pilot Plant with Regard to Compliance with 40 CFR 191, Subpart B.* SAND92-0427. Albuquerque, NM: Sandia National Laboratories.

Butcher, B.M., C.F. Novak, and M. Jercinovic. 1991a. *The Advantages of a Salt/Bentonite Backfill for Waste Isolation Pilot Plant Disposal Rooms.* SAND90-3074. Albuquerque, NM: Sandia National Laboratories.

Butcher, B.M., T.W. Thompson, R.G. VanBuskirk, and N.C. Patti. 1991b. *Mechanical Compaction of Waste Isolation Pilot Plant Simulated Waste*. SAND90-1206. Albuquerque, NM: Sandia National Laboratories.

Callahan, G.D. 1993. "Appendix A: Further Discussion of the TRU Waste Model," *A Summary of the Models Used for the Mechanical Response of Disposal Rooms in the Waste Isolation Pilot Plant with Regard to Compliance with 40 CFR 191, Subpart B*. B.M. Butcher and F.T. Mendenhall. SAND92-0427. Albuquerque, NM: Sandia National Laboratories. A-27 through A-30.

Callahan, G.D., and K.L. DeVries. 1991. *Analyses of Backfilled Transuranic Wastes Disposal Rooms.* SAND91-7052. Albuquerque, NM: Sandia National Laboratories.

Freeze, G.A., K.W. Larson, P.B. Davies, and F.T. Mendenhall. 1993. "Modeling Salt Deformation with a Multiphase Flow Code to Couple the Effects of Repository Consolidation and Brine and Gas Flow at the Waste Isolation Pilot Plant," *EOS Transactions, American Geophysical Union, 1993 Fall Meeting, San Francisco, CA, December 6-10, 1993*. Vol. 74, no. 43, 285. (Abstract only.)

Freeze, G.A., K.W. Larson, and P.B. Davies. 1995a. *Coupled Multiphase Flow and Closure Analysis of Repository Response to Waste-Generated Gas at the Waste Isolation Pilot Plant (WIPP).* SAND93-1986. Albuquerque, NM: Sandia National Laboratories.

Freeze, G.A., K.W. Larson, and P.B. Davies. 1995b. *A Summary of Methods for Approximating Salt Creep and Disposal Room Closure in Numerical Models of Multiphase Flow*. SAND94-0251. Albuquerque, NM: Sandia National Laboratories.

Freeze, R.A., and J.A. Cherry. 1979. *Groundwater*. Englewood Cliffs, NJ: Prentice-Hall. Chapter 8, Section 8.7.

Holcomb, D.J., and D.W. Hannum. 1982. *Consolidation of Crushed Salt Backfill Under Conditions Appropriate to the WIPP Facility.* SAND82-0630. Albuquerque, NM: Sandia National Laboratories.

Holcomb, D.J., and M. Shields. 1987. *Hydrostatic Creep Consolidation of Crushed Salt With Added Water.* SAND87-1990. Albuquerque, NM: Sandia National Laboratories

Krieg, R.D. 1984. *Reference Stratigraphy and Rock Properties for the Waste Isolation Pilot Plant (WIPP) Project.* SAND83-1908. Albuquerque, NM: Sandia National Laboratories.

Labreche, D.A., M.A. Beikmann, J.D. Osnes, and B.M. Butcher. 1995. *A Sensitivity Analysis of the WIPP Disposal Room Model: Phase 1*. SAND94-0890. Albuquerque, NM: Sandia National Laboratories.

Larson, K.W. 1994. "The PHENIX Coupled Room Closure and Multiphase Flow Code."

Memo to B.M. Butcher, August 17. See Appendix B.

Luker, R.S., T.W. Thompson, and B.M. Butcher. 1991. "Compaction and Permeability of Simulated Waste," *Rock Mechanics as a Multidisciplinary Science: Proceedings of the 32nd U.S. Symposium, The University of Oklahoma, Norman, OK, July 10-12, 1991*. Ed. J-C. Roegiers. SAND90-2368C. Brookfield, VT: A.A. Balkema. 693-702.

Morgan, H.S. 1993a. "Appendix A: TRU Storage Room Calculation with Stratigraphy," *A Summary of the Models Used for the Mechanical Response of Disposal Rooms in the Waste Isolation Pilot Plant with Regard to Compliance with 40 CFR 191, Subpart B.* B.M. Butcher and F.T. Mendenhall. SAND92-0427. Albuquerque, NM: Sandia National Laboratories. A-91 through A-103.

Morgan, H.S. 1993b. "Appendix A: Estimate of the Time Needed for TRU Storage Rooms to Close," *A Summary of the Models Used for the Mechanical Response of Disposal Rooms in the Waste Isolation Pilot Plant with Regard to Compliance with 40 CFR 191, Subpart B.* B.M. Butcher and F.T. Mendenhall. SAND92-0427. Albuquerque, NM: Sandia National Laboratories. A-67 through A-89.

Munson, D.E. 1992. "Appendix A: Mechanical Parameters for Volume 3, SAND92-0700," *Preliminary Performance Assessment for the Waste Isolation Pilot Plant, December 1992. Volume 3: Model Parameters.* Sandia WIPP Project. SAND92-0700/3. Albuquerque, NM: Sandia National Laboratories. A-107 through A-123.

Munson, D.E., A.F. Fossum, and P.E. Senseny. 1989a. *Advances in Resolution of Discrepancies Between Predicted and Measured In Situ WIPP Room Closures.* SAND88-2948. Albuquerque, NM: Sandia National Laboratories. (See also: Munson, D.E., and K.L. DeVries. 1991. "Development and Validation of a Predictive Technology for Creep Closure of Underground Rooms in Salt," *Proceedings of the 7th International Congress on Rock Mechanics, Aachen, FRG, September 16-20, 1991*. Ed. W. Wittke. SAND90-1147. Vol. 7, 127-134.)

Munson, D.E., A.F. Fossum, and P.E. Senseny. 1989b. *Approach to First Principles Model Prediction of Measured WIPP In Situ Room Closure in Salt*. SAND88-2535. Albuquerque, NM: Sandia National Laboratories.

Pruess, K. 1987. *TOUGH User's Guide*. NUREG/CR-4645, SAND86-7104, LBL-20700. Washington, DC: Division of Waste Management, Office of Nuclear Material Safety and Safeguards, U.S. Nuclear Regulatory Commission.

Pruess, K. 1991. *TOUGH2 - A General-Purpose Numerical Simulator for Multiphase Fluid and Heat Flow*. LBL-29400. Berkeley, CA: Lawrence Berkeley Laboratory.

Sandia WIPP Project. 1992. *Preliminary Performance Assessment for the Waste Isolation Pilot Plant, December 1992. Volume 3: Model Parameters.* SAND92-0700/3. Albuquerque NM: Sandia National Laboratories.

Sjaardema, G.D., and R.D. Krieg. 1987. *A Constitutive Model for the Consolidation of WIPP Crushed Salt and Its Use in Analyses of Backfilled Shaft and Drift Configurations*.

SAND87-1977. Albuquerque, NM: Sandia National Laboratories.

Stone, C.M. 1997. *Final Disposal Room Structural Response Calculations*. SAND97-0795. Albuquerque, NM: Sandia National Laboratories.

Stone, C.M., and J.G. Argüello. 1993. "Appendix A: Panel Scale Calculations for the Waste Isolation Pilot Plant (WIPP)," *A Summary of the Models Used for the Mechanical Response of Disposal Rooms in the Waste Isolation Pilot Plant with Regard to Compliance with 40 CFR 191, Subpart B.* B.M. Butcher and F.T. Mendenhall. SAND92-0427. Albuquerque, NM: Sandia National Laboratories. A-121 through A-134.

Stone, C.M., R.D. Krieg, and L.J. Branstetter. 1981. *The Effects of Clay Seam Behavior on WIPP Repository Design.* SAND81-0768. Albuquerque, NM: Sandia National Laboratories.

Stone, C.M., R.D. Krieg, and Z.E. Beisinger. 1985. *SANCHO, A Finite Element Computer Program for the Quasistatic, Large Deformation, Inelastic Response of Two-Dimensional Solids.* SAND84-2618. Albuquerque, NM: Sandia National Laboratories.

US EPA (Environmental Protection Agency). 1985. "40 CFR 191: Environmental Standards for the Management and Disposal of Spent Nuclear Fuel, High-Level and Transuranic Radioactive Wastes; Final Rule," *Federal Register*. Vol. 50, no. 182, 38066-38089.

US EPA (Environmental Protection Agency). 1993. "40 CFR Part 191 Environmental Radiation Protection Standards for the Management and Disposal of Spent Nuclear Fuel, High-Level and Transuranic Radioactive Wastes; Final Rule," *Federal Register.* Vol. 58, no. 242, 66398-66416.

Weatherby, J.R., W.T. Brown, and B.M. Butcher. 1991. "The Closure of WIPP Disposal Rooms Filled with Various Waste and Backfill Combinations," *Rock Mechanics as a Multidisciplinary Science, Proceedings of the 32nd U.S. Symposium, University of Oklahoma, Norman, OK, July 10-12, 1991*. Ed. J.C. Roegiers. SAND90-2399C. Brookfield, VT: A.A. Balkema. 919-928.

WIPP PA (Performance Assessment) Department. 1992. *Preliminary Performance Assessment for the Waste Isolation Pilot Plant, December 1992. Volume 1: Third Comparison with 40 CFR 191, Subpart B.* SAND92-0700/1. Albuquerque, NM: Sandia National Laboratories.

WIPP PA (Performance Assessment) Department. 1993. *Preliminary Performance Assessment for the Waste Isolation Pilot Plant, December 1992. Volume 4: Uncertainty and Sensitivity Analyses for 40 CFR 191, Subpart B.* SAND92-0700/4. Albuquerque, NM: Sandia National Laboratories.

WIPP PA (Performance Assessment) Division. 1991. *Preliminary Comparison with 40 CFR Part 191, Subpart B for the Waste Isolation Pilot Plant, December 1991. Volume 3: Reference Data*. SAND91-0893/3. Eds. R.P. Rechard, A.C. Peterson, J.D. Schreiber, H.J. Iuzzolino, M.S. Tierney, and J.S. Sandha. Albuquerque, NM: Sandia National Laboratories.

APPENDICES

CONTENTS

APPENDIX A: B.M. Butcher and R.C. Lincoln, "Completion of Milestone DR11M, 5/31/93, Which States That a Method will be Provided to PA for Defining the Effects of Human Intrusion from the Porosity Surface Data (No Brine Flow); WBS 1.1.1.2.3."

APPENDIX B: K.W. Larson, "The PHENIX Coupled Room Closure and Multiphase Flow Code."

APPENDIX C: J.G. Argüello, "Backfill Sensitivity Study—Creep Closure Behavior of an `Equivalent' Empty Room at the North End of the WIPP Subjected to Gas Generation."

APPENDIX A: Completion of Milestone DR11M, 5/31/93, Which States That a Method will be Provided to PA for Defining the Effects of Human Intrusion from the Porosity Surface Data (No Brine Flow); WBS 1.1.1.2.3

Sandia National Laboratories

Albuquerque, New Mexico 87185

date: May 28, 1993

to: D. R. Anderson, 6342

B.M. Butcher R.C. Lincoln

from: B. M. Butcher, R. C. Lincoln, 6345

subject: Completion of milestone DR11M, 5/31/93, which states that a method will be provided to PA for defining the effects of human intrusion from the porosity surface data (no brine flow); WBS 1.1.1.2.3.

Summary:

A preliminary method for defining the effect of a human intrusion on the post-intrusion closure history of a disposal room containing backfill and waste was proposed in the memorandum from B. M. Butcher to R. C. Lincoln, October 26, 1992. Additional calculations have shown this approach to be only partially correct; the refinements described this memorandum show that the estimated post-intrusion closure history is simpler than was previously presented. In fact, if the assumption is made that gas pressurization of the repository is not likely to increase much above lithostatic pressure because of fracturing of the interbeds, then the PA assumption that the room porosity remains constant is considered an adequate approximation of post-intrusion closure.

Elastic-plastic waste response:

The mechanical responses of wastes stored in the WIPP repository are modeled as elastic-plastic materials in numerical closure analyses. This feature of material response is neglected in the preliminary human intrusion model. Justification for modeling waste as elastic-plastic is derived from the compaction response of the various waste materials.

Experimental compaction loading-unloading curves for the principal waste components are shown in Figures 1 to 4. These curves have the common characteristic of different response during unloading than during loading. Density changes caused by unloading are very much smaller than density changes caused by compaction, particularly when the sample is still under an appreciable load. In addition, reloading after unloading, though not shown, is known to proceed up along a path much closer to the unloading curve than along the original compaction curve. This observation is approximated in the waste compaction model by assuming that the response of the waste during unloading/reloading is elastic, and therefore that the strains associated with the expansions are small. Any hysteresis in unloading/reloading paths is also neglected.

The reason the previous model of closure after human intrusion was partially in error was because it did not recognize the way the waste responds during unloading. Suppose, for example, the waste material has been compacted to a given maximum stress level. At this point, The stress is removed from the material unloading it elastically. It is important to remember in the discussion that follows that any additional irreversible compaction of the

waste is possible only when the load on the waste exceeds the previous maximum stress level that produced compaction.

Now consider gas pressurization in a disposal room within WIPP. Initially compaction of the waste occurs as the room closes, but if sufficient room pressurization occurs, a minimum in the closure curve (porosity v time) is reached. With additional generation of gas, the room starts to expand. Recognizing that the waste acts as a skeletal framework having the gas contained in the interconnected space within it, the minimum in the closure curve is associated with the maximum stress that the waste can support without continued irreversible compaction.

To proceed one step further, the maximum load the waste has to eventually support if no gas were present would be the overburden load. A corollary is that because the room is closing very slowly, the sum of the stress supported by the waste and the gas pressure is usually close to the overburden load. This means that the waste supports part of the load, and the gas supports the remainder of the load required to hold the ceiling up. If additional gas is now generated and gas pressure increases, the waste does not have to support as large a portion of the load, and it begins to unload. The extreme would be when the gas pressure increases to lithostatic, when contact between the backfill and the ceiling is lost and a gap forms. In this circumstance the waste is almost completely unloaded. If, on the other hand, the gas pressure falls below the level that existed at the minimum, then the load on the waste will exceed the previously established level for irreversible compaction, and compaction will begin again.

A diagram of the tradeoff between gas pressure and the load supported by the waste is shown in Figure 5. In the top figure, the backfill and waste are in contact with ceiling, and supports some overburden load. The portion of the load supported by the waste and backfill depends on the gas pressure. In the bottom figure, contact has been broken and the ceiling is held up by the gas pressure alone. These features of room closure are the reason closure after an intrusion cannot be computed by the method described in the previous memorandum.

Human Intrusion Closure Histories

A) Definition of the boundary of a disposal room

The boundary of the disposal room is defined as the heavy line shown in Figure 6. We assume that gas can flow through this boundary at any time during closure, so that the room is not sealed. When a specific quantity of gas is considered, it is the amount of gas within the boundary. All excess gas is assumed to flow out into additional gas storage volume, such as might exist within the interbeds. In addition the assumption is made that the external gas storage reservoir is in pressure equilibrium with the room pressure. The assumption that gas escaping through the boundary (such as into the interbeds) does not influence the closure process is considered reasonable.

B) Assumed Sequences of Gas Generation:

The porosity surface is used to explore the consequences of various gas generation assumptions. The following gas generation sequence will be used for the examples that follow. The method to be described is not limited to this sequence, but is applicable to any

other sequence that can be represented as a path on the porosity surface.

Time years	Description
0 - 550	gas generation at 1.36 x 10^4 moles/year/room (2 moles/drum/year).
550 - 1000	gas generation at 0.68 x 10^4 moles/year/room (1 mole/drum/year).
1000	human intrusion: gas pressure decrease to 7.7 MPa.
1000 - 1050	gas generation at 1 mole/drum/year.
1050 - 1425	gas leakage at 680 moles/year/room (0.1 mole/drum/year).
1425 - 2500	gradual increase in pore pressure (gas + brine, until it becomes equal to the far-field pore pressure.

In this sequence, 7.7 MPa is the hydrostatic pressure of brine at the repository horizon, and 10 MPa is assumed to be the far-field pore pressure.

The reader is again reminded that these assumptions do not necessarily represent the total amount of gas that is produced, but instead the amount of gas that remains in the room.

C) Post-Intrusion Histories

Two different cases are examined in the following discussion to illustrate how compaction of the waste controls the response of the waste. Case 1, where the gas pressure in the room is allowed to exceed lithostatic pressure, is presented first because it is easier to explain. However, it is not now considered typical of room closure. In addition, SANTOS results are available that permit a direct comparison of porosity surface estimates for Case 1 with computational results obtained from the disposal room model. Case 2 is considered the more likely response of the disposal room. Gas pressure within the room is limited in Case 2 to 14.8 MPa, to simulate opening of fractures in the interbeds at lithostatic pressure. The results for this case show that while the response is more complicated than that of Case 1, the estimated response of the room after intrusion is closer to the assumption made for the Preliminary Performance Assessment for WIPP, December 1992. This assumption was that closure completely stops after a human intrusion.

1) Case 1: Pressure in the room exceeds lithostatic pressure.

Case 1 represents the closure history when the pressure in the room was allowed to exceed lithostatic pressure. For this case, the gas generation history was modified slightly from the full sequence by omitting any leakage after 1050 years. With this simplification, the gas sequence was an exact duplicate of the assumptions for one of the SANTOS human intrusion calculations. Figure 7 illustrates the closure history derived from the porosity surface.

Significant events before and after the intrusion in Figure 7 are marked with letters and are described next. Gas generation and pressurization histories are shown in Figures 8 and 9.

(1) Point H: After waste emplacement, the disposal room closes until equilibrium is reached between the gas pressure and the waste/backfill compaction. If the amount of gas is insufficient, this condition may never occur, but if it does, a minimum occurs in the porosity history curve (Figure 7). For this case the minimum occurs at 200 years and corresponds to an average porosity of 38.14%, and a gas pressure of 8.87 MPa. The number of moles of gas is $2.7 \cdot 10^7$ moles/room. The minimum represents the time when the combined backstress exerted by the waste skeleton and the gas is approximately equal to the load exerted on the disposal room boundary by the overburden. In addition, continued compaction will occur only when the load supported by the waste at this time is exceeded. The SANTOS curve in Figure 7 is different from the porosity surface prediction, because the SANTOS calculation was more recent than the calculations used to construct the porosity surface, and contains improvements that were not previously available. A new surface needs to be constructed that includes these improvements.

(2) Segment H-I: Additional gas is now generated and gas pressure within the room continues to increase to lithostatic pressure at Point I. The simplest interpretation of the elastic-plastic response of the waste would suggest that the porosity remain constant during this segment, but the more exact calculation shows a slight increase.

(3) Segment I-J: Contact between the waste, backfill and the ceiling (back) of the room is broken at point I and a gas-filled cavity or plenum is created above the waste as the disposal room continues to expand. The waste supports little or no load when the gas pressure is equal to lithostatic pressure, as will be evident from the discussion of Case 2.

(4) Point J: The assumption of human intrusion at this time is that the gas pressure within the disposal room almost instantaneously drops to a lower pressure. A pressure of 7.7 MPa was assumed for this calculation. Before the intrusion, the average porosity of the room was 50.72%, the gas pressure was 20.58 MPa, and the number of moles of gas was $10.5 \cdot 10^7$ moles/room. After the intrusion, the number of moles of gas was $4.0 \cdot 10^7$, still above the gas content at the minimum porosity of $2.7 \cdot 10^7$ moles/room. Gas is still being generated.

(5) Segment J-L: The waste continues to reload as the porosity decreases because of the drop in pressure caused by the intrusion.

(6) Point L: Gas generation ceases.

(8) Point N: The porosity of the room has dropped to the minimum porosity value of 38.14, and thereafter will remain constant because the room contains more gas than existed at Point H. No leakage was allowed in this example, but had leakage been postulated, the gas content in the room would eventually drop below the content at point H, and compaction would again begin.

2) Case 2: Pressure in the room limited to lithostatic pressure.

Figure 10 illustrates the closure history derived from the porosity surface for the prescribed gas generation history, assuming that gas pressure within the room never gets any higher than lithostatic pressure. Significant events before and after the intrusion in Figure 10 are marked with letters and are described next. Gas and pressurization histories are shown in Figures 8 and 11.

(1) Point H: Conditions at this point are the same as for Case 1. We assume that after waste emplacement the disposal room continues to close until gas pressurization becomes sufficient to prevent additional decrease in porosity. For this case, as for Case 1, the minimum occurs at 200 years and corresponds to an average porosity of 38.14%, and a gas pressure of 8.87 MPa. The number of moles of gas is $2.7 \cdot 10^7$ moles/room. The minimum represents the time when the combined backstress exerted by the waste skeleton and the gas is equal to the load exerted on the disposal room boundary by the overburden. Continued compaction will occur only when the load supported by the waste at this time is exceeded.

(2) Segment H-I: Additional gas is generated and gas pressure within the room continues to increase until lithostatic pressure is reached. As the pressure increases, the load supported by the waste-backfill skeleton decreases until it becomes almost 0 at lithostatic pressure (Figure 11). The increase in strain in the waste during unloading is considered insignificant.

(3) Point I: The pressure of the gas in the room reachs lithostatic pressure, the porosity is 39.17 % and the quantity of gas is $4.7 \cdot 10^7$ moles/room at 350 years.

(4) Segment I-J: The contact between the waste, backfill and the ceiling (back) of the room may be broken at Point I, depending on how far the room pressure gets above lithostatic pressure. Whether or not contact with the back is lost at Point I is unimportant, however, because there will be no significant room expansion. A much more important observation is that at Point I the waste supports little or no load during the time the gas pressure is equal to lithostatic pressure (Figure 11).

A critical assumption in deriving this part of the path from the porosity surface is that the room porosity will remain constant, because the pressure remains constant. In contrast, the SANTOS solution for this segment will probably show that the porosity is slowly changing because of backfill creep consolidation and/or changes in the stress gradients within the halite adjacent to the rooms. No SANTOS results are presently available to confirm this conclusion, but this feature of closure will be explored in greater detail in future calculations.

(5) Point J: We assume that a human intrusion occurs at this time, which almost instantaneously drops the gas pressure in the disposal room to a lower pressure. A pressure of 7.7 MPa was assumed. The waste reloads as the drop in pressure occurs, but not necessarily to the load that it supported at Point H. Before the intrusion, the average porosity of the room was 39.17%, the gas pressure was 14.8 MPa, and the

number of moles of gas was $4.7 \cdot 10^7$ moles/room. After the intrusion, the number of moles of gas was $2.5 \cdot 10^7$, below the gas content at the minimum porosity of $2.7 \cdot 10^7$ moles/room. If a gas-filled cavity existed in the room prior to the intrusion, this cavity would first close before any load was taken up by the waste, as was illustrated in Case 1.

(6) Segment J-K: After the human intrusion, the amount of gas in the room drops briefly below the amount of gas at Point H, the previous minimum.

(7) Point K: A new minimum in porosity is established as gas generation continues. The quantity of gas in the room at 1015 years has increased to $2.6 \cdot 10^7$ moles/room and is still increasing. The porosity of the room constant at 38.01%.

(8) Segment K-L-M: The porosity of the room remains constant.

(9) Point L: Gas generation ceases at 1050 years, after which gas begins leak out of the room. The room porosity remains constant because the amount of gas within the room is greater than the amount of gas at greatest compaction, Point K.

(10) Point M: Conditions in the room have returned to exactly the same conditions as encountered at the previous point of greatest compaction at Point K, and compaction begins again. Point M occurs at 1325 years

(11) Segment M-N: Gas pressure in the room drops continuously because of the leakage, accompanying by continued compaction of the waste.

(12) Point N: The sum of the stress supported by the waste and the gas pressure is equal to the overburden and the porosity of the room has dropped to 36.6% after 1430 years. After point N, the porosity path is speculative and must be determined by two-phase flow analysis.

3) Discussion of Case 2

The assumption made by PA for the 1992 comparison was that closure completely stopped after a human intrusion even if the pre-intrusion pressurized state of the repository was above lithostatic pressure: i.e. upon release of gas, the pressure was assumed to drop to a pressure characteristic of the drilling fluid at constant porosity, which for this case is the porosity at Point J of 39.2%. The porosity was assumed to remain at this value as time increased.

The 1993 PA calculations are expected to show that gas pressure within the repository is limited to around lithostatic pressure because of incorporation of the interbed fracture model. Therefore, Case 2 is considered a good representation of the anticipated response of the disposal room. Instead of remaining constant after the intrusion, however, the porosity surface prediction for Case 2 shows that the porosity drops very gradually to 36.6% and then remains constant. Since (1) the additional change in porosity after the human intrusion estimated from the porosity surface prediction is only 2.6%, and (2) because this difference is likely to be of the same order of magnitude as the uncertainty of the porosity surface, we conclude that for the conditions examined in this analysis the assumption of constant porosity after the intrusion

is a suitable approximation of room response. The small difference between the porosity surface results and the PA assumption represents the difference between the porosity at the minimum porosity point and the porosity when lithostatic pressure is reached. Since the closure history in this region is slowly changing, a relatively small difference is to be expected for all gas pressurization conditions that eventually reach lithostatic pressure.

As a further check on the generality of the observations from Case 2, the calculation was repeated, assuming 1/5 the gas generation rates assumed for the Case 2 calculation, with gas generation over 1050 years. This assumption is thought to be close to the lower bound of expected response, that of insignificant or no gas generation. The results in Figure 12 show that even less change in porosity was observed after the intrusion than for Case 2. The reason for this response was that there was insufficient gas produced at these rates to permit much release during the intrusion, and the disposal room under these conditions is essentially unaffected by it.

Justification for the proposed method for defining the effects of human intrusion from porosity surface data

Although relatively few calculations have been completed to support the conclusion that little porosity change occurs after a human intrusion when gas pressures are limited to lithostatic pressure, it is considered to be fairly general. Several parameters dominate response.

First, the response of the disposal room in Case 2 is controlled by the amount of gas that can be stored in the room when the gas pressure reaches lithostatic pressure, which is largely independent of the total potential for gas production: the gas storage volume depends on the initial reversal point or minimum in the porosity versus time curve, assuming that enough gas is generated to produce such response. The parameters for this point are more sensitive to the rate of gas generation than the gas generation potential. Thus, the conditions examined in Case 2 are considered to be very severe because they represent a more rapid rise in gas pressure than is observed from most of the compliance calculations. Lesser rates produce lower values of the initial minimum porosity, and less gas available for release during the intrusion to cause additional closure.

The hydraulic pressure exerted by the drilling fluid is another parameter influencing the state of the repository after an intrusion: the gas pressure depends entirely on the hydraulic pressure exerted by the drilling fluid, and is independent of any prior pressurization history.

In summary, according to the simple method presented in this memorandum, if (1) values for these parameters are known; and (2) the gas pressure is known to never increase much above lithostatic pressure, then (3) the state of the repository after an intrusion is defined, without the need for any additional knowledge of prior closure history, and (4) the constant porosity assumption can be used. If a limit on the gas pressure is not imposed, then it is sufficient to keep track of the minimum porosity condition as closure proceeds, and estimate post-intrusion closure as described for Case 1.

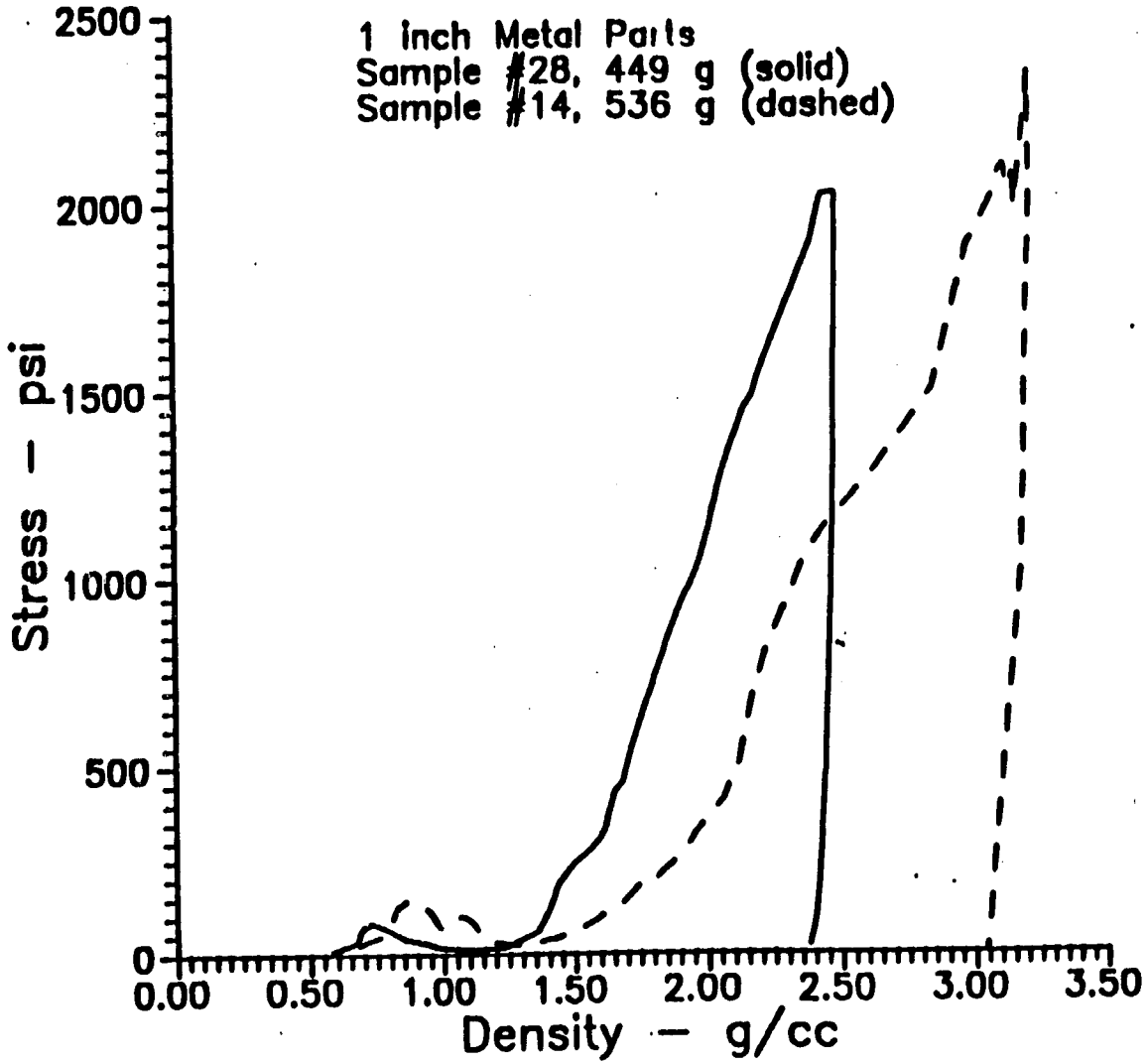


Figure 1: Stress versus density compaction curves for a mixture various of 1 inch in dimension metal parts simulating metallic waste.

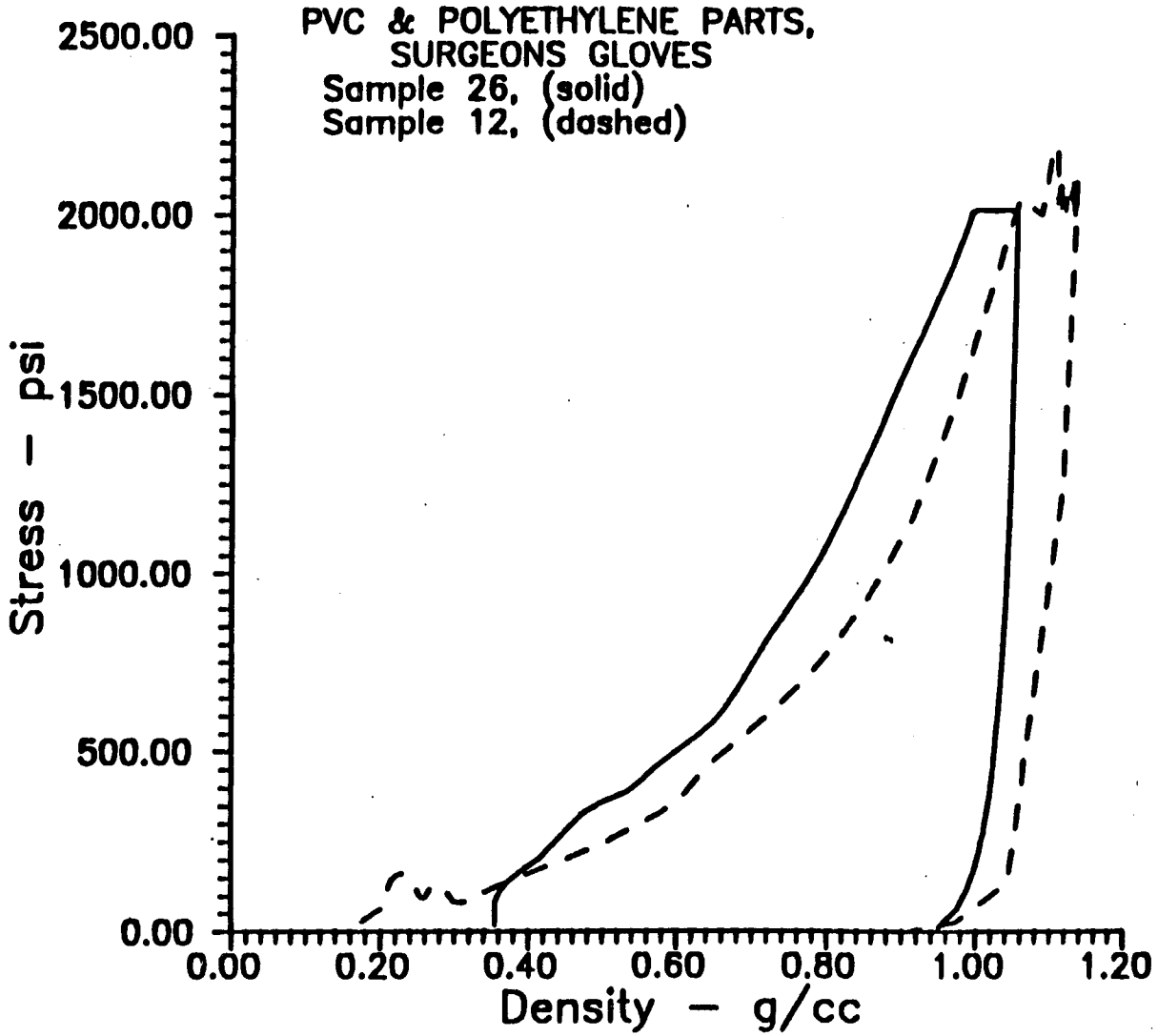


Figure 2: Stress versus density compaction curves for a mixture of polyvinyl chloride parts, polyethylene parts, and surgeons gloves, simulating plastics waste.

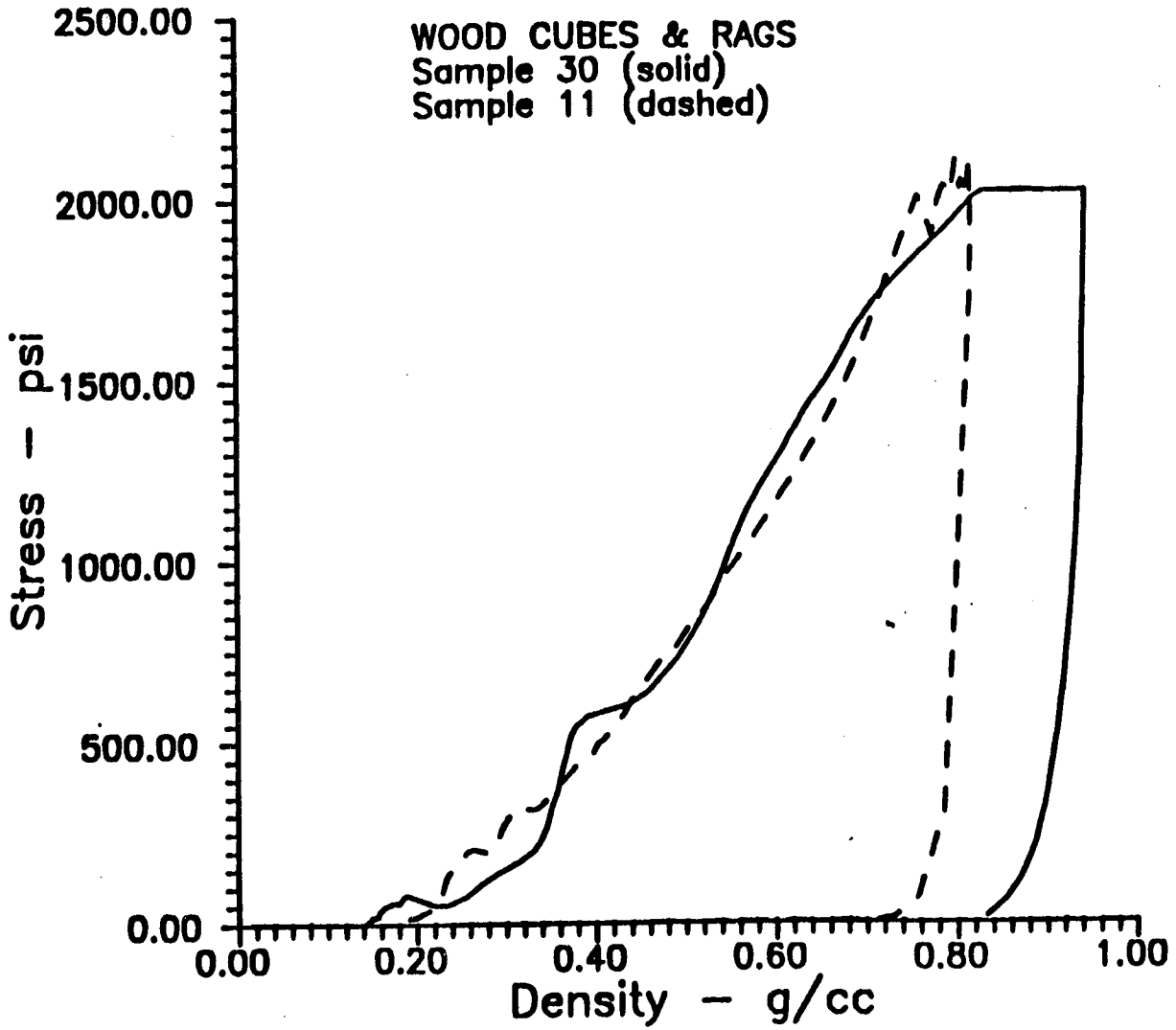


Figure 3: Stress versus density compaction curves for a mixture of wood cubes and rags simulating cellulosic waste.

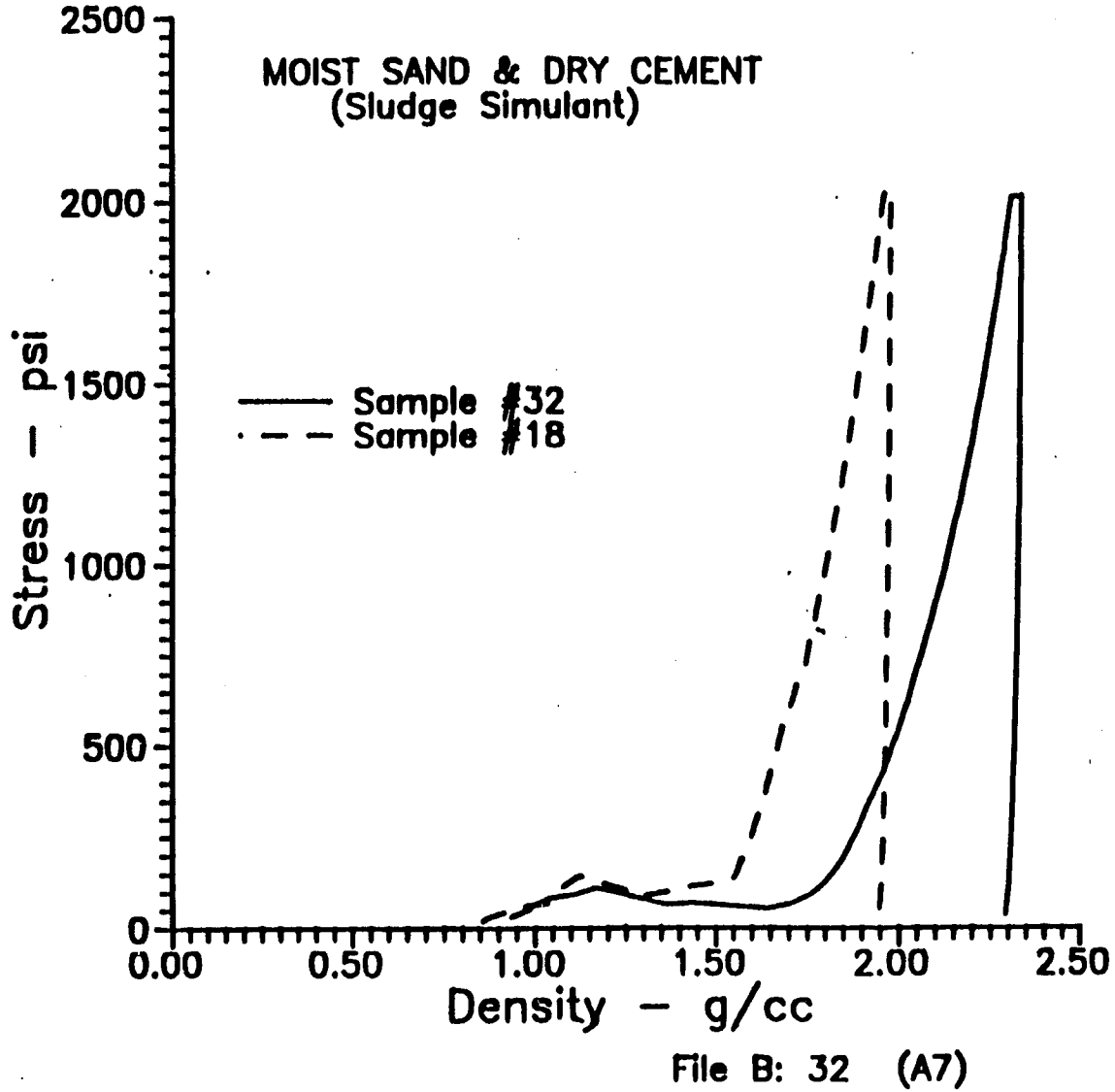
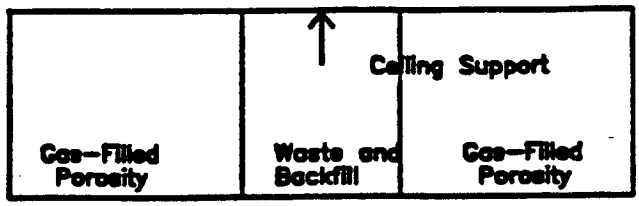
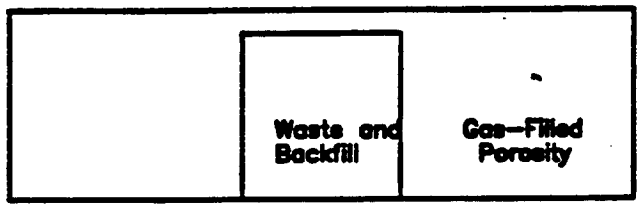


Figure 4: Stress versus density compaction curves for a mixture of moist sand and dry cement simulating sludges.



Waste and backfill in contact with room ceiling, partially supporting it.



No contact between the backfill and the room ceiling: the ceiling is supported entirely by gas pressure.

Figure 5: A schematic representation of the tradeoff between gas pressure and the load supported by waste and backfill within the disposal room.

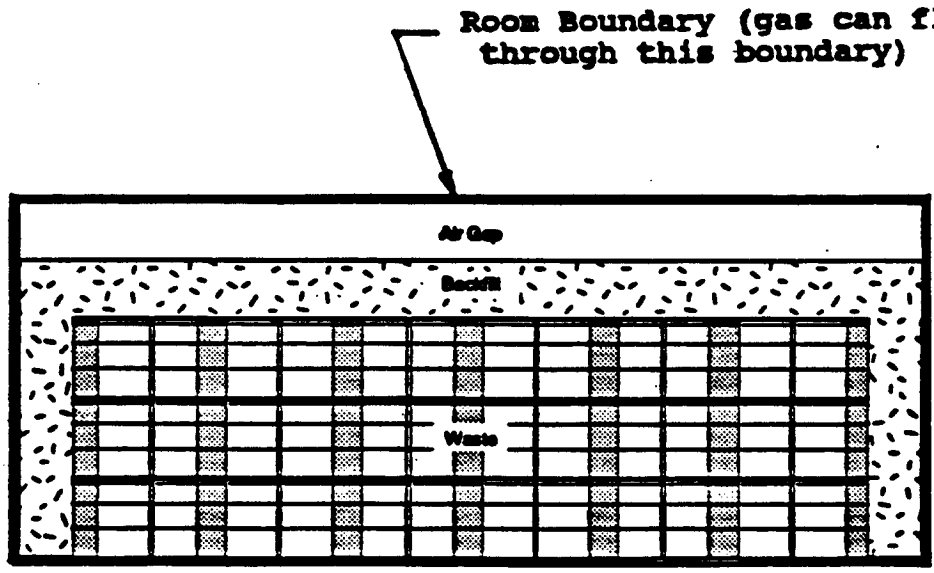


Figure 6: The boundary of the disposal room assumed for calculations. The room is not sealed and gas can flow through the boundary at any time during closure. However, when a specific quantity of gas is quoted it refers to the amount of gas contained inside the boundary.

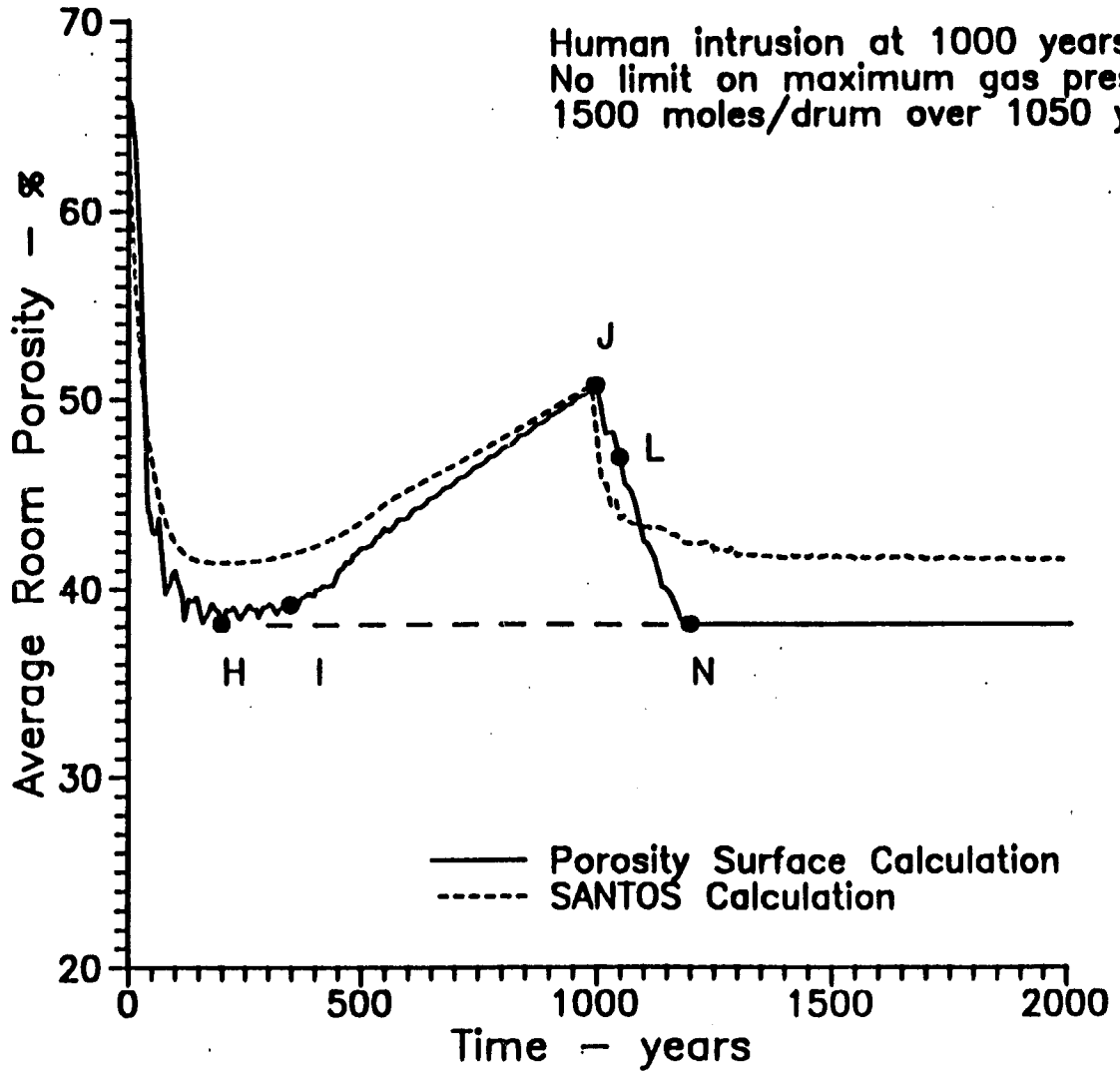


Figure 7: The average room porosity history of a disposal room as a function of time assuming that there is no limit on maximum gas pressure (Case 1).

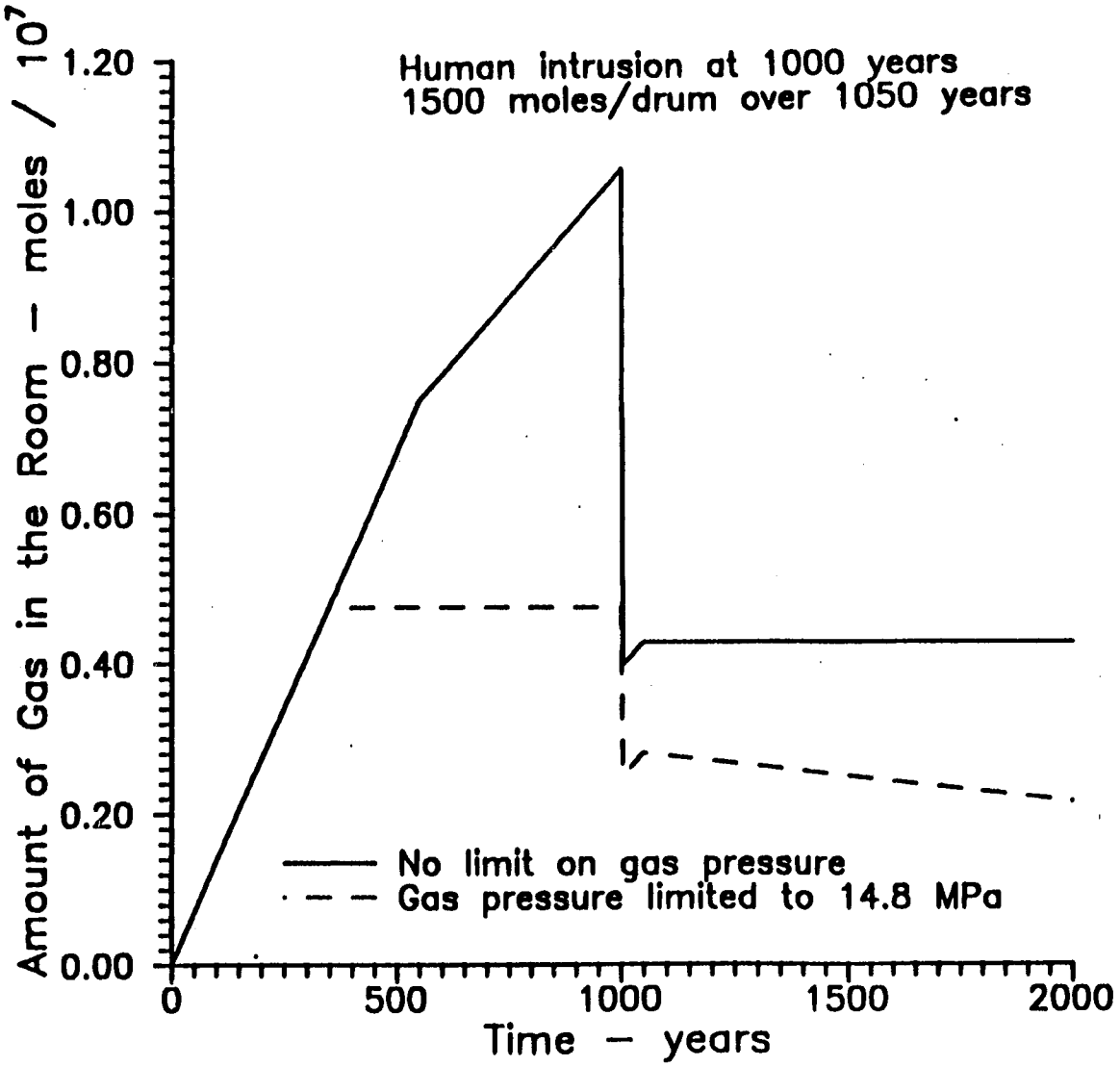


Figure 8: The assumed gas generation sequence for Case 1 and Case 2 porosity surface post-intrusion predictions.

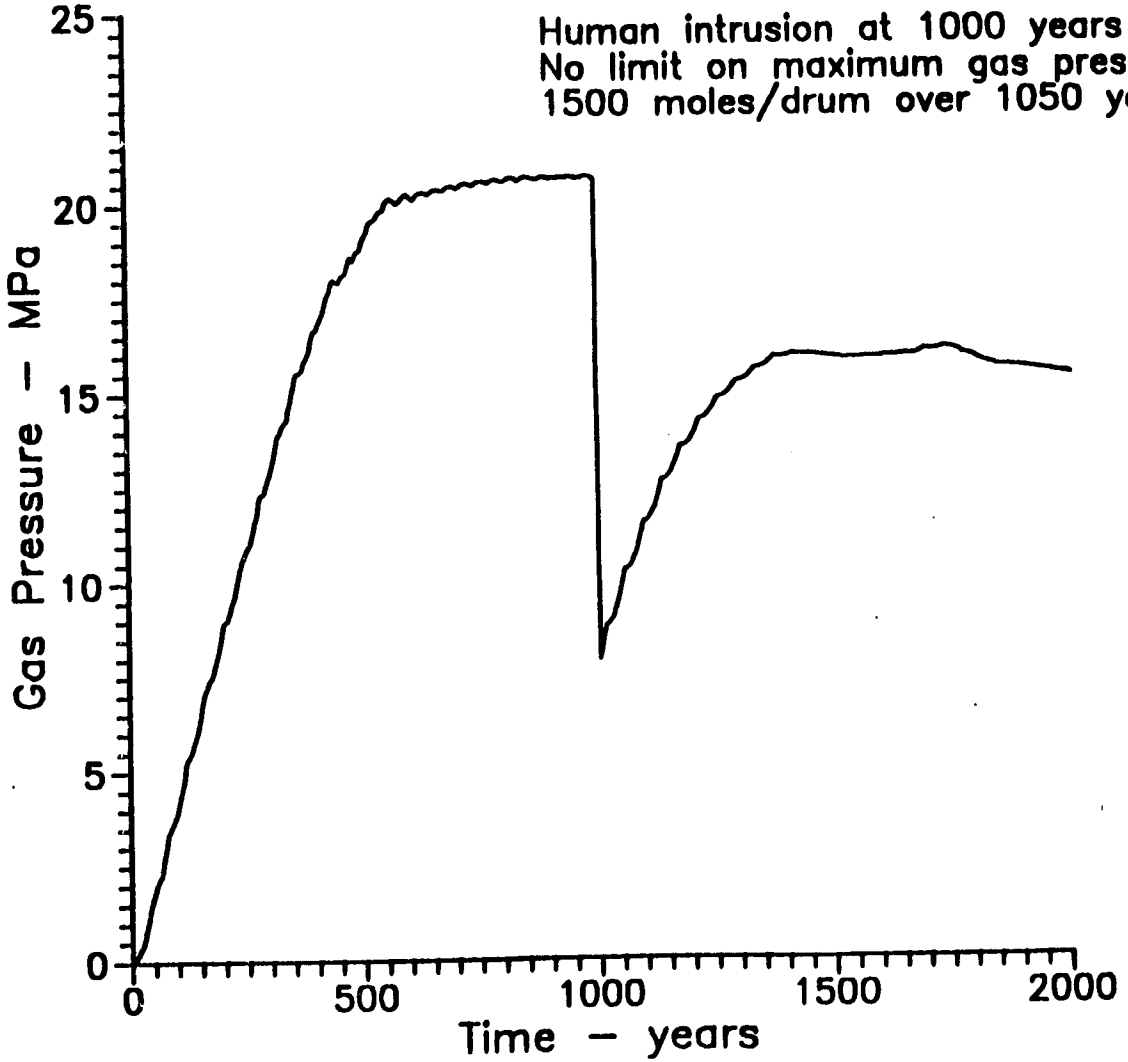


Figure 9: Gas pressure within a disposal room as a function of time assuming that there is no limit on maximum gas pressure.

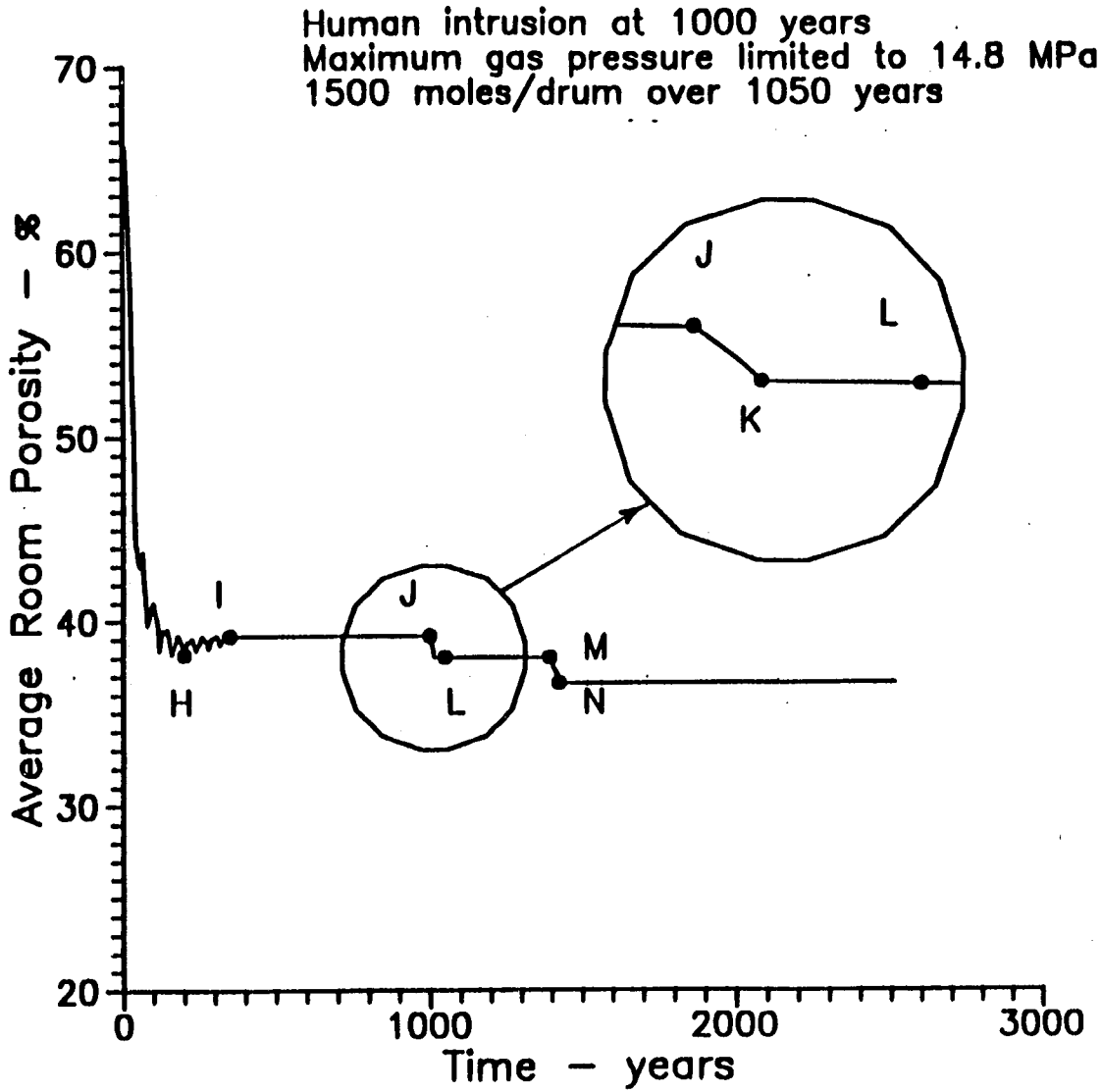


Figure 10: The average room porosity history of a disposal room as a function of time assuming the gas pressure can not exceed lithostatic pressure (Case 2).

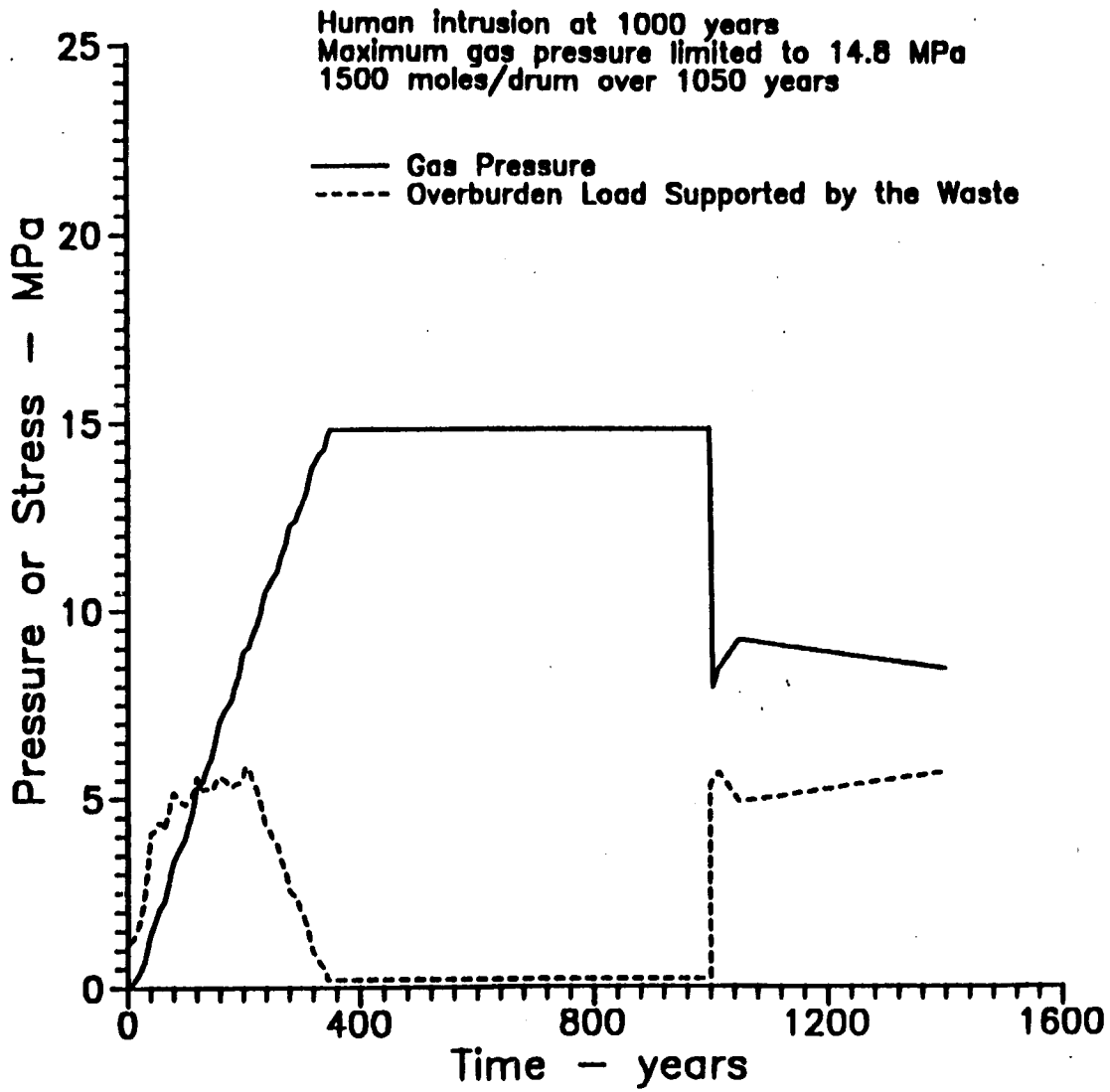


Figure 11: Gas pressure within a disposal room as a function of time assuming that the gas pressure can not exceed lithostatic pressure.

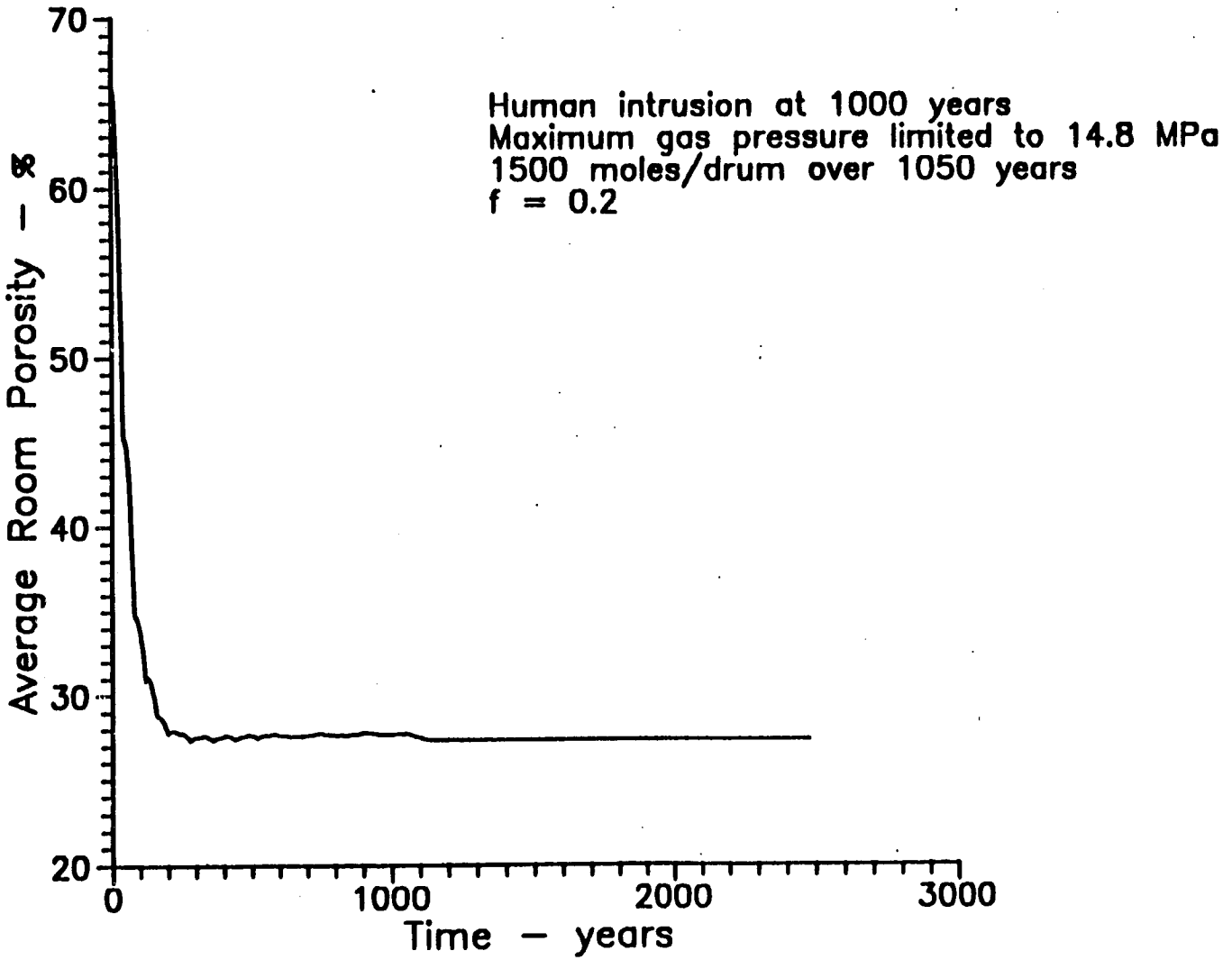


Figure 12: The average room porosity history of a disposal room with 1/5 the gas generation rate of Case 2 as a function of time. Gas generation is assumed to cease after 1050 years, and the gas pressure never exceeds lithostatic pressure.

APPENDIX B: The PHENIX Coupled Room Closure and Multiphase Flow Code

Errata:

The text references to Freeze et al., 1994 and Freeze et al., 1994a refer to SAND94-0251 and SAND93-1986. Those reports were printed in October 1995.

In the citation given as Freeze et al., 1994b, the report number should be corrected to: SAND93-1986.

Sandia National Laboratories

Albuquerque, New Mexico 87185

date: August 17, 1994

to: Barry M. Butcher 6348

from: Kurt W. Larson INTERA/6115

subject: **The PHENIX Coupled Room Closure and Multiphase Flow Code**

ABSTRACT

The PHENIX code is described, including a synopsis of results to date. PHENIX was created to begin development of a method to couple the effects of salt deformation on fluid flow at the WIPP. PHENIX simulates one aspect of the problem, room closure and multiphase fluid flow between disposal rooms and the Salado Formation. SANTOS is used to calculate room closure, and TOUGH2/EOS8 is used to calculate fluid flow and room pressures. Coupling is accomplished by an explicit, backward-in-time method. Several test simulations demonstrate the effectiveness of the coupling method, and comparisons are made to SANCHO results, SANTOS results, and TOUGH2/EOS8 results. PHENIX is available within SNL/WIPP for further studies. Particularly useful may be the ability with PHENIX to couple room closure with brine-dependent gas generation rates such as the type used by WIPP PA. PHENIX is currently an experimental code and has not been baselined in the SNL/WIPP QA system. Continued use by WIPP PA of the pressure-line interpolation method is recommended.

1.0 Background

The impact of disposal room closure due to salt creep on room volume is considered significant by the WIPP project. Among other impacts, room closure affects porosity by collapsing voids in the waste and backfill and gas pressure by compression. Due to closure, disposal room porosity is expected to reduce by a factor of about 3 from an initial 0.66, and gas pressures will increase by the same magnitude relative to an initial-volume room. Incorporating room volume changes of this magnitude is important in models of gas and brine flow between the room and Salado Formation (Freeze et al., 1994).

Due to the complexity of both multiphase flow codes and salt deformation codes, WIPP PA is currently not able to model room deformation directly. Instead, independent simulations with the code SANCHO (Stone, 1992), which uses an elastic-secondary creep constitutive model for room deformation, are the basis for incorporating room closure information into BRAGFLO, the primary PA flow

code. Room porosities are correlated with time and pressure by a suite of SANCHO simulations assuming a sealed room (no mass flux through room walls), and assuming a certain gas generation history. Porosities are assigned to room volumes in BRAGFLO by interpolation and extrapolation on the SANCHO data set with time and pressure. There are two principal concerns with this method. First, the effects of brine and gas flow on room closure may not be accurately captured. Second, the coupling is dependent on the gas generation history in BRAGFLO being similar to the gas generation history used in SANCHO (Freeze et al., 1994). Because gas generation in BRAGFLO is influenced by flow, and because parameters in BRAGFLO are chosen stochastically, this condition cannot be assured.

A study of methods developed to incorporate room closure effects in multiphase flow codes was undertaken by Freeze et al. (1994). The present PA method, called pressure-lines interpolation, was found likely to be adequate. However, a more complex method, called fluid-phase salt, was both conceptually more realistic, and had significantly different results for gas generation histories different than the SANCHO suite. The fluid-phase salt method is too complex for use in PA calculations. Because of lingering uncertainty in the adequacy of using the pressure-lines interpolation method for PA use, an effort was made to simultaneously solve the salt creep constitutive relations and multiphase flow consititive relations to better couple room closure and fluid flow.

2.0 PHENIX

PHENIX is a hybrid code created from an explicit (backwards-in-time) coupling of two codes, SANTOS (Stone, 1993) and TOUGH2/EOS8 (Pruess, 1991; Freeze et al., 1994a). It was developed collaboratively by Kurt Larson, of INTERA/6115, and C. Mike Stone of 1561, during the summer and fall of 1993. SANTOS is the successor to SANCHO and is essentially the same code but has been optimized for the Cray and has dramatically improved performance. SANTOS also has provision for single-phase fluid flow, which is not utilized in PHENIX. TOUGH2/EOS8 is a multiphase flow code with hydrogen gas and liquid brine components. In PHENIX, SANTOS is used to calculate room volume change due to salt creep, and TOUGH2/EOS8 is used to calculate room pressures, which are influenced both by volume change nad brine and gas flow.

A time-step sequence initiates with SANTOS and TOUGH2/EOS8 at the same initial time, room pressure, and room volume. At constant room pressure, SANTOS begins stepping forward with its own internal time-step procedure, changing room volume according to the elastic-creep constitutive relations. When a predetermined coupling time, typically half of a year, is reached, SANTOS execution is temporarily halted, and the coupling-time room volume is passed to

TOUGH2/EOS8. TOUGH2/EOS8 starts stepping from the initial time towards the coupling time, varying room pressure according to multiphase consititutive relations, and setting room volume by linear interpolation between the initial room volume and the coupling-time room volume just calculated by SANTOS. When the coupling time is reached by TOUGH2/EOS8, TOUGH2/EOS8 execution is temporarily halted, room pressure is passed to SANTOS, and a new time-step sequence is ready to begin. Salt creep output is controlled by SANTOS, and flow output is controlled by TOUGH2/EOS8. The domains in the two codes need not have the same discretization, which allows for flexible specification of problem parameters.

PHENIX is classified as an experimental code, is computationally inefficient (primarily because the most efficient TOUGH2/EOS8 solver is currently not robust on the Cray), and requires much user interaction for successful execution. Currently, 2,000 year simulations requires several hours of Cray machine time. It is not ready for 'production-mode' simulations or general release. A User's Manual has not been written, and the code and initial results have not been QA'd following SNL/WIPP QA procedures. These impediments to further use could be overcome with modest effort.

3.0 Results

A series of simulations was performed to demonstrate the viability of PHENIX for coupling room closure with multiphase flow. An isolated room simulation benchmarks PHENIX against SANTOS. A time-step convergence study demonstrates the effect of different time intervals between SANTOS-TOUGH2 coupling. Inclusion of far-field salt and interbeds in the TOUGH2/EOS8 domain demonstrates the effect of fluid flow between room and rock. The effect of different gas-generation assumptions is shown with a run using a brine-dependent gas generation rate. Finally, comparison is made to TOUGH2/EOS8 simulations using the Fluid-Phase Salt method for incorporating room closure.

3.1 Isolated Room Calibration

Figures 1 and 2 present room gas pressure and room porosity values for a 2000 year simulation. In these figures, SANTOS results are compared with PHENIX results, labelled here as SANTOS-TOUGH coupling. Both models use a sealed room, i.e. one in which mass flux across room walls is not allowed, and the same gas generation history. Although the results are not identical, the strong similarity encourages use of PHENIX for more complex situations. The disparity is attributed to the change from implicit to explicit coupling of pressure and volume, which is expected to be less accurate than implicit coupling.

3.2 Time-Step Convergence Study

The baseline simulation presented in Figures 1 and 2 coupled pressure and volume every 20 SANTOS time steps, or every 0.5 years. To verify that this frequency of coupling is adequate for accurate simulation, PHENIX was run with couplings occurring every 5 steps, or 0.125 years. Results are shown in Figures 3 and 4. The 5 step coupling is slightly more accurate than the 20 step coupling, but not significantly so. The 5 step coupling is more accurate, i.e. is more similar to the SANTOS solution (Figures 1 and 2), than the 0.5 year coupling. Increasing accuracy is generally expected from explicit methods as the time step decreases.

3.3 Salado Flow Coupling

A simplified, two-dimensional representation of the Salado Formation with two rock types, halite and anhydrite, and two anhydrite beds, was used to demonstrate the difference between a sealed room and a system in which fluid may flow between the room and Salado Formation. The representation has been used extensively in past models of the Salado Formation (for example, Freeze et al., 1994), and a recent study (Webb and Frear, in preparation) found that the stratigraphic simplification likely preserves sufficient detail for defensible results. Figures 5 and 6 show that porosity is similar for the two cases until 500 years, wheras pressure is higher for the fluid flow case. This occurs because brine seeping into the room occupies some pore space which is then inacessible to gas. After 500 years, porosity and pressure are lower when fluid flow between the room and rock is allowed. This happens because gas is expelled from the room, allowing both decreased pressure and decreased porosity. Similar results have been described for some other methods of simulating closure of waste disposal rooms (Freeze et al., 1994).

WIPP PA uses sealed room results, from SANCHO, and applies them to rooms open to fluxes. The difference between the baseline sealed room case and the baseline with interbeds case supports the concern that the PA room closure coupling may not yield sufficiently accurate results. However, PHENIX results to not warrant the conclusion that the WIPP PA method, pressure-lines interpolation, is inadequate.

3.4 Brine-Dependent Gas Generation Rate

A single simulation was performed with the gas generation rate being determined as a linear function of the brine saturation in the room. This method is described in Freeze et al. (1994). Figures 7 and 8 show results. Due to low total brine inflow, gas generation proceeds at a near-humid rate, which is much slower than

the brine-inundated rates assumed in the baseline simulations. Because there is less gas, pressures are lower (Figure 8), and room closure is accordingly greater (Figure 7).

3.5 Comparison to Fluid-Phase Salt Method

Comparison of PHENIX results to results based on the SANCHO models is hampered by a change in domain configuration that took place at some time prior to PHENIX development. SANCHO simulations (Stone, 1992) used a domain in which the air gap at the top of the room was represented with a physical material, whereas the SANTOS and PHENIX simulations reported here used a model in which the air gap was explicitly modeled. There is a marked difference in the results of the two models that occurs near the time of minimum room porosity for the f=1.0 case. This difference is shown in Figure 9. Because of this difference, comparison of PHENIX simulations to TOUGH2/EOS8 simulations with the Fluid-Phase Salt method can be made only by mentally accounting for the difference between SANCHO and SANTOS results.

Freeze et al. (1994) determined the Fluid-Phase Salt method to be the most accurate method for coupling room closure with multiphase fluid flow up until PHENIX. Comparison of PHENIX and Fluid-Phase Salt methods for the sealed room (baselline), Salado, and brine-dependent generation rate cases are shown in Figures 10 and 11. The Fluid-Phase Salt method is calibrated to the SANCHO series of simulations, so the spread at the porosity low is evident in these figures. Taking into account the difference between SANCHO and SANTOS, agreement between PHENIX and Fluid-Phase Salt appears very good. This result lends support to the conclusions of Freeze et al (1994) regarding the adequacy of the current WIPP PA method for incorporating room closure.

4.0 For the Future

PHENIX is a tool with great promise in studies of coupled room closure, gas generation, and brine and gas flow. If required, PHENIX could:

- be used to explore the effect of gas-generation potential, brine-dependent rates, room closure more explicitly than previously possible. This would increase confidence or reveal suspected weaknesses in the current PA coupling methods;
- be used to develop a new pressure-lines interpolation surface that better takes into account (1) brine and gas flow between the room and formation, and (2) brine-dependent gas-generation rates;

- serve as a starter platform for the development of a code that couples salt deformation with fluid flow both in the room and far-field formation.

5.0 Conclusions

Several simulations have been successfully performed with PHENIX. Several of the simulations demonstrate that PHENIX works as intended by the developers. Additional simulations begin to explore the effect on room volume and room pressure of room closure coupled with brine and gas flow. Because the most accurate constitutive relations available for room closure (in SANTOS) and brine and gas flow (in TOUGH2/EOS8) are observed by PHENIX, PHENIX results are regarded as more accurate and defensible than other methods of coupling previously investigated. However, because of a favorable comparison of PHENIX and the Fluid-Phase Salt method, previous conclusions and recommendations (Freeze et al. 1994) to PA regarding the coupling of room closure and brine and gas flow are still supported. PHENIX is an experimental code, not presently quality assured, that requires much user support to run, but the major impediments to more robust execution have been identified and are correctable. Therefore, it is expected that with modest additional effort, a quality-assured, production-mode version of PHENIX would be available to SNL/WIPP should more investigation of room-fluid flow interactions be necessary.

6.0 References

Freeze, G.A., K.W. Larson, and P.B. Davies. 1994a (Approved for Release, In Publication). A Summary of Methods for Approximating Salt Creep and Disposal Room Closure in Numerical Models of Multiphase Flow. SAND94-0251. Albuquerque, NM: Sandia National Laboratories.

Freeze, G.A., K.W. Larson, and P.B. Davies, 1994b (In Management Review). Coupled Multiphase Flow and Closure Analysis of Repository Response to Waste-Generated Gas at the Waste Isolation Pilot Plant (WIPP). SAND93-1936. Albuquerque, NM: Sandia National Laboratories.

Pruess, K. 1991. TOUGH2 - A General-Purpose Numerical Simulator for Multiphase Fluid and Heat Flow. LBL-29400. Berkeley, CA: Lawrence Berkeley Laboratory.

Stone, C.M., R.D. Krieg, and Z.E. Beisinger. 1985. SANCHO, A Finite Element Computer Program for the Quasistatic, Large Deformation, Inelastic

Response of Two-Dimensional Solids. SAND84-2618. Albuquerque, NM: Sandia National Laboratories.

Stone, C.M. 1992. "Creep Closure Behavior of Waste Disposal Rooms in Bedded Salt due to Gas Generation Produced by Several Alternatives of the Engineered Alternatives Task Force," memorandum to B.M. Butcher (October 6). Albuquerque, NM: Sandia National Laboratories. (See Appendix C of Freeze et al., 1994a, cited above).

Stone, C.M. 1993. "Application of SANTOS to Waste Disposal Room Problems Including a Demonstration of Coupled Structural/Porous Flow Capability," memorandum to B.M. Butcher (March 31). Albuquerque, NM: Sandia National Laboratories (see Appendix C of Freeze et al., 1994a, cited above).

Copy to:

C.M. Stone	1561
T. Corbet	6307
F.T. Mendenhall	6308
P.B. Davies	6115
P. Vaughn	6342
G.A. Freeze	INTERA
V.A. Kelley	INTERA

6303 SWCF HYD
WBS 1.1.4.2.2 - Salado Hydrology and Transport - Model Development

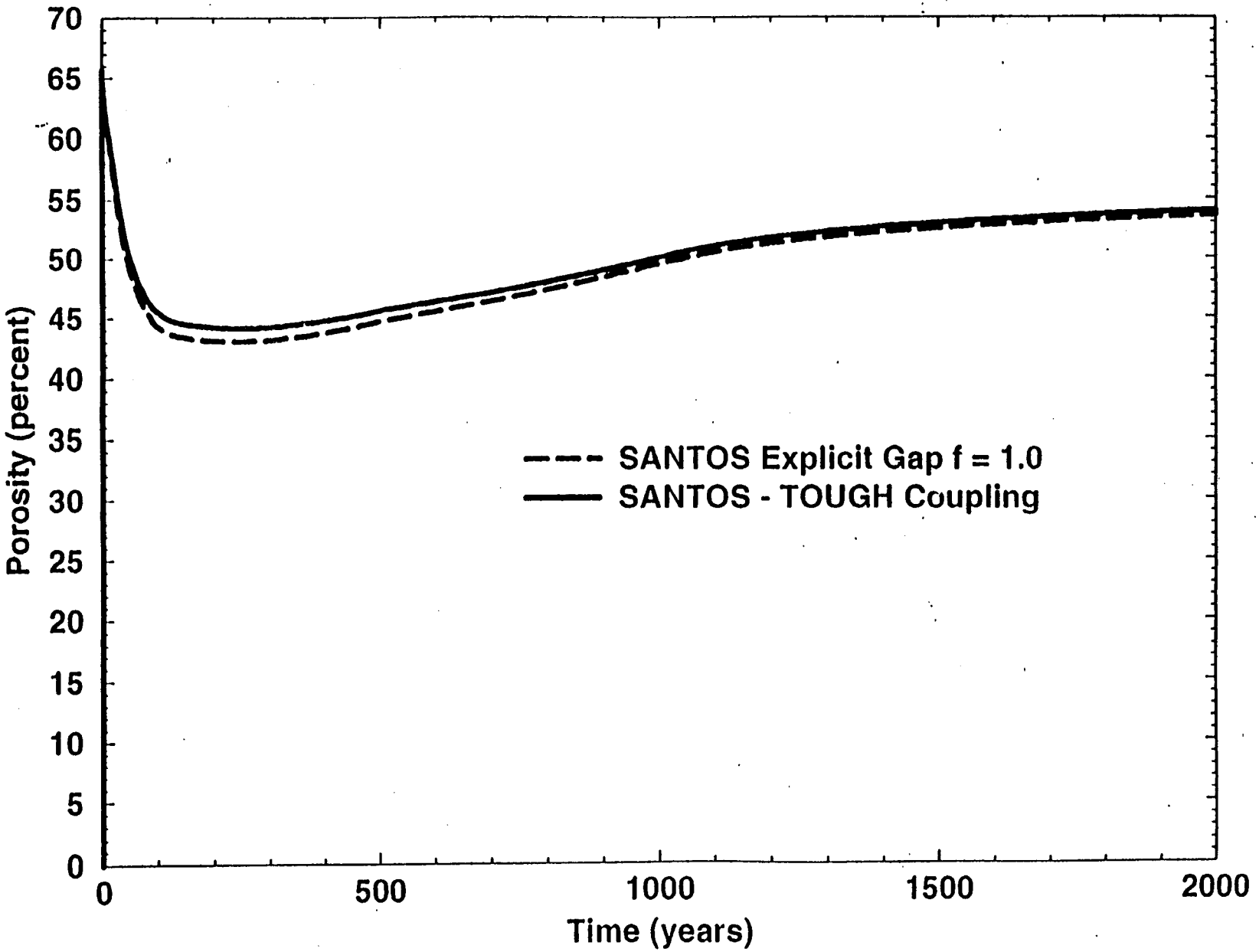


Figure 1. Comparison of SANTOS and PHENIX (here labelled SANTOS-TOUGH Coupling) porosity for a sealed disposal room.

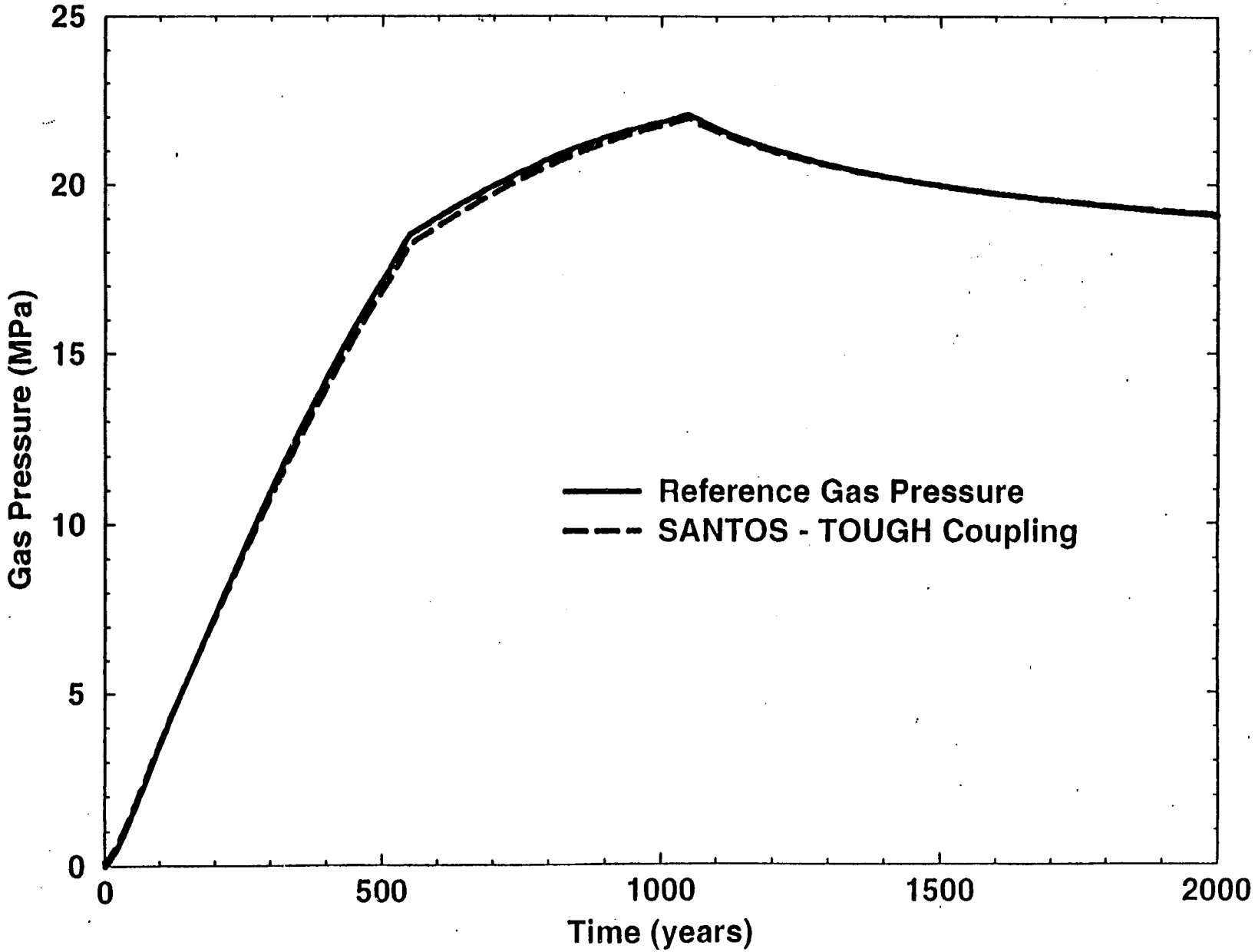


Figure 2. Comparison of SANTOS and PHENIX (here labelled SANTOS-TOUGH Coupling) gas pressure for a sealed disposal room.

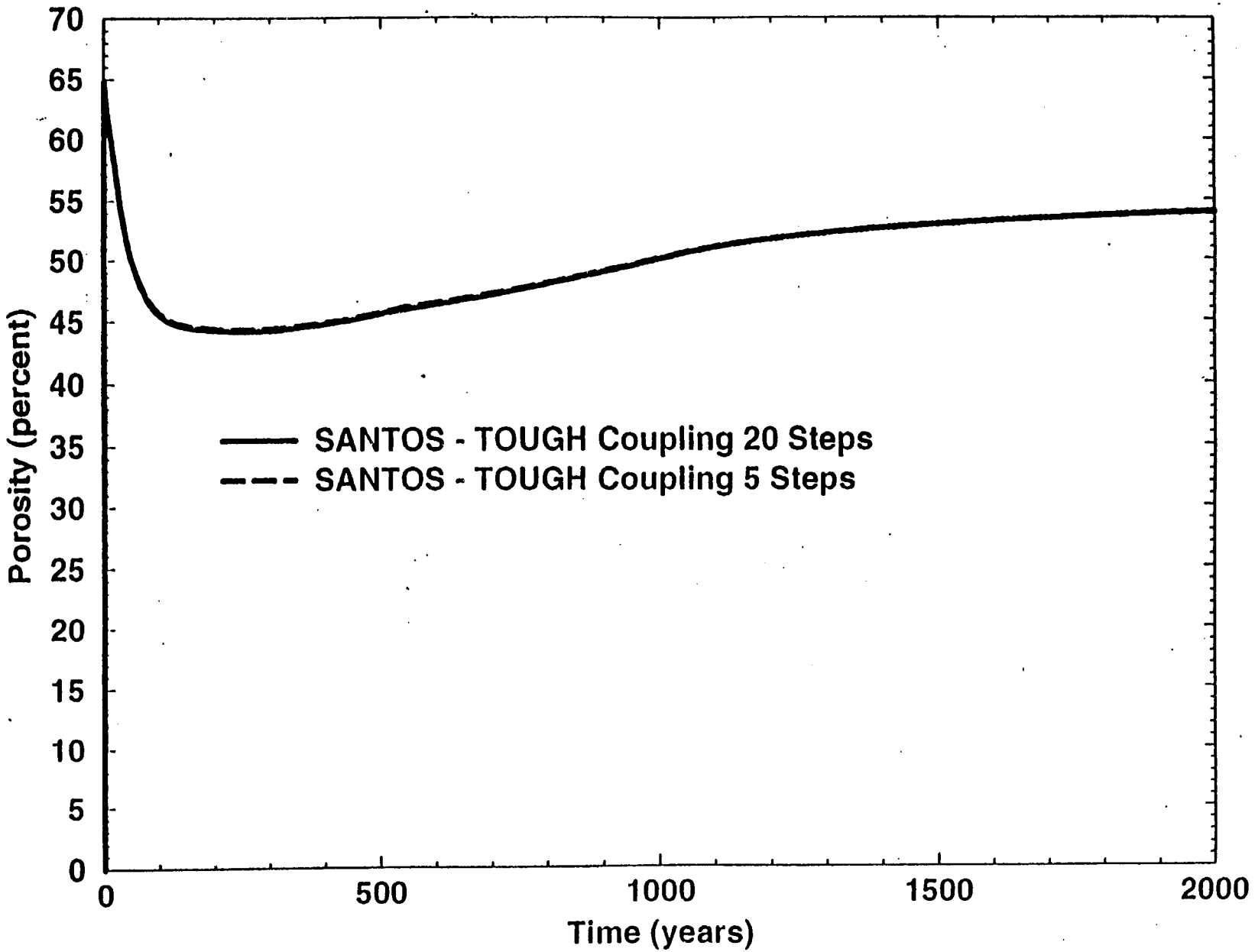


Figure 3. Effect of frequency of time-step coupling in PHENIX (here labelled SANTOS-TOUGH Coupling) on porosity.

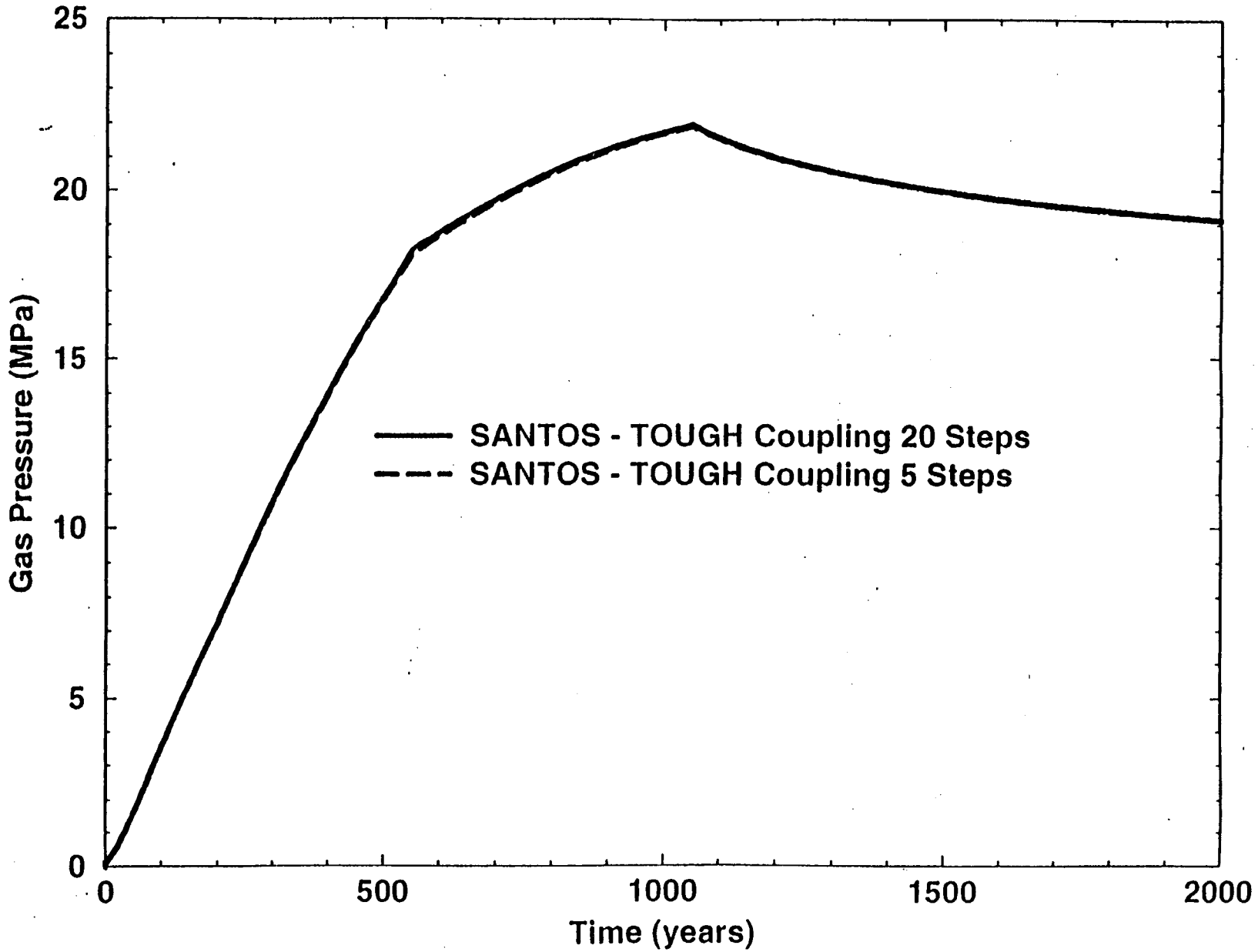


Figure 4. Effect of frequence of time-step coupling in PHENIX (here labelled SANTOS-TOUGH Coupling) on gas pressure.

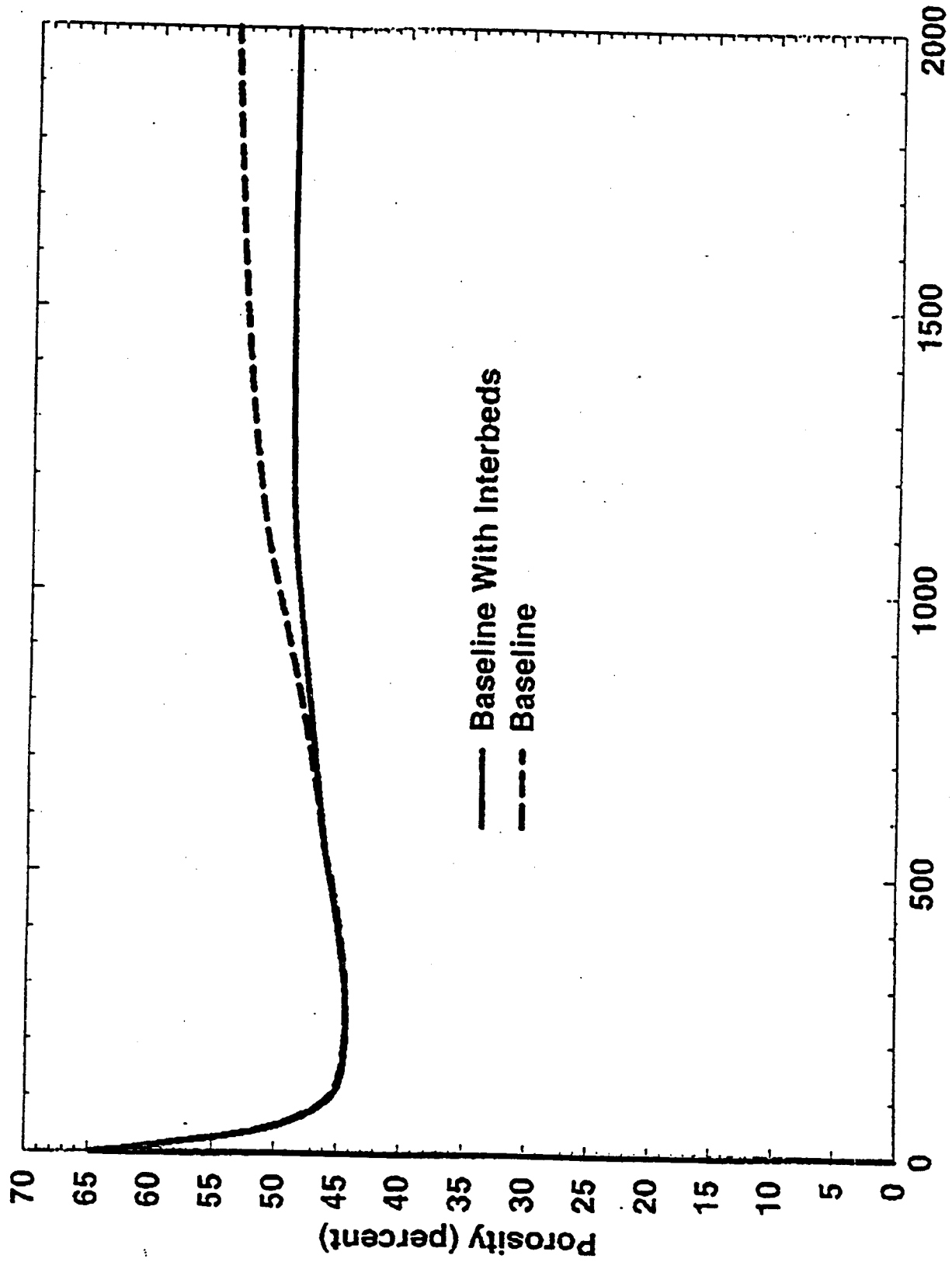


Figure 5. Effect on porosity of adding halite and interbeds to the fluid flow domain in PHENIX.

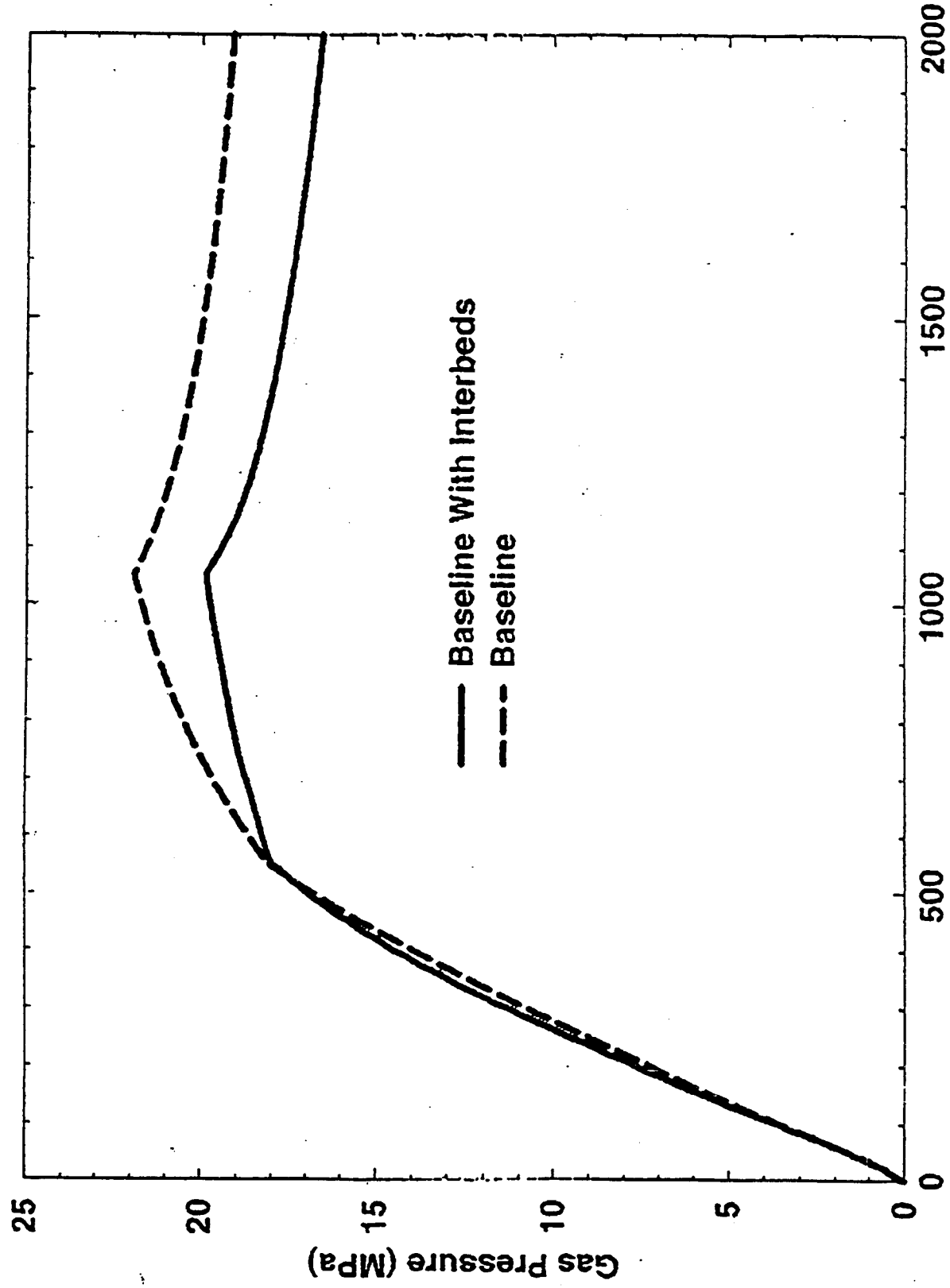


Figure 6. Effect on gas pressure of adding halite and interbeds to the fluid flow domain in PHENIX.

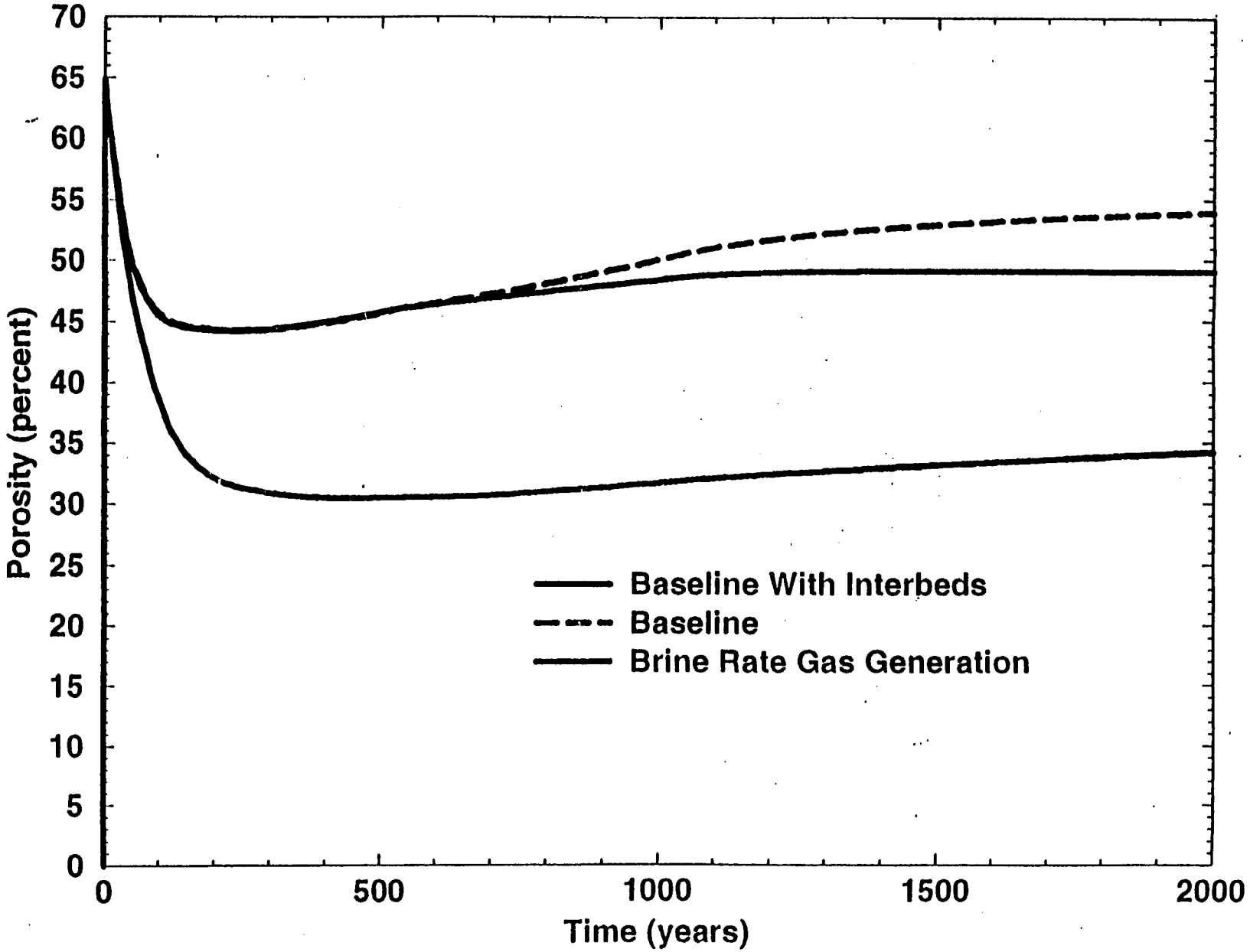


Figure 7. Comparison of porosity for f = 1.0 sealed room and f = 1.0 halite and interbeds simulations to a brine-dependent gas generation simulation.

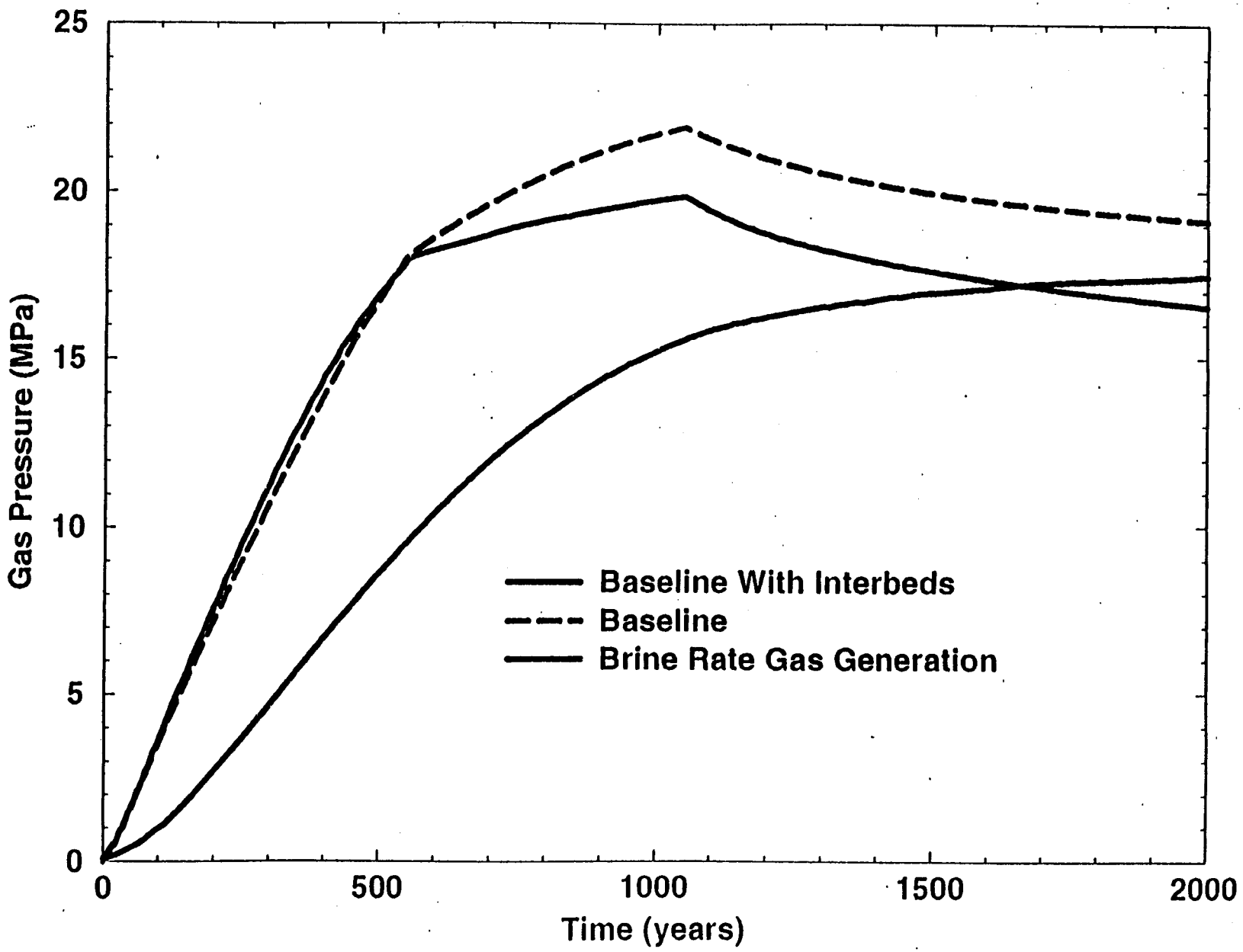


Figure 8. Comparison of gas pressure for f = 1.0 sealed room and f = 1.0 halite and interbeds simulations to a brine-dependent gas generation simulation.

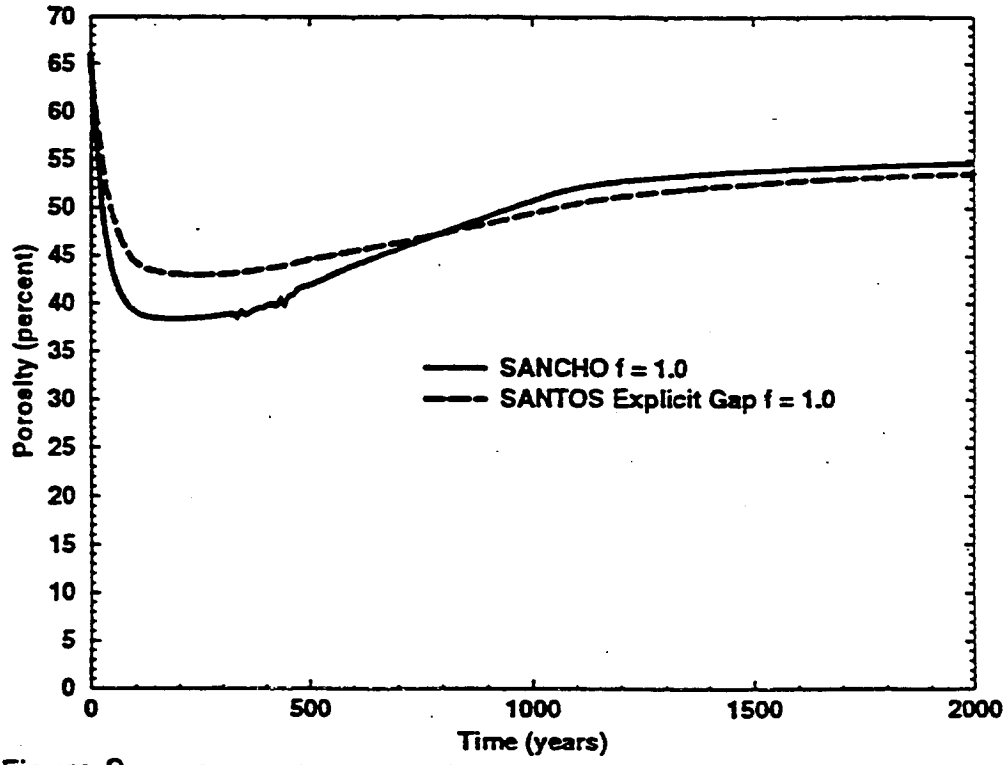


Figure 9. Comparison of Effective Disposal Room Porosity Calculations Between a Reference Model Analysis With SANCHO and SANTOS With the Headspace Explicitly Modeled.

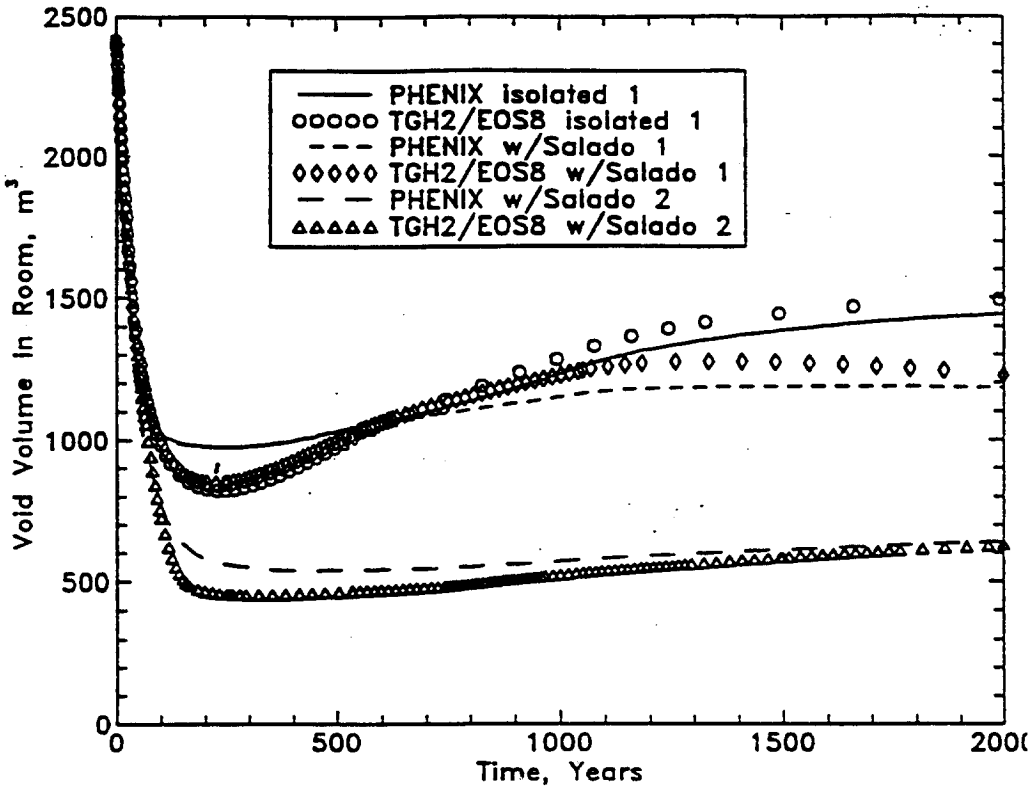


Figure 10.– Comparison of void volume for several simulations calculated with PHENIX to comparable simulations calculated with the Fluid-Phase Salt method in TOUGH2/EOS8. Sealed room, halite and interbed, and brine dependent gas generation rate results are plotted.

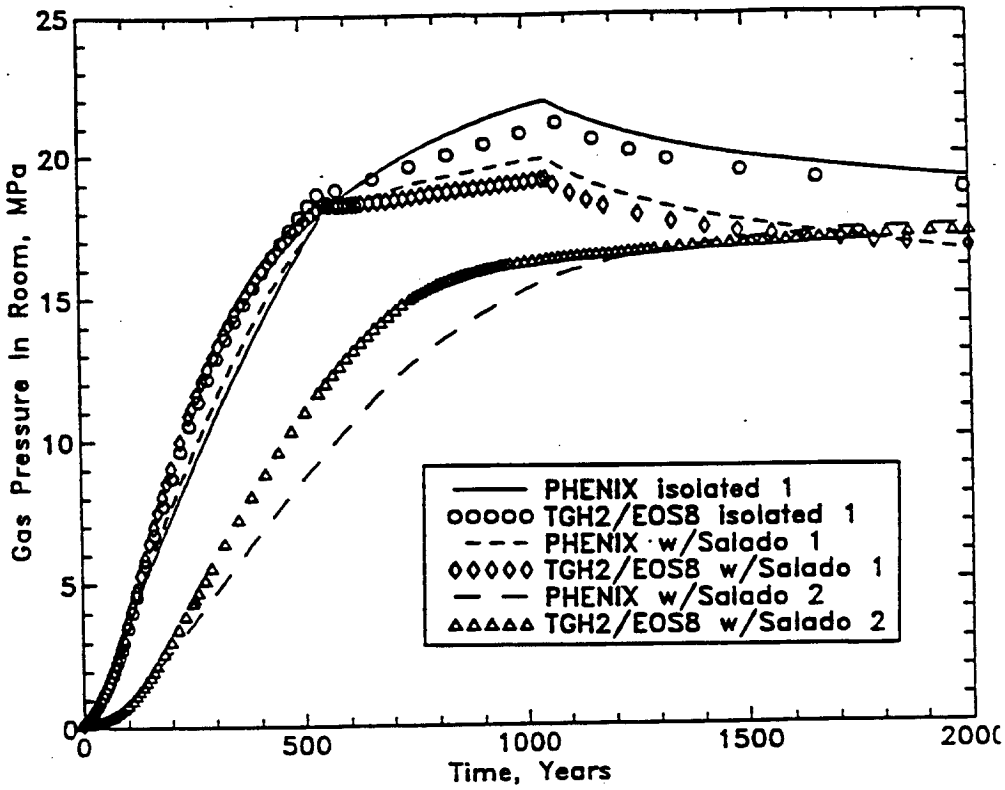


Figure 11. Comparison of gas presure for several simulations calculated with PHENIX to comparable simulations calculated with the Fluid-Phase Salt method in TOUGH2/EOS8. Sealed room, halite and interbed, and brine dependent gas generation rate results are plotted.

APPENDIX C: **Backfill Sensitivity Study-Creep Closure Behavior of an "Equivalent" Empty Room at the North End of the WIPP Subjected to Gas Generation.**

Sandia National Laboratories

Albuquerque, New Mexico 87185

date: August 29, 1994

to: B. M. Butcher, 6345 (MS1341)

from: J. Guadalupe Argüello, 1561

subject: Backfill Sensitivity Study – Creep Closure Behavior of An "Equivalent" Empty Room at the North End of the WIPP Subjected to Gas Generation

Introduction

The WIPP Performance Assessment organization is responsible for the development of the performance assessment model to be used for determining if the repository is in compliance with the EPA standard (40 CFR Part 191). A part of this overall repository model is the Disposal Room model which provides information regarding the response of the disposal rooms in the Waste Storage Area of the WIPP. Of particular interest is information about the porosity of the waste and the backfill at any point in time. Porosity is important because it gives estimates of how much brine could be available within the disposal room for transporting radionuclides from the repository and their rate of transport.

In addition to the information regarding the response of the disposal rooms in the Waste Storage Area of the WIPP, information is also needed regarding the response of the rooms, drifts, and haulage-ways comprising the North End of the WIPP, i.e., the Experimental Region. Under a current disposal scenario being investigated, for purposes of sensitivity analyses on the consequences of backfilling or lack thereof, these excavated areas comprising the North End will not be backfilled with either waste or crushed-salt backfill. As such, there will be nothing to impede their creep closure other than the gas that might potentially be generated within the disposal rooms of the Waste Storage Area, which could then escape into these empty rooms and drifts in the North End and pressurize them.

This memorandum documents the mechanical creep closure analyses performed for an "equivalent" long room representative of the North End of the WIPP. The information required from these analyses are curves of room void volume as a function of time for various values of the gas generation rate. The generated curves can then be combined to produce a porosity surface for use in the repository Performance Assessment model. The next section of this memo describes how the North End was idealized into the resulting "equivalent" room as well as the gas generation conditions that were used in the analyses. This is followed by a section that discusses the geomechanical model used and one discussing the results obtained from the analyses. A final section summarizes what was learned from this study.

Idealization of North End and Gas Generation

The area of interest for these analyses is shown in Figure 1 and includes the various rooms,

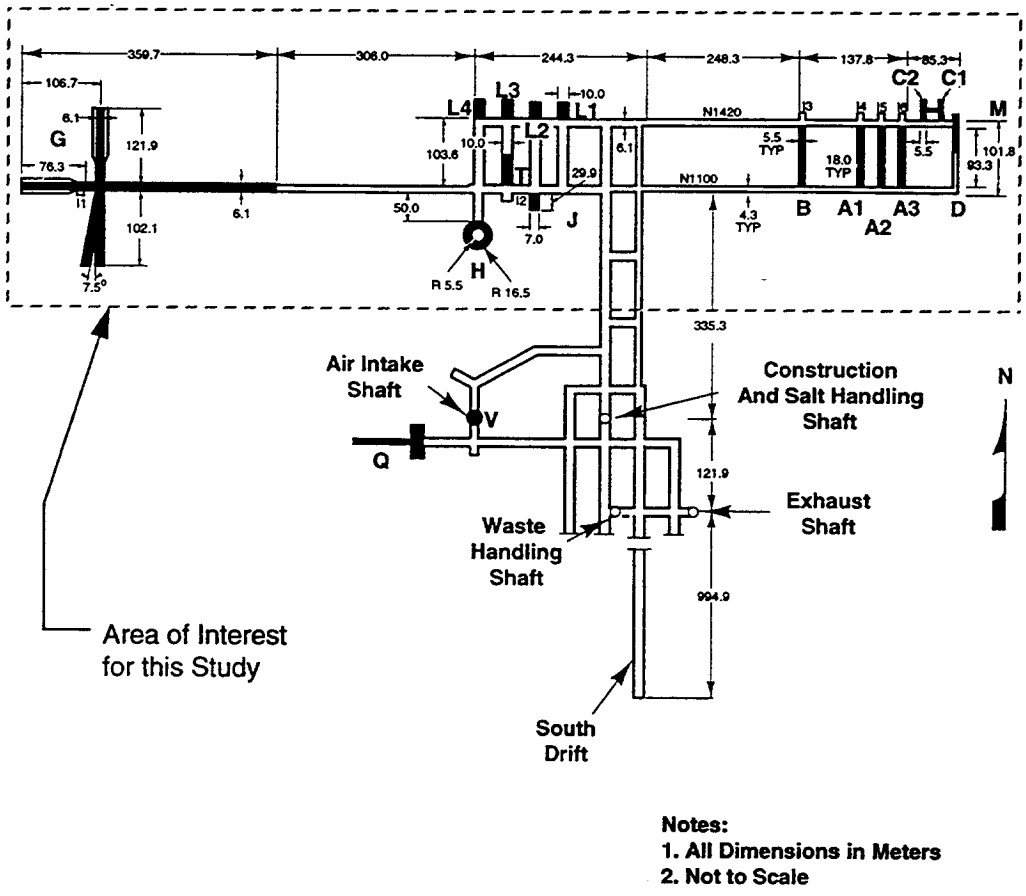


Figure 1 Layout of North End of WIPP

drifts, and haulage-ways of the Experimental Region. The figure clearly shows that there are a variety of cross-sectional dimensions and lengths for these excavations. According to Butcher [1], the total excavated area in question is approximately 21,610 m^2 and constitutes a total volume of approximately 71,900 m^3. This volume has in turn been translated [1] to an "equivalent" average room height, width, and length of 3.33 m, 5.94 m, and 3,635 m, respectively. Using this information, Butcher [2] determined that to produce the same final state in the North End as in the Waste Storage Area (using a maximum gas potential of 1600 moles/drum for the waste in the Waste Storage Area), the gas generation rate into the North End of the WIPP should be 400,000 moles/year for the first 550 years and 200,000 moles/year for the next 500 years, with gas generation terminating at the end of 1,050 years. This was later revised [3] to use a maximum gas potential of 3,200 moles/drum. Thus, the gas generation rates used in these analyses were 800,000 moles/year for the first 550 years and 400,000 moles/year for the next 500 years. As before, gas generation

stopped at the end of 1,050 years. The total gas potential into the North End with time is thus shown in Figure 2.

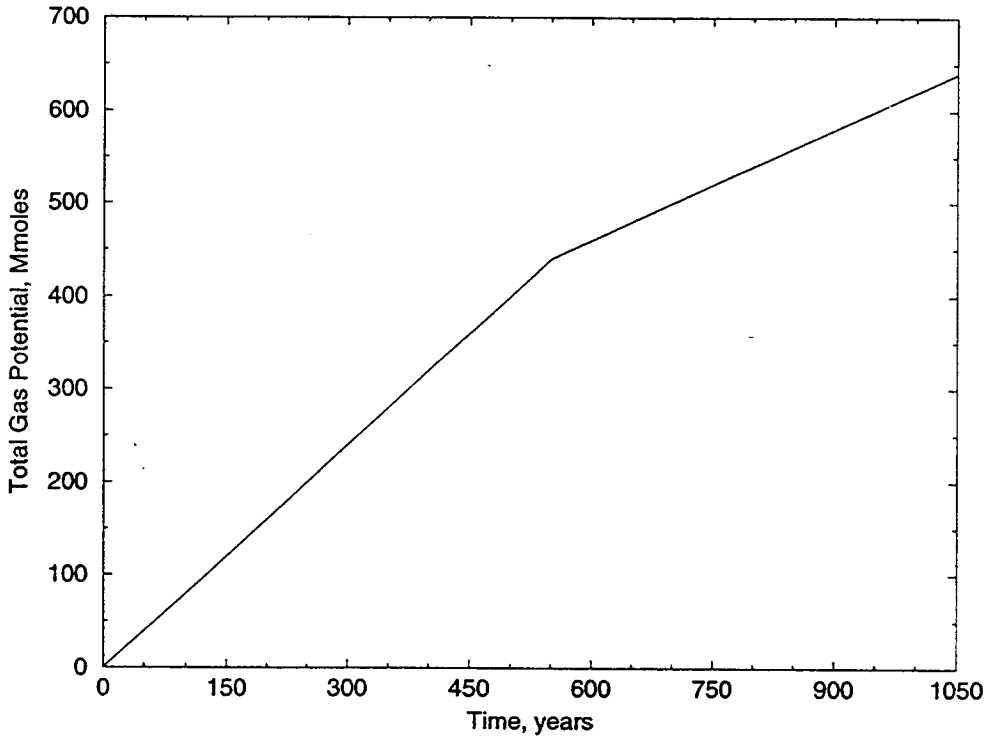


Figure 2 Total Gas Potential for North End of WIPP

The quasi-static, large deformation finite element code SANTOS [4] was used for the analyses. It has been modified to compute the room pressure and to apply the resulting forces to nodes on the room boundary. The gas pressure was computed from the ideal gas law based on the current free volume in the room. Specifically, the gas pressure, p_g, was computed with the following relationship:

$$p_g = f\frac{NRT}{V}, \qquad \text{(EQ 1)}$$

where N, R, and T are the mass of gas in g-moles, the universal gas constant, and the absolute temperature in degrees Kelvin. The variable V is the current volume of the "equivalent" empty room. After each iteration in the analysis, the current room volume is calculated based on the locations of the nodes on the boundary of the room. The variable f is a multiplier used in the study to scale the pressure by varying the amount of gas generation. A value of f=1 corresponds to an analysis with full gas generation, while a value of f=0 corresponds to no internal pressure increase due to gas generation.

Geomechanical Model

A two-dimensional plane strain disposal room model, as shown in Figure 3, was used for

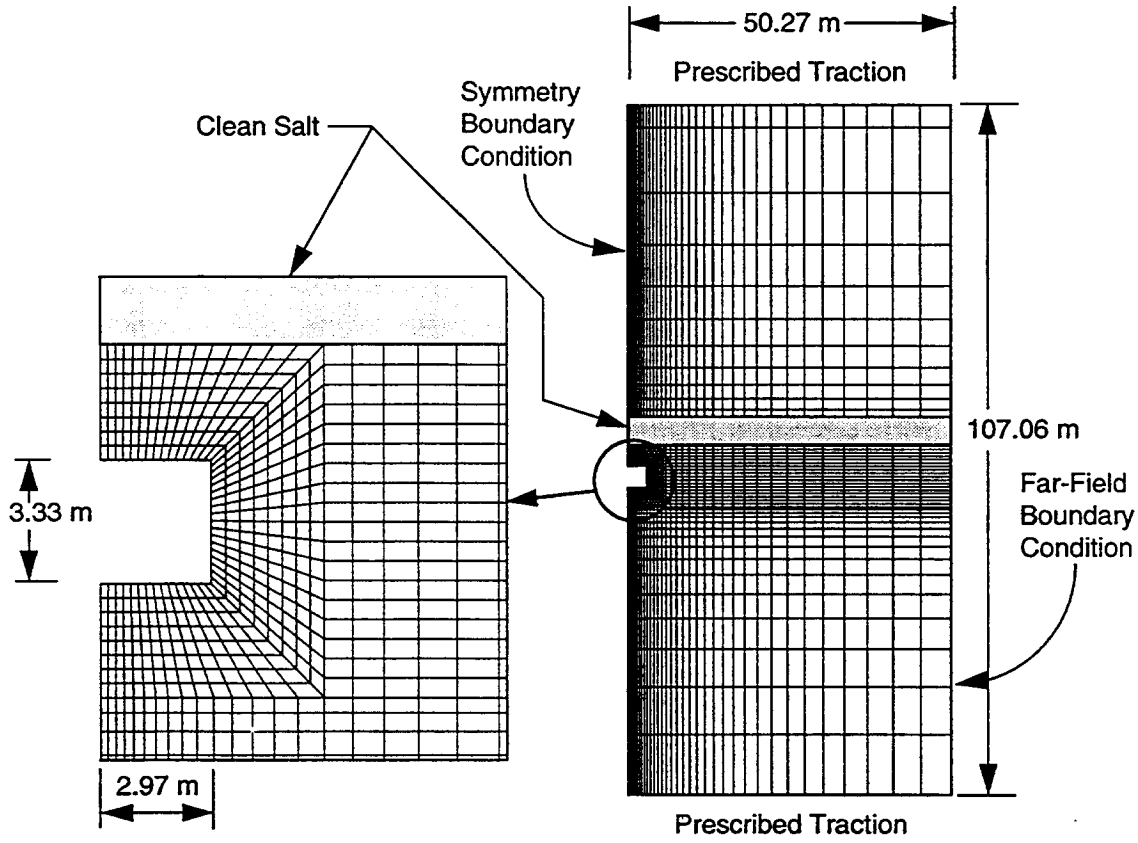


Figure 3. Finite Element Mesh and Boundary Conditions Used in SANTOS Analyses

the SANTOS analyses. The model represents the room as an isolated room located at the repository horizon. Making use of symmetry, only half of the room needed to be modeled. The left boundary is a plane of symmetry and the right boundary, located approximately 50 m away, represents a far-field boundary. The upper and lower boundaries are also located approximately 50 m from the room. A lithostatic stress ($\sigma_x = \sigma_y = \sigma_z$) that varies with depth is used as the initial stress on the configuration and gravity forces are included. The idealized stratigraphy for the WIPP underground used in the geomechanical model is the stratigraphy as redefined by Munson [5]. However, as has been typically done in other analyses for Munson [5], it is further assumed that the configuration is composed of only clean salt and argillaceous salt. The single layer of clean salt is labelled in the figure with the rest of the material in the configuration being argillaceous salt. The model contains 1,829 elements and 1,937 nodal points. A zero-displacement boundary condition in the horizontal direction was applied on both the left and right boundaries of the model. A prescribed normal traction of -13.57 MPa was applied on the upper boundary and another of -15.98 MPa was applied on the lower boundary to simulate the overburden load. As

previously described, within the room a pressure, p_g, was applied along the room boundary.

A combined transient-secondary creep constitutive model for rock salt attributed to Munson and Dawson [6] and described by Munson, et. al [5] was used for the clean and argillaceous salt. The model can be decomposed into an elastic volumetric part defined by,

$$\varepsilon_{kk} = \frac{\sigma_{kk}}{3K}, \qquad \text{(EQ 2)}$$

(where the ε_{ij} and the σ_{ij} are the total strain and stress components, respectively, and K is the elastic bulk modulus) and a deviatoric part defined by,

$$\dot{s}_{ij} = 2G\left(\dot{e}_{ij} - F\dot{\varepsilon}_s \left[\frac{\cos 2\theta}{\cos 3\theta \sqrt{J_2}} s_{ij} - \frac{\sqrt{3}\sin\theta}{\cos 3\theta J_2} \{ s_{ip}s_{pj} - \frac{2J_2}{3}\delta_{ij} \} \right] \right), \qquad \text{(EQ 3)}$$

where the second term of the above equation represents the creep contribution. In the above equation, s_{ij} is the deviatoric stress defined as $s_{ij} = \sigma_{ij} - \frac{\sigma_{kk}}{3}$, G is the elastic shear modulus, and e_{ij} is the deviatoric strain defined by $e_{ij} = \varepsilon_{ij} - \frac{\varepsilon_{kk}}{3}$.

In the creep term of Equation 3, F is a multiplier on the steady-state creep rate to simulate the transient creep response according to the following,

$$F = \begin{cases} e^{\Delta[1-\zeta/\varepsilon_t^*]^2}, & \zeta < \varepsilon_t^* \\ 1, & \zeta = \varepsilon_t^* \\ e^{-\delta[1-\zeta/\varepsilon_t^*]^2}, & \zeta > \varepsilon_t^* \end{cases}, \qquad \text{(EQ 4)}$$

where Δ and δ are work-hardening and recovery parameters, respectively, and ε_t^* is the so-called transient strain limit. Finally, ζ is an internal state variable whose rate of change is determined by the following evolutionary equation,

$$\dot{\zeta} = (F-1)\,\dot{\varepsilon}_s. \qquad \text{(EQ 5)}$$

In Equation 4, the work-hardening parameter Δ is defined as $\Delta = \alpha + \beta \log(\bar{\sigma}/G)$ where α and β are constants. The variable $\bar{\sigma}$ is the equivalent Tresca stress given by

$\bar{\sigma} = 2\sqrt{J_2}\cos\theta$ where $\theta = \frac{1}{3}\text{asin}\left[\frac{-3\sqrt{3}J_3}{2(J_2)^{3/2}}\right]$ is the Lode angle and is limited to the range $-\frac{\pi}{6} \le \theta \le \frac{\pi}{6}$. The variables J_2 and J_3 are the second and third invariants of the stress deviator given by $J_2 = \frac{1}{2}s_{pq}s_{qp}$ and $J_3 = \frac{1}{3}s_{pq}s_{qr}s_{rp}$, respectively. The recovery parameter δ is held constant. The transient strain limit is given by $\varepsilon_t^* = K_o e^{cT}(\bar{\sigma}/G)^M$ where K_o, c, and M are constants.

The steady-state, or secondary creep, strain rate, $\dot{\varepsilon}_s$, is given by

$$\dot{\varepsilon}_s = A_1 e^{-Q_1/RT}\left(\frac{\bar{\sigma}}{G}\right)^{n_1} + A_2 e^{-Q_2/RT}\left(\frac{\bar{\sigma}}{G}\right)^{n_2} + |H|\left[B_1 e^{-Q_1/RT} + B_2 e^{-Q_2/RT}\right]\sinh\left[\frac{q(\bar{\sigma}-\sigma_o)}{G}\right]; \quad \text{(EQ 6)}$$

where the A_is and B_is are constants, the Q_is are activation energies, T is the absolute temperature, R is the universal gas constant, the n_is are the stress exponents, q is the so-called stress constant, σ_o is the stress limit of the dislocation slip mechanism, and $|H|$ is the Heaviside step function with the argument $(\bar{\sigma} - \sigma_o)$. The material constants corresponding to the clean and argillaceous salt, used in the analyses, are given in Table 1 and Table 2.

The SANTOS analyses were carried out to a simulation time of 10,000 years. Seven cases of gas generation were investigated, these were for f=0.0, 0.01, 0.1, 0.2, 0.4, 0.6, and 1.0. The input file for one of the SANTOS analyses is included in Appendix I. The other files are identical except for the title line, and the fact that a different value of f was used for each run (this feature was internal to the code and did not change the input file).

Results of the Analyses

The results of interest are the pressure buildup in the "equivalent" room and the corresponding room volume (from which porosity can be deduced). Figure 4 shows the "equivalent" room pressure histories for the various values of f. Obviously for f=0, the amount of gas generation is zero resulting in a zero pressure in the room for all times. As would be expected in all other cases, the room pressure rises during the gas generation period of 1,050 years. Thereafter in time, there appears to be a transition in the character of the response at about f=0.2. For f values greater than 0.2, the room pressure begins to drop after gas generation stops, and for values less than 0.2, the room pressure continues to rise

Table 1: Elastic Properties

G MPa	E MPa	ν
12,400	31,000	0.25

Table 2: Creep Properties

Parameters (units)	Clean Salt	Argillaceous Salt
A_1 (/sec)	8.386E22	1.407E23
Q_1 (cal/mole)	25,000	25,000
n_1	5.5	5.5
B_1 (/sec)	6.086E6	8.998E6
A_2 (/sec)	9.672E12	1.314E13
Q_2 (cal/mole)	10,000	10,000
n_2	5.0	5.0
B_2 (/sec)	3.034E-2	4.289E-2
σ_o (MPa)	20.57	20.57
q	5,335	5,335
M	3.0	3.0
K_o	6.275E5	2.470E6
c (/T)	9.198E-3	9.198E-3
α	-17.37	-14.96
β	-7.738	-7.738
δ	0.58	0.58

throughout the 10,000 year simulation. For example with f=1.0 (full gas generation) the room pressure increases monotonically during the period of gas generation and reaches a value slightly larger than 24 MPa at 1,050 years. When the gas generation ceases at this time, the room pressure begins to drop reaching a value slightly less than 19 MPa at 10,000 years. On the other end of the range for f, an interesting case is f=0.01 (i.e., one percent of full gas generation). The figure clearly shows that for even this tiny amount of gas generation, the pressure in the room rises significantly (4 MPa at the end of 10,000 years) to approximately 27 % of the value of the lithostatic stress at the repository horizon.

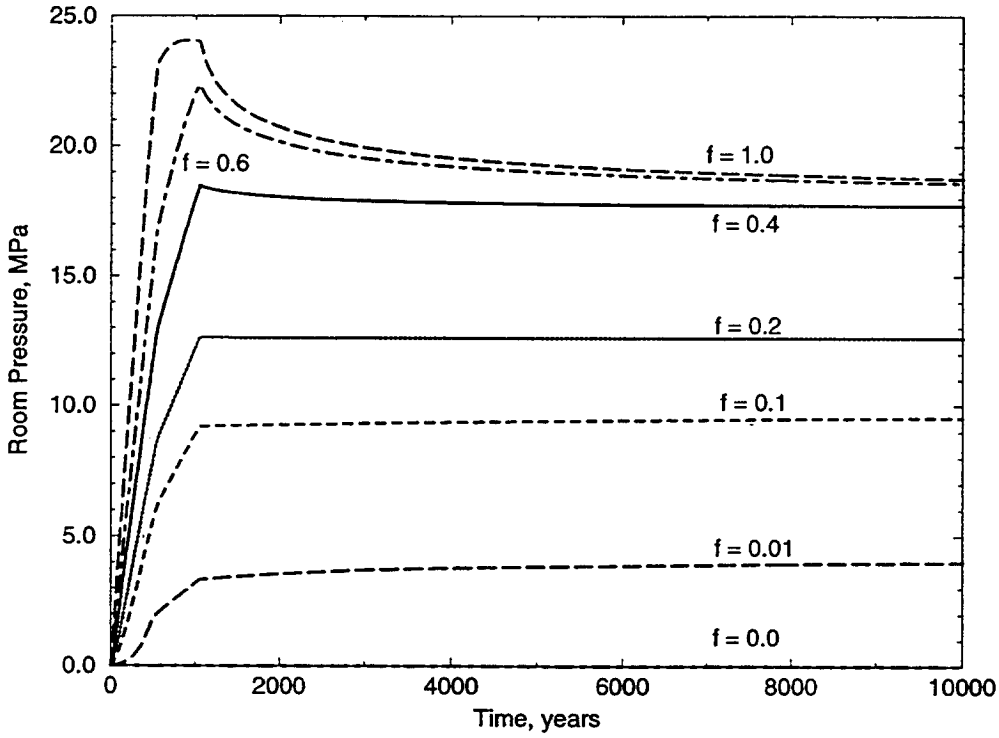


Figure 4 Room Pressure Histories for "Equivalent" Room at WIPP North End

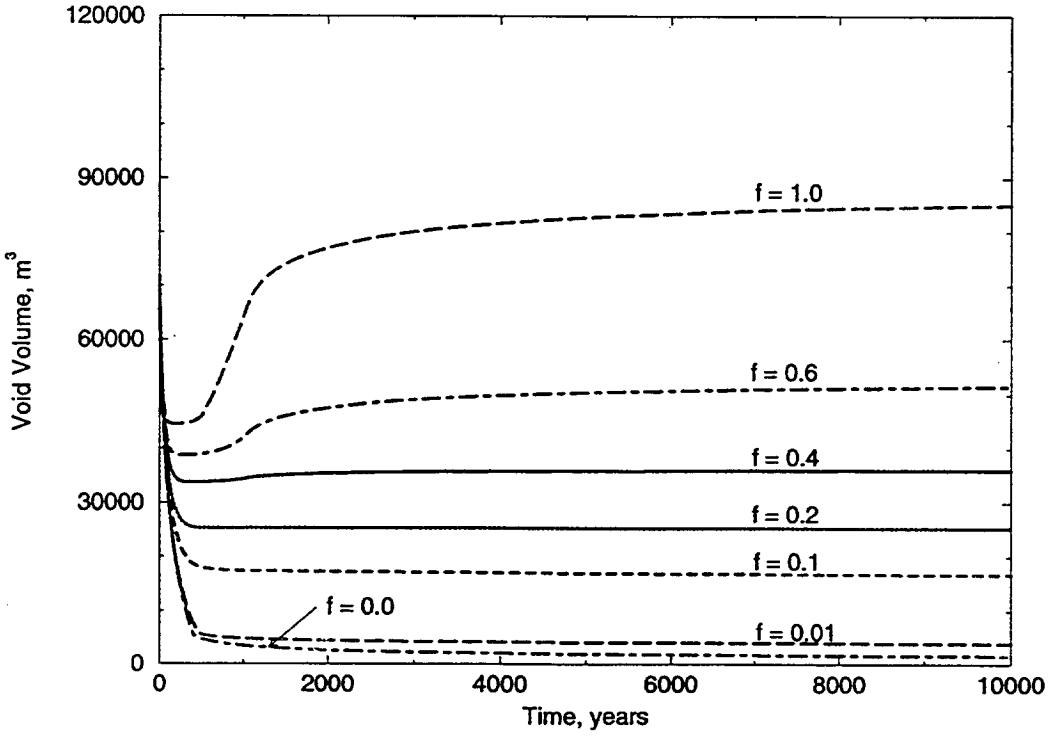


Figure 5 Room Volume Histories for "Equivalent" Room at WIPP North End

Figure 5 shows the "equivalent" room void volume histories for the seven cases of gas generation considered. As would be expected, the void volume drops monotonically from

its initial value of 71,900 m^3 for the first 100 to 500 years, depending on the value of f. Thereafter, once again, there appears to be a transition in response at about f=0.2. For values of f below that value, the volume continues to decrease with time but at a slower rate, as the roof and floor and ribs start coming into contact with one another. For values of f greater than 0.2, the volume starts to increase. In fact, for the full gas generation case of f=1, the room actually inflates to a volume of about 85,000 m^3 at the end of the simulation, which is greater than the original volume. The volume reached at this same time for the case without any gas generation, f=0, is approximately 1600 m^3. Even though a significant percentage of lithostatic stress was reached in terms of room pressure for f=0.01, the volume for this case at 10,000 years is seen to be only about 4,000 m^3, slightly more than twice that for the f=0 case.

Summary of Results

Calculations of the mechanical creep closure response of an "equivalent" room in the North End of the WIPP have been performed to allow three-dimensional porosity surfaces of the North End to be constructed for WIPP Performance Assessment activities. Data supplied to B. M. Butcher consisted of room pressure and volume histories for various gas generation rates for a period of 10,000 years following excavation. Closure results from the calculations show rapid closure of the "equivalent" room occurring during the first 100 to 500 years following excavation. Depending upon the gas generation rate, the room will either continue to experience a decrease in volume, but at a slower rate, due to continued creep closure of the room or an increase volume due to the action of the internally generated pressure acting on the room boundaries.

References

1. Butcher, B. M., "Backfill Sensitivity Study Parameters," Memorandum to and J. G. Argüello, Jr., 1561, 0443, Sandia National Laboratories, Albuquerque, New Mexico, June 8, 1994.

2. Butcher, B. M., "Backfill Sensitivity Study Parameters: Correction," Memorandum to and J. G. Argüello, Jr., 1561, 0443, Sandia National Laboratories, Albuquerque, New Mexico, June 21, 1994.

3. Butcher, B. M., Personal Communication (Telephone Conversation of June 30, 1994 during which preliminary results were discussed).

4. Stone, C. M., SANTOS – *A Two-Dimensional Finite Element Program for the Quasistatic, Large Deformation, Inelastic Response of Solids*, SAND90-0543, Sandia National Laboratories, Albuquerque, New Mexico, in preparation.

5. Munson, D. E., A. E. Fossum, and P. E. Senseny, Advances in Resolution of Discrepancies Between Predicted and Measured In Situ WIPP Room Closures, SAND88-2948, Sandia National Laboratories, Albuquerque, New Mexico, 1989.

6. Munson, D. E. and P. R. Dawson, *A Transient Creep Model for Salt During Stress Loading and Unloading*, Sandia National Laboratories, Albuquerque, New Mexico, 1982.

Input File for SANTOS (Version 1.0.0) Run

```
TITLE
PRESSURIZED (f=0.2) 5.94m X 3.33m EMPTY ROOM - STRAT. W/ MD (3200 moles/
    drum)
PLANE STRAIN
INITIAL STRESS = USER
GRAVITY = 1 = 0. = -9.8066 = 0.
PLOT ELEMENT, STRESS, STRAIN, VONMISES, PRESSURE
PLOT NODAL, DISPLACEMENT, RESIDUAL
PLOT,STATE, EQCS, DENSITY, EV
RESIDUAL TOLERANCE = 0.5
MAXIMUM ITERATIONS = 1000
MAXIMUM TOLERANCE = 100.
INTERMEDIATE PRINT = 100
ELASTIC SOLUTION
PREDICTOR SCALE FACTOR = 1.0
AUTO STEP .02 2.592E6 NOREDUCE 1.E-5
HOURGLASS STIFFENING = .005
STEP CONTROL
 120000  3.1536e11
END
OUTPUT TIME
 120   3.1536e11
END
PLOT TIME
 120   3.1536e11
END
 MATERIAL, 1, MUNSON DAWSON, 2300. $ ARGILLACEOUS HALITE
TWO MU = 24.8E9
BULK MODULUS = 20.66E9
A1 = 1.407E23
Q1/R = 41.94
N1 = 5.5
B1 = 8.998E6
A2 = 1.314E13
Q2/R = 16.776
N2 = 5.0
B2 = 4.289E-2
SIG0 = 20.57E6
QLC = 5335.
M = 3.0
K0 = 2.47E6
C = 2.759
ALPHA = -14.96
BETA = -7.738
DELTLC = .58
RN3 = 2.
AMULT = .95
```

Input File for SANTOS (Version 1.0.0) Run (cont'd)

```
END
 MATERIAL, 2, MUNSON DAWSON, 2300. $ PURE HALITE
TWO MU = 24.8E9
BULK MODULUS = 20.66E9
A1 = 8.386E22
Q1/R = 41.94
N1 = 5.5
B1 = 6.086E6
A2 = 9.672E12
Q2/R = 16.776
N2 = 5.0
B2 = 3.034E-2
SIG0 = 20.57E6
QLC = 5335.
M = 3.0
K0 = 6.275E5
C = 2.759
ALPHA = -17.37
BETA = -7.738
DELTLC = .58
RN3 = 2.
AMULT = .95
END
NO DISPLACEMENT X = 1
NO DISPLACEMENT X = 3
NO DISPLACEMENT Y = 3
PRESSURE, 20, 1, 13.57E6
PRESSURE, 10, 1, 15.98E6
ADAPTIVE PRESSURE, 400, 0., -6.4
CONTACT SURFACE 200 100 0. 1.E-6 1.E40
CONTACT SURFACE 300 200 0. 1.E-6 1.E40
CONTACT SURFACE 100 300 0. 1.E-6 1.E40
FUNCTION,1  $ FUNCTION TO DEFINE PRESCRIBED PRESSURE
0., 1.
6.3072E20, 1.
END
FUNCTION,2
 0., 0.
.0323, .02833E6
.741, .733E6
.898, 1.1333E6
1.029, 1.667E6
1.18, 2.8E6
1.536, 10.167E6
END
EXIT
```

Distribution:

MS0439	1434	D. R. Martinez
MS0841	1500	D. J. McCloskey
MS0836	1501	C. W. Peterson
		Route to: 1512, 1513, 1551, 1552
MS0827	1502	P. J. Hommert
		Route to: 1503 1511, 1553, 1554
MS0443	1561	H. S. Morgan
MS0443	1561	E. L. Hoffman
MS0443	1561	C. M. Stone
MS0443	1561	J. R. Weatherby
MS0437	1562	R. K. Thomas
MS1322	6121	J. R. Tillerson
MS1322	6121	D. E. Munson
MS1328	6342	D. R. Anderson
MS1328	6342	P. Vaughn
MS1328	6342	J. D. Schreiber
MS1328	6342	J. E. Bean
MS1341	6345	R. C. Lincoln
MS1341	6345	F. T. Mendenhall
MS0443	1561	J. G. Argüello

WIPP
UC721 - DISTRIBUTION LIST
SAND97-0794

Federal Agencies

US Department of Energy (4)
Office of Civilian Radioactive Waste Mgmt.
Attn: Deputy Director, RW-2
Acting Director, RW-10
Office of Human Resources & Admin.
Director, RW-30
Office of Program Mgmt. & Integ.
Director, RW-40
Office of Waste Accept., Stor., & Tran.
Forrestal Building
Washington, DC 20585

Attn: Project Director
Yucca Mountain Site Characterization Office
Director, RW-3
Office of Quality Assurance
P.O. Box 30307
Las Vegas, NV 89036-0307

US Department of Energy
Albuquerque Operations Office
Attn: National Atomic Museum Library
P.O. Box 5400
Albuquerque, NM 87185-5400

US Department of Energy
Research & Waste Management Division
Attn: Director
P.O. Box E
Oak Ridge, TN 37831

US Department of Energy (5)
Carlsbad Area Office
Attn: G. Dials
D. Galbraith
M. McFadden
R. Lark
J. A. Mewhinney
P.O. Box 3090
Carlsbad, NM 88221-3090

US Department of Energy
Office of Environmental Restoration and
Waste Management
Attn: M Frei, EM-30
Forrestal Building
Washington, DC 20585-0002

US Department of Energy (3)
Office of Environmental Restoration and
Waste Management
Attn: J. Juri, EM-34, Trevion II
Washington, DC 20585-0002

US Department of Energy
Office of Environmental Restoration and
Waste Management
Attn: S. Schneider, EM-342, Trevion II
Washington, DC 20585-0002

US Department of Energy (2)
Office of Environment, Safety & Health
Attn: C. Borgstrom, EH-25
R. Pelletier, EH-231
Washington, DC 20585

US Department of Energy (2)
Idaho Operations Office
Fuel Processing & Waste Mgmt. Division
785 DOE Place
Idaho Falls, ID 83402

US Environmental Protection Agency (2)
Radiation Protection Programs
Attn: M. Oge
ANR-460
Washington, DC 20460

Boards

Defense Nuclear Facilities Safety Board
Attn: D. Winters
625 Indiana Ave. NW, Suite 700
Washington, DC 20004

Nuclear Waste Technical Review Board (2)
Attn: Chairman
J. L. Cohon
1100 Wilson Blvd., Suite 910
Arlington, VA 22209-2297

State Agencies

Attorney General of New Mexico
P.O. Drawer 1508
Santa Fe, NM 87504-1508

Environmental Evaluation Group (3)
Attn: Library
7007 Wyoming NE
Suite F-2
Albuquerque, NM 87109

NM Energy, Minerals, and Natural
Resources Department
Attn: Library
2040 S. Pacheco
Santa Fe, NM 87505

NM Environment Department (3)
Secretary of the Environment
Attn: Mark Weidler
1190 St. Francis Drive
Santa Fe, NM 87503-0968

NM Bureau of Mines & Mineral Resources
Socorro, NM 87801

Laboratories/Corporations

Battelle Pacific Northwest Laboratories
Battelle Blvd.
Richland, WA 99352

Los Alamos National Laboratory
Attn: B. Erdal, INC-12
P.O. Box 1663
Los Alamos, NM 87544

Tech Reps, Inc. (3)
Attn: J. Chapman (1)
Loretta Robledo (2)
5000 Marble NE, Suite 222
Albuquerque, NM 87110

Westinghouse Electric Corporation (5)
Attn: Library
J. Epstein
J. Lee
B. A. Howard
R. Kehrman
P.O. Box 2078
Carlsbad, NM 88221

S. Cohen & Associates
Attn: Bill Thurber
1355 Beverly Road
McLean, VA 22101

**National Academy of Sciences,
WIPP Panel**

Howard Adler
Oxyrase, Incorporated
7327 Oak Ridge Highway
Knoxville, TN 37931

Tom Kiess
Board of Radioactive Waste Management
GF456
2101 Constitution Ave.
Washington, DC 20418

Rodney C. Ewing
Department of Geology
University of New Mexico
Albuquerque, NM 87131

Charles Fairhurst
Department of Civil and Mineral Engineering
University of Minnesota
500 Pillsbury Dr. SE
Minneapolis, MN 55455-0220

B. John Garrick
PLG Incorporated
4590 MacArthur Blvd., Suite 400
Newport Beach, CA 92660-2027

Leonard F. Konikow
US Geological Survey
431 National Center
Reston, VA 22092

Carl A. Anderson, Director
Board of Radioactive Waste Management
National Research Council
HA 456
2101 Constitution Ave. NW
Washington, DC 20418

Christopher G. Whipple
ICF Kaiser Engineers
1800 Harrison St., 7th Floor
Oakland, CA 94612-3430

John O. Blomeke
720 Clubhouse Way
Knoxville, TN 37909

Sue B. Clark
University of Georgia
Savannah River Ecology Lab
P.O. Drawer E
Aiken, SC 29802

Konrad B. Krauskopf
Department of Geology
Stanford University
Stanford, CA 94305-2115

Della Roy
Pennsylvania State University
217 Materials Research Lab
Hastings Road
University Park, PA 16802

David A. Waite
CH_2 M Hill
P.O. Box 91500
Bellevue, WA 98009-2050

Thomas A. Zordon
Zordan Associates, Inc.
3807 Edinburg Drive
Murrysville, PA 15668

Universities

University of New Mexico
Geology Department
Attn: Library
141 Northrop Hall
Albuquerque, NM 87131

University of Washington
College of Ocean & Fishery Sciences
Attn: G. R. Heath
583 Henderson Hall, HN-15
Seattle, WA 98195

Libraries

Thomas Brannigan Library
Attn: D. Dresp
106 W. Hadley St.
Las Cruces, NM 88001

Government Publications Department
Zimmerman Library
University of New Mexico
Albuquerque, NM 87131

New Mexico Junior College
Pannell Library
Attn: R. Hill
Lovington Highway
Hobbs, NM 88240

New Mexico State Library
Attn: N. McCallan
325 Don Gaspar
Santa Fe, NM 87503

New Mexico Tech
Martin Speere Memorial Library
Campus Street
Socorro, NM 87810

WIPP Public Reading Room
Carlsbad Public Library
101 S. Halagueno St.
Carlsbad, NM 88220

Foreign Addresses

Atomic Energy of Canada, Ltd.
Whiteshell Laboratories
Attn: B. Goodwin
Pinawa, Manitoba, CANADA R0E 1L0

Francois Chenevier (2)
ANDRA
Route de Panorama Robert Schumann
B. P. 38
92266 Fontenay-aux-Roses, Cedex
FRANCE

Claude Sombret
Centre d'Etudes Nucleaires de la Vallee Rhone
CEN/VALRHO
S.D.H.A. B.P. 171
30205 Bagnols-Sur-Ceze
FRANCE

Commissariat a L'Energie Atomique
Attn: D. Alexandre
Centre d'Etudes de Cadarache
13108 Saint Paul Lez Durance Cedex
FRANCE

Bundesanstalt fur Geowissenschaften und
Rohstoffe
Attn: M. Langer
Postfach 510 153
D-30631 Hannover
GERMANY

Bundesministerium fur Forschung und
Technologie
Postfach 200 706
5300 Bonn 2
GERMANY

Institut fur Tieflagerung
Attn: K. Kuhn
Theodor-Heuss-Strasse 4
D-3300 Braunschweig
GERMANY

Gesellschaft fur Anlagen und Reaktorsicherheit
(GRS)
Attn: B. Baltes
Schwertnergasse 1
D-50667 Cologne
GERMANY

Shingo Tashiro
Japan Atomic Energy Research Institute
Tokai-Mura, Ibaraki-Ken, 319-11
JAPAN

Netherlands Energy Research Foundation ECN
Attn: J. Prij
3 Westerduinweg
P.O. Box 1
1755 ZG Petten
THE NETHERLANDS

Svensk Karnbransleforsorjning AB
Attn: F. Karlsson
Project KBS (Karnbranslesakerhet)
Box 5864
S-102 48 Stockholm
SWEDEN

Nationale Genossenschaft fur die Lagerung
Radioaktiver Abfalle (2)
Attn: S. Vomvoris
P. Zuidema
Hardstrasse 73
CH-5430 Wettingen
SWITZERLAND

AEA Technology
Attn: J. H. Rees
D5W/29 Culham Laboratory
Abington, Oxfordshire OX14 3DB
UNITED KINGDOM

AEA Technology
Attn: W. R. Rodwell
044/A31 Winfrith Technical Centre
Dorchester, Dorset DT2 8DH
UNITED KINGDOM

AEA Technology
Attn: J. E. Tinson
B4244 Harwell Laboratory
Didcot, Oxfordshire OX11 ORA
UNITED KINGDOM

Internal

MS	Org.	
1324	6115	P. B. Davies
1320	6831	E. J. Nowak
1322	6121	J. R. Tillerson
1328	6849	D. R. Anderson
1328	6848	H. N. Jow
1335	6801	M. Chu
1341	6832	J. T. Holmes
1395	6800	L. Shephard
1395	6821	M. Marietta
0443	9117	J. G. Arguello
0443	9117	C. M. Stone
0443	9117	A. Fossum
0443	9117	G. D. Sjaardema
0815	5932	F. T. Mendenhall
0425	5932	R. C. Lincoln
0716	6113	D. E. Munson
1341	6822	K. W. Larson
1395	6801	P. Swift
1341	6832	L. H. Brush
3128	6848	D. M. Stoelzel
1328	6849	P. Vaughn
1324	6115	A. R. Lappin
1324	6115	S. W. Webb
1345	6832	B. M. Butcher (5)
1330	6811	K. Hart (2)
1330	4415	NWM Library (20)
9018	8940-2	Central Technical Files
0899	4916	Technical Library (5)
0619	12690	Review and Approval Desk (2), For DOE/OSTI